CONDENSATION AND EVAPORATION COEFFICIENTS OF LIQUIDS

A Thesis submitted to The University of London

for the Degree of

DOCTOR OF PHILOSOPHY

by

PETER BARBER, B.Sc..

Department of Chemical Engineering,

Imperial College of Science and Technology,

London, S.W.7.

December 1966.

ABSTRACT

An attempt has been made to use an existing apparatus designed (by Johnstone[47]) for the investigation of unsteady-state evaporation and condensation of relatively high vapour pressure liquids (e.g.: water) with a view to determining their evaporation coefficients, α. The main feature of the apparatus was the use of an interferometric technique for accurate measurement of the temperature of the liquid at and near its surface. Consideration of the unsteady-state procedure and the proposed method of analysis of results has shown both to be unsatisfactory. In addition, the possibility of adapting the apparatus for use with steady-state evaporation or condensation experiments was considered but was found to be impracticable. Use of the apparatus was abandoned and the design and construction of a new system undertaken.

In view of the unsatisfactory nature of the interferometric technique a system was designed to provide stirring at the evaporating liquid surface in an attempt to eliminate surface cooling and hence allow the assumption that surface temperature equals bulk temperature.

The materials used in the investigation were benzyl alcohol and n-butyric acid. It was found that the evaporation coefficient, α, (as defined by equation (1.1-6)) increased as the vapour pressure above the evaporation surface was decreased and in particular the increase became very rapid as the vapour pressure approached zero (i.e.: as "free evaporation" conditions were approached). Indications were that α was unity at "free evaporation " conditions. As far as is known, in all previous work with liquids, α has been considered to be a constant for a given material at a given temperature and independent of the undersaturation in the vapour.

There was evidence that, despite stirring, a high temper-

ature gradient existed in the liquid over a small distance at the surface (estimated to be about 0.2 mm.). A method of estimation of the true surface temperature was devised, but the continued need for a satisfactory method of measuring surface temperature under these conditions was evident.

ACKNOWLEDGEMENTS

The author wishes to thank Dr R.F. Strickland-Constable who, in his capacity as supervisor, has given valuable criticism and continual encouragement throughout this work.

Thanks are also due to Professor K.G. Denbigh in whose Section the work was carried out and who, as Cortaulds Professor of Chemical Engineering, made available a maintenance grant from the Cortaulds Trust Fund.

The many helpful discussions with Mr J.S. Oakley and the workshop staff are also gratefully acknowledged.

TABLE OF CONTENTS.

CHAPTER 1.

INTRODUCTION.

1.1 The Simple Kinetic Theory Approach.

If a gas of molecular weight M is at a pressure P and temperature T, it can be shown from the kinetic theory that the rate of mass flow, W, through a "window" of unit area in the gas is as follows:-

$$W = (M/2\pi RT)^{\frac{1}{2}} . P$$

If we now consider a volatile material in equilibrium with its vapour, since no net transfer is taking place from one phase to the other, it can be said that if all molecules striking the material surface from the gas phase condense, then the rate of evaporation from the surface must be equal to the rate of bombardment of the surface from the gas phase. Hence, if the vapour pressure of the material is P, molecular weight M, and the temperature T, then both the rate of condensation, W_c , and the rate of evaporation, W_e , are given by the above equation as follows:-

$$W_e = W_c = (M/2\pi RT)^{\frac{1}{2}} . P \qquad (1.1\text{-}1)$$

At this point it is assumed that the processes of condensation and evaporation are going on independently of one another, so that if the space above the surface of the volatile material were evacuated, it would continue to evaporate at the rate given in equation (1.1-1), provided that the surface were maintained at the temperature T. This rate will be referred to as the "kinetic evaporation rate" of a material since it is the theoretical maximum possible rate.

Herz[1] used equation (1.1-1) to calculate the evaporation rate of mercury at 100°C, and subsequently found that only about 15% of this rate could be achieved experimentally. It is reported by Langmuir[2]

that close examination of Herz's experimental conditions showed readily that his results must have been much too low and that a rate equal to the calculated kinetic rate was most likely. In fact, Knudsen[3] has accurately determined the rate of evaporation of mercury in a high vacuum and has been able to show conclusively that with a clean mercury surface the rate of evaporation is at least 99% of the calculated kinetic rate.

If we now consider a material evaporating into an atmosphere of its own vapour rather than into a vacuum, it is obvious from the assumption of independence of evaporation and condensation that the net flux is the difference between the kinetic evaporation rate and the rate of bombardment of the evaporating surface from the vapour space. If the surface temperature is T_1, the corresponding vapour pressure P_1, and the pressure and temperature in the vapour space are P_2 and T_2 respectively, the following equation results:-

$$W_{net} = (M/2\pi RT_1)^{\frac{1}{2}}.P_1 - (M/2\pi RT_2)^{\frac{1}{2}}.P_2 \qquad (1.1\text{-}2)$$

If it can further be assumed that the temperature of the vapour is equal to that of the evaporating surface, equation (1.1-2) becomes:-

$$W_{net} = (M/2\pi RT_1)^{\frac{1}{2}}.(P_1 - P_2) \qquad (1.1\text{-}3)$$

If we now consider the possibility that not all molecules striking the material surface condense, we can introduce the concept of a reflection coefficient, "r", such that r is the fraction of molecules striking the surface which condenses (and hence the fraction (1 - r) is reflected). Equation (1.1-1) then becomes:-

$$W_c = W_e = r(M/2\pi RT)^{\frac{1}{2}}.P \qquad (1.1\text{-}4)$$

It is clear from equation (1.1-4) that the kinetic rate of evaporation must also be multiplied by the reflection coefficient, r (r is assumed to be a constant depending only on the material used). When the reflection coefficient is incorporated in equation (1.1-3) the following is obtained:-

$$W_{net} = r(M/2\pi RT_1)^{\frac{1}{2}}.(P_1 - P_2) \qquad (1.1\text{-}5)$$

It has been the practice in this work to relate experimental rates of mass transfer to the kinetic rate given in equations (1.1-1) and (1.1-3) by means of an evaporation coefficient, α, defined by the following equation:-

$$W_{net}\ (\text{experimental}) = \alpha(M/2\pi RT_1)^{\frac{1}{2}}.(P_1 - P_2) \qquad (1.1\text{-}6)$$

It should be noted that experimentally determined values of α will not necessarily be equal to the reflection coefficient r in equation (1.1-5) but will certainly incorporate such a factor if it exists. However, interpretation of the experimental evaporation coefficient has in the past always resembled the reflection coefficient concept in that α has been taken to be a constant for a given substance and has been assumed to be applicable to the gross condensation and gross evaporation processes separately.

1.2 A Brief Review of Published Experimental Work.

The early experiments in this field were mostly similar to the mercury evaporation experiments of Herz and Knudsen in that they were concerned with the evaporation into vacuum of heavy metals having monatomic vapours. It was found that these materials evaporated at rates very close to the kinetic rate and hence no question of interpretation of

the factor α arose. It is worth noting also that these materials all have relatively low vapour pressures which means that the evaporating flux in these experiments was relatively low. This fact, coupled with the existence of high thermal conductivity of the bulk material, means that surface cooling was a negligible factor, unlike in many more recent experiments. An account of the early experimental work in this field is given in some detail by Knacke and Stranski[4].

Interest in evaporation of materials other than metals was shown towards both liquids and solids. The work on solids has been almost entirely confined to the measurement of rates of evaporation into vacuum, as exemplified by the work of Alty[5] who used iodine, camphor, naphthalene and benzoic acid as his test materials. Because of inevitable surface cooling, it became necessary with materials such as these to make an attempt to measure surface temperature. Alty, for example, used a thermocouple in the form of a loop such that the junction could be held hard in contact with the evaporating surface (which was convex) by applying tension to the leads.

In Alty's experiments and in others since then [6 - 13], weighing (direct or indirect) was used to determine the rate of evaporation. However, another method is to measure the recoil force on the evaporating surface. Rideal and Wiggins[14] used this technique in the following way. They suspended on a quartz fibre a horizontal arm on each end of which was fixed a rhombic sulphur crystal. The crystals were partially masked with metal foil such that the exposed surfaces evaporating into the vacuum gave rise to a couple and a consequent deflection of the horizontal arm which was measured by means of a mirror and scale arrangement. Knowing the torque produced, it was possible to calculate the

"evaporation pressure" from a simple relationship, and the evaporation pressure expressed as a fraction of the saturation pressure gave the evaporation coefficient directly. This technique has been used by subsequent workers [15,11] and in particular it is of interest to note that the work of Paul and Lyon[11] was of more than academic interest, since their work on biphenyl was initiated because of the possibility of using the recoil force of evaporating biphenyl as a means of propulsion for satellites in space.

The main point emerging from the mass of results representing the study of evaporation of solids to date is that a good number of materials appear to have evaporation coefficients less than unity. This appears to be so despite a good deal of discrepancy in some cases between the results of different investigators for the same material.

Littlewood and Rideal[16] put forward the idea that all substances have an evaporation coefficient of unity and that any experimental values less than this are due to experimental error. Their major argument was that wherever a value of evaporation coefficient less than unity is obtained, heat transfer to the evaporating surface has been the governing factor and efforts to measure the surface cooling have been inadequate.

Further criticism of experimental technique was expressed by Burrows[17] who considered theoretically the question of evaporation at low pressures from a liquid or solid surface to a condenser. He has pointed out that the geometry of the experimental system is critical in determining whether all molecules leaving the evaporating surface reach the condenser without colliding with another molecule or re-entering the

evaporating surface. In other words, he has claimed that the assumption of "free evaporation" conditions (zero pressure above the evaporating surface) in many cases is invalid. He has carried out sample calculations on some published experimental results to show that if allowance is made for collision and reflection of molecules, the values of evaporation coefficient are increased to approximately unity.

Sherwood and Johannes[9] set out to determine evaporation coefficients under conditions which were not subject to the criticisms of Littlewood and Rideal. They measured the surface temperatures of the evaporating materials by means of a thermocouple technique, but at the same time checked this temperature independently using a thermistor bolometer. The two determinations agreed within $0.1^{\circ}C$. At the same time, the evaporating surfaces were spherical and were surrounded by the condensing surface under conditions where the mean free path of the vapour molecules was considerably greater than the dimensions of the apparatus, so that assumption of free evaporation conditions was reasonably valid. Despite these precautions, these authors obtained values of evaporation coefficient ranging from 1.00 for hexadecanol to 0.14 for thymol.

Alty[5] pointed out that for the materials he studied, those which gave an evaporation coefficient of unity (iodine and naphthalene) have a zero dipole moment whereas camphor and benzoic acid, having dipole moments of 2.95×10^{-18} and 0.8×10^{-18} respectively, were found to have evaporation coefficients of 0.17 and 0.29 respectively. This led him to put forward the view that evaporation coefficient decreases with increase in dipole moment, and this is related to the "free angle ratio" interpretation of evaporation coefficient which is discussed in Section 1.3.

It is worth noting that not all workers have found α to be dependent on dipole moment in the way that Alty noticed. For example, Sherwood and Johannes[9] (whose results can be considered to be as reliable as any) found that four of the materials they used (naphthalene, biphenyl, camphor and thymol) gave evaporating coefficients which increased in order of decreasing dipole moment, but the fifth material (hexadecanol) did not comply with this trend.

The fact that some materials have an evaporation coefficient less than unity is not the only point emerging from the work on solids. So far only "free evaporation " experiments with solids have been considered but some work has been done on the evaporation of solids into an atmosphere of their own vapour [10,12,15]. The values of evaporation coefficients in these experiments were calculated from the simple equation (1.1-6). Jaeckel and Peperle[10] noticed that for the materials they used (sodium chloride, potassium iodide, antimony trisulphide and sulphur) the evaporation coefficient was not constant over the range of experimental conditions used. They found that it was smallest at the smallest undersaturation used and increased by a factor of 3 to 5 for "free evaporation" into vacuum. The authors offer an explanation of these results in terms of increased roughening of the crystal surface at higher undersaturation.

More recently, Cordes and Cammenga[12] have made a study of the effect of relative undersaturation, $(P_1 - P_2)/P_1$, on the evaporation coefficient for hexamethylenetetramine. They were able to obtain a small range of values of relative undersaturation (from 0.06 to 0.18) and found that evaporation coefficient gradually increased throughout this

range. Kitchener and Strickland-Constable[15] report (for work on benzophenone and rhombic sulphur) that the slope of the curve representing growth rate versus relative supersaturation decreased in the region of the origin both in the evaporation and growth regions (i.e.:- both negative and positive supersaturation). Since the slope of these curves is a measure of evaporation coefficient, these authors had the same trend in their results as reported above. Consideration of this trend makes it clear that it is possible to interpret the results in terms of the vapour pressure above the evaporating surface as well as in terms of the relative undersaturation or supersaturation. In these terms, the evaporation coefficient tends to increase as the vapour pressure above the evaporating surface is decreased.

Experimental work on the evaporation of liquids in many cases involved the problem of the existence of much higher vapour pressures than encountered with solids and the consequent difficulty in carrying out experiments at free evaporation conditions. In addition, the higher undersaturations obtainable, and consequent higher evaporation fluxes, led to even greater surface cooling problems than encountered with solids.

Some of the early work on liquids was carried out by Alty[18] who set out to test the kinetic theory prediction for the absolute rate of evaporation of water (equation (1.1-1)). He attempted to overcome the above problems by measuring surface cooling (using a thermocouple) as a function of the vapour pressure above the evaporating surface (which was regulated by means of a series of leaks to a vacuum pump) and then extrapolating to zero pressure to give an estimate of surface cooling at

"free evaporation" conditions. In the same way, the observed rate of evaporation was plotted and extrapolated to zero pressure and the value of evaporation coefficient obtained using these extrapolated quantities was about 0.01. In later work, Alty and Mackay[19] had developed an experimental technique whereby drops of water were formed on the end of a capillary and dropped through an atmosphere of water vapour at known pressure (undersaturated) into a reservoir covered with a layer of oil (to prevent further evaporation). The surface temperature of the evaporating drop was determined from the relationship of the size of the drop with surface tension, which in turm is related to temperature. This method was meant to overcome the difficulty of measuring surface temperature without "interfering" with the system in the way that a thermocouple does (for example). In this case there was no attempt by Alty and Mackay to extrapolate to "free evaporation" conditions and hence equation (1.1-6) was used as the basis for analysis of the results. The values obtained by this method for the evaporation coefficient of water ranged from 0.0053 to 0.0392 but a value of 0.036 is quoted by the authors. In view of the reported increase of evaporation coefficients of solids as the vapour pressure above the evaporating surface was decreased [10,12], it is interesting to note at this point that the higher values of evaporation coefficient obtained by Alty and Mackay for water (around 0.03) were obtained under conditions where the pressure in the vapour space was 5-10 mm. Hg., whereas for the lower values of evaporation coefficient (0.005 - 0.01) the pressure in the vapour space was 16 - 26 mm. Hg.. However, using the same technique these authors obtained an evaporation coefficient of unity for carbon tetrachloride.

Baranaev[20] carried out experimental work similar to the original work of Alty[5]. He evaporated liquids into their own vapours, the pressures of which were regulated at an undersaturated value and he measured the temperatures of the evaporating surfaces using a thermocouple. However, Baranaev did not attempt to extrapolate his results to "free evaporation"conditions and hence used equation (1.1-6) to determine the evaporation coefficients. The liquids investigated were methyl alcohol, ethyl alcohol, propyl alcohol, benzene, toluene and chloroform and the evaporation coefficients obtained ranged from 0.02 for ethyl alcohol to about 0.9 for benzene. Baranaev made an attempt to explain his results in terms of the surface energy of a liquid.

Prüger[21] investigated the rate of evaporation of water and carbon tetrachloride on boiling at atmospheric pressure (without actual formation of vapour bubbles). A steady-state system in which air was was excluded from contact with the evaporating surface was achieved by use of an inverted bell-jar arrangement fitted with a reflux condenser. Since the pressure and hence boiling point were fixed by atmospheric conditions it remained only to measure the superheating of the liquid at the evaporating surface. The technique for doing this was the main feature of the work. Prüger used a very thin "strip" thermocouple junction (0.04 mm. thick and 0.7 mm. long) which was immersed parallel to the liquid surface and was hence capable of establishing the temperature profile in the surface layer (about 0.3 mm. thick) as the liquid level dropped due to evaporation losses. The temperature profile established in this way was found to be linear until very near the surface so that extrapolation of the linear section was used to establish the actual surface temperature.

Prüger pointed out that the thickness of the thermocouple junction was critical in this technique and carried out a similar procedure with a 0.55 mm. thick junction to show that it gave a much lower temperature gradient than the thin junction. Prüger obtained an evaporation coefficient of about 0.02 for water and unity for carbon tetrachloride.

A further attempt to measure the surface temperature of water during evaporation, without "interfering" with the surface, was made by Hammeke and Kappler[22] who used a thermopile to measure the infra-red radiation from the evaporating surface. It is claimed by these authors that since the coefficient of extinction is very large for water, the radiation reaching the thermopile came from a surface layer only 0.01 mm. thick. They found the evaporation coefficient for water at room temperature to be 0.045.

The experimental work referred to so far has been carried out under steady-state conditions. Bucka[23], however, measured evaporation coefficients by a method which depended on continuous measurement of vapour pressure in the vapour space after isolation of the experimental system from the vacuum pump. The following equation was derived from the simple kinetic theory:-

$$\frac{dP_2}{dt} = \alpha \cdot \frac{F}{V} \cdot (RT_1/2\pi M)^{\frac{1}{2}} \cdot (P_1 - P_2) \qquad (1.2\text{-}1)$$

where F = area of evaporating surface

V = volume of vapour space

Bucka designed his experiment for ethyl alcohol such that all the liquid had evaporated before saturation pressure in the vapour space could be reached. A thermocouple installed at the bottom of the

recess containing the evaporating alcohol gave a minimum temperature reading corresponding to completion of evaporation of the alcohol . This temperature was then taken to be the temperature of the alcohol surface throughout the experiment. Point values of the slope of the curve of pressure versus time were then used to determine the evaporation coefficient from equation (1.2-1). The value obtained was 0.024.

A modification of Bucka's method was used by Bogdandy, Kleist and Knacke[24]. These workers used the integrated form of equation (1.2-1) on the assumption that T_1 and hence P_1 were constant throughout the experiment (Bucka in fact had also assumed this). The evaporating liquid in this case was contained in a narrow bore copper tube in a constant temperature bath and the surface temperature was taken to be equal to the bath temperature throughout an experiment. The evaporation coefficient was obtained from the slope of the straight line obtained by plotting $\ln (P_1 - P_2)$ against time, t. The fact that these workers did obtain a linear relationship between $\ln (P_1 - P_2)$ and t led them to believe that their original assumption of constant surface temperature was valid. Using this method they obtained evaporation coefficients of 0.036, 0.99, and 0.96 for ethyl alcohol, carbon tetrachloride and stannous tetrachloride respectively.

Bucka's method has been used recently in a series of experiments by Delaney and coworkers[25 - 27] to determine the evaporation coefficients of water, carbon tetrachloride, deuterium oxide and methanol. The equipment used was considerably more elegant than Bucka's apparatus. For example, the surface temperature (measured by thermistor) and pressure (measured with an "Alphatron" gauge) were recorded during a run on two

continuous balancing electronic recorders with adjustable range and zero, each having a response time of less than one second for full-scale pen deflection. Equation (1.2-1) was used for analysis of results and evaporation coefficients of approximately 0.04, 1.0, 0.02, and 0.02 respectively were obtained for the four materials mentioned above. Regarding the work on deuterium oxide, the authors[26] have pointed out that an error in measurement of surface temperature of from 1°C to 4°C (depending on the experimental conditions) could mean that the true value of α is unity, and that although 1°C is large compared with the accuracy of a thermistor, large temperature gradients may exist at the evaporating surface (as pointed out by Prüger) such that the size of the sensing element is critical.

Not all the work on the evaporation of liquids has been concerned with the higher vapour pressure materials. Wyllie[28] determined the evaporation coefficient of glycerol under "free evaporation" conditions by employing the principles of a Knudsen effusion cell. Here the rate of effusion per unit area of effusion hole is equivalent to the rate of evaporation per unit area of liquid with evaporation coefficient of unity (the pressure in the cell being the saturation pressure). Hence by comparing the rate of weight loss per unit area of effusion hole with the rate of weight loss per unit area of exposed glycerol surface (effusion cap removed) the value of evaporation coefficient for glycerol was found to be about 0.05. Because of the very low evaporation rates involved, surface cooling was considered to be negligible in this experiment.

Bradley and coworkers[29 - 31] carried out a series of experiments in which they were basically interested in the rates of evapor-

ation of low vapour pressure materials in the presence of a non-condensible gas. The materials studied were n-dibutylphthalate and long chain hydrocarbons and fluorocarbons. From their determinations of diffusion coefficients, these workers were able to deduce that the evaporation coefficient was unity for these materials over the whole range of experimental conditions used.

A new approach to the problem was introduced by the work of Hickman and Trevoy[32] with low vapour pressure liquids (2-ethyl hexyl phthalate and 2-ethyl hexyl sebacate). The liquid concerned was continuously recycled in such a way that the evaporating surface was the surface of a falling stream of liquid which was surrounded by a cylindrical condenser wall divided into a number of collecting zones. The system was thoroughly degassed and the temperature of the condenser was such that "free evaporation" conditions were assumed. Also surface cooling was claimed to be negligible in these experiments since evaporation rates obtained from upper and lower collecting zones of the condenser showed no difference. For lower liquid temperatures and hence vapour pressures (e.g.:- 115°C, 1 micron) the value of evaporation coefficient was found to be unity, whereas at higher temperatures (e.g.:- 180°C, 160 microns) it fell to a value of 0.75. (Trevoy[53] makes reference to this work in a later publication and points out that the value of 0.75 was in fact most probably due to surface cooling.) On the basis of these results, Hickman and Trevoy put forward the idea that freshly formed surfaces of all liquids evaporate at the theoretical maximum rate.

In view of this postulation, Trevoy[33] adapted the same experimental system for use with glycerol in order to check the evaporation

coefficient of 0.05 obtained by Wyllie[28]. Temperatures ranging from 70.1°C (17 microns) to 18.2°C (0.069 microns) were used, and over the whole range, α was found to be unity within experimental error. Trevoy claimed that the value of unity obtained was entirely due to the renewal of surface or maintenance of a clean surface that his technique provided.

The natural advancement from these experiments was to attempt to use the same technique for a high vapour pressure material. Hickman[34] modified the apparatus design so that water could be used as the test liquid . Since "free evaporation" conditions were still to be used, it was necessary to provide for a very short exposure time by shortening the length of the falling stream and increasing the stream velocity. Water temperatures corresponding to a vapour pressure of 7 - 8 mm. Hg. were used (6°C) but even so the majority of runs lasted less than five seconds before ice appeared. Some successful runs were obtained but it was obviously necessary here to make allowance for surface cooling and this was done by assuming that the sole source of latent heat was the outer 0.1 mm. thickness of the falling stream. Also, assumption of "free evaporation" conditions was not valid and an "escape coefficient" had to be introduced to take into account resistances in the apparatus resulting in the existence of a back pressure at the evaporating surface. After making these allowances, an average value of evaporation coefficeint of 0.424 was obtained, but Hickman points out that if the outer surface of the evaporating liquid stream were as low as -6°C, then the evaporation coefficient obtained would be unity.

Following on from the disagreement between the results of Wyllie and Trevoy for the evaporation coefficient of glycerol, Heideger

and Boudart[35] carried out a further determination using a combination of Wyllie's effusion cell technique and the integrated unsteady-state technique used by Bogdandy et al.. The times for increase of vapour pressure in the isolated system from one chosen level to another were determined both with and without the effusion cap fitted to the cell. It was necessary to know only the ratio of these times and the ratio of the areas of effusion hole and liquid surface to calculate the evaporation coefficient. These workers also included a turbine agitator to permit stirring which could be arranged to give continuous renewal of the evaporating surface. Despite this precaution, they found the value of evaporation coefficient to be 0.05 (in agreement with the work of Wyllie) and indepindent of stirring.

Experimental techniques so far had involved only a net evaporation process. However, Nabavian and Bromley[36] approached the problem from an engineering point of view in that they carried out determinations of the overall heat transfer coefficients for the condensation of saturated water vapour at low pressures. It is under these conditions that the liquid-vapour interfacial resistance (normally assumed to be zero) becomes significant compared with the other heat transfer resistances in the system (see Appendix 1). Every effort was made to reduce the other resistances involved by using as the condenser surface a specially grooved copper tube cooled internally by high velocity iced water. This made it possible to measure accurately the "interfacial heat transfer coefficient", a concept used by Silver and Simpson[37] and described in Appendix 1. Since the interfacial heat transfer coefficient is dependent on the evaporation coefficient, it was possible for Nabavian and Bromley to calculate

values of α for water and these ranged from 0.35 to 1.0. The authors claim that by means of a thorough error analysis they were able to show that the values obtained near unity were more likely to be correct than those near the lower limit.

Other recent determinations of evaporation coefficient based on condensation experiments have been carried out by Miller and Daen.[38]. These workers caused liquid condensation on glass tube walls by inducing shock waves in the vapour phase which caused compression in the boundary layer at the wall. The growth of the liquid films occurred over very short times and was observed optically. The materials studied were 2-butanol, ethanol, hexane, carbon tetrachloride and chloroform and the values of α reported compare reasonably well with previously determined values with the exception of carbon tetrachloride. For this material a value of 0.05 ± 0.01 was obtained whereas all previous investigators had found the value to be unity .

Jamieson[39] has reported recent condensation experiments employing a radioactive tracer technique. A known area of water surface in the form of a cylindrical jet of unactivated water was passed through an atmosphere of water vapour labelled with tritium. The number of water molecules striking the water jet from the vapour was calculated from the known temperature, vapour pressure and surface area, whilst the number of molecules actually condensed was obtained from the activity acquired by the collected water. The difficulty with this method was the obvious possibility of the re-evaporation of tritiated molecules from the water jet during its passage through the vapour space. It is clear that this would give a lower apparent value of α (condensation coefficient in this

case) than the true value. To overcome this problem, the residence time of the water jet in the vapour was reduced as far as possible. The value of α was found to increase markedly with reduction of residence time such that for a residende time of about 1 second the apparent value of α was of the order of 10^{-4}, whereas at the lowest residence time attainable (about 10^{-5} seconds) the value was about 0.3, and it appeared that further reduction of residence time would increase the value even further. Jamieson pointed out that this investigation was still proceeding within the Fluids Group at the National Engineering Laboratory, East Kilbride, Glasgow.

1.5 A Review of Theoretical Interpretations.

The theory of evaporation (or growth) of solids is dependent on the postulated nature and/or condition of the evaporating (or growing) surface and consequently is more complex than the corresponding concepts for liquid surfaces. For example, in their discussion of the evaporation of dislocation-free crystals, Hirth and Pound[40] (p.96) have derived an expression for evaporation coefficient for a specific set of conditions. Evaporation is said to take place by the following mechanism:- dissociation of molecules from kink sites to positions at ledges; diffusion along the ledge; dissociation from the ledge to an adsorbed position; diffusion of the adsorbed molecule and desorption to the vapour. Applying this mechanism to the case of a clean crystalline surface evaporating into a monatomic vapour phase, Hirth and Pound obtain the following expression:-

$$\alpha = (\sqrt{2}\,\bar{X}/\lambda).\tanh(\lambda/\sqrt{2}\,\bar{X})$$

where $\bar{X}$ = mean free path of diffusion on a surface

λ = interledge spacing

In discussing the evaporation of liquids, these authors suggested that simply bonded liquids which evaporate or grow by exchange of single atoms with a monatomic vapour should exhibit no surface constraint (i.e.:- no interface control) in the kinetics because each surface site may be considered equivalent and because elastic reflection of incident atoms is unlikely (in other words, the evaporation coefficient for such a liquid should be unity).

Hirth and Pound also report a theoretical treatment of the evaporation of an atomic liquid which in essence uses the approach of absolute rate theory and describes the evaporation frequency by the product of a frequency of decomposition and the probability of occupancy of the activated state. This treatment predicts that evaporation coefficient will be unity, and the authors point out that liquids with spherically symmetrical molecules which do not have appreciable entropies of activation should follow similar kinetics and hence also exhibit evaporation coefficients of unity.

It has been mentioned in Section 1.2 that Alty[5] noticed in his experimental results that materials having zero dipole moment had an evaporation coefficient of unity, whilst those having a dipole moment exhibited values less than unity. It was about this time that Herzfeld[41] pointed out the importance of rotation in evaporation. He and others[42] have shown that if it is considered that a molecule is restricted in a rotational degree of freedom in the activated state but not in the vapour, the evaporation coefficient then becomes equivalent to an additional factor introduced into the absolute rate theory. This factor is equal to the ratio of the partition function for the restricted rotation of the

molecule in the activated state to the partition function for its free rotation in the gas phase, and was given the name "free angle ratio" by Kincaid and Eyring[43]. These authors have proposed a number of methods for estimation of this quantity.

Wyllie[28] was the first to point out that for some materials the observed evaporation coefficient and calculated free angle ratio were nearly equal. Hirth and Pound[40] (p.83) have set out a table of experimental evaporation coefficients and the corresponding values of free angle ratio for various polar compounds. For some of the earlier work in this field [20,23,28] the agreement between α and free angle ratio is encouraging, and this includes the controversial liquids glycerol and water.

It is equally clear however that the results obtained by Hickman and Trevoy[33,34] for glycerol and water (α equal to or approaching unity) do not fit the free angle ratio theory. Hirth and Pound offer the explanation that since these workers were using moving streams of liquid, the turbulence of the stream could continuously disturb the liquid-vapour interface and thus disrupt the surface dipole such that the rotational partition function for the molecule in the activated state approaches that of the freely rotating molecule in the gas phase.

The evaporation coefficients for most of the remaining materials in the table (e.g.:- hexadecanol, n-dibutylphthalate) have been determined to be unity despite the fact that they are polar. Mortensen and Eyring[42] have noted that all these substances have either long chain molecules or large planar molecules and have suggested that such molecules might be expected to evaporate in segments such that each segment which has broken loose from the surface gains additional freedom of motion. They

suggested that by the time the molecule finally breaks away from the surface its internal motion is essentially like those of the molecules in the vapour phase so that rotational degrees of freedom are operative in the activated state and the free angle ratio becomes unity.

When discussing the interpretation of experimental evaporation coefficients less than unity the conclusions of Littlewood and Rideal[16] cannot be ignored. Low results may be due to temperature measurement errors occasioned by the existence of large temperature gradients at evaporating surfaces.

1.4 A More Detailed Discussion of the Kinetic Theory Approach.

The simple form of equation (1.1-3) was obtained as a result of assuming the applicability of the simple kinetic theory of gases to the vapour in contact with the liquid or solid surface. That is to say, the vapour phase at the interface has been assumed to be a uniform gas for which the molecules have a Maxwellian velocity distribution function. Under equilibrium conditions (i.e.:- no net mass transfer) this assumption is likely to be valid, but Schrage[44] (p.50) has pointed out that under conditions of net mass transfer, if uniform gas conditions were to be maintained in the vapour phase right up to the interface, an unreasonable law for the velocity distribution of molecules emitted from the liquid or solid surface would be required. In other words, the velocity distribution in the vapour at the interface must be other than Maxwellian.

However, it is clear that even if uniform gas conditions can be assumed up to the interface, the rate of bombardment of the liquid or solid surface under conditions of net mass transfer will not be given

by the simple equation (1.1-1) since this does not provide for the mass motion of vapour to or from the interface. Schrage has treated this problem mathematically for the case where velocity distribution in the vapour right up to the interface is considered to be that of a uniform gas (Maxwellian) in simple mass motion. The temperature of the vapour at the interface is not assumed equal to the temperature of the liquid or solid surface. On this basis, Schrage has obtained an expression for the rate at which mass strikes the phase interface as follows:-

$$W_{o-} = - \left(\frac{\gamma_o}{\gamma_s}\right) \cdot \left(\frac{T_o}{T_s}\right)^{\frac{1}{2}} \Gamma \; W_{s+}$$

where W_{s+} = mass rate of flow per unit area from the interface (kinetic evaporation rate)

γ_o = mass density of vapour at interface

γ_s = mass density of vapour at equilibrium with liquid (or solid) surface

T_o, T_s = temperature of vapour at interface and of liquid (or solid) surface respectively

Γ = a "velocity of approach" correction factor

The factor, Γ , is a collection of rather complex terms and has therefore been presented graphically by Schrage as a function of a more simple quantity, ϕ , defined as follows:-

$$\phi = \frac{1}{2\pi^{\frac{1}{2}}} \cdot \frac{W}{W_{s+}} \cdot \left(\frac{T_o}{T_s}\right)^{-\frac{1}{2}} \cdot \left(\frac{\gamma_o}{\gamma_s}\right)^{-1}$$

where W = net rate of mass transfer at interface

By introducing an evaporation coefficient, α (assumed to be applicable to both the gross evaporation process and the gross condensation process) Schrage has obtained the net rate of mass transfer as the

sum of the two quantities αW_{s+} and αW_{o-}. The final expression obtained is as follows:-

$$\frac{W}{W_{s+}} = \alpha \left[1 - \left(\frac{\gamma_o}{\gamma_s} \right) \cdot \left(\frac{T_o}{T_s} \right)^{\frac{1}{2}} \cdot \Gamma \right] \qquad (1.4\text{-}1$$

Schrage points out that equation (1.4-1) is equivalent to equation (1.1-6) if T_o is assumed equal to T_s and if Γ is assumed to be unity, conditions which apply strictly only at equilibrium ($\Gamma < 1$ for net evaporation, $\Gamma > 1$ for net condensation). He also points out that the assumption $T_o = T_s$ might not be a bad one provided that all the energy transfer necessary for condensation or evaporation occurs through the liquid (or solid) rather than through the vapour phase.

Schrage has also considered the problem of the exact description of the vapour at the phase interface but his treatment, of necessity, involves merely the assumption of a velocity distribution other than Maxwellian. In a similar way, Zwick[45] has proposed a kinetic model in which molecules are assumed to evaporate into a one sided Maxwellian velocity distribution at the liquid surface and molecules reaching the surface from the vapour are assumed to form part of an ellipsoidal velocity distribution. Both of these treatments are complex, and the resulting solutions show no resemblance to the simple equation (1.1-3).

A thorough analysis of evaporation and condensation has been presented by Wilhelm[46] who has written, in addition to the normal mass transfer equation (based on Schrage's expression, equation (1.4-1)), the kinetic theory equations of momentum transport and energy transport. He has also written an expression tonormalise the composite velocity distribution for vapour at the interface, and these four equations together

with the ideal gas law gave a set of five equations, the simultaneous solution of which depended strongly on the assumed velocity distribution of vapour molecules reflected from the liquid surface. Wilhelm used a computer to solve these equations for six chosen sets of conditions (some parameters had to be fixed) but was not able to produce physically consistent results (heat flux and overall thermal driving force were inconsistent).

Available mercury film-condensing data was analysed using the mass, momentum and energy transfer equations, and as a result, it was concluded by Wilhelm that heat transfer coefficients and condensation coefficients obtained experimentally cannot be directly compared without due regard for the experimental system conditions.

Wilhelm claims to have revealed serious shortcomings in the kinetic theory of condensation and it is his opinion that an adequate theory of condensing vapour transport at the vapour-liquid interface remains to be developed. Probably the most interesting point made is that no supporting reasonswere found for the common assumption that the evaporation coefficient is applicable to the gross condensation and gross evaporation processes separately.

On consideration of the more recently attempted theoretical treatments, it seems, in view of discrepancies between experimental evaporation coefficients reported in the literature and the consequent doubt as to the adequacy of experimental procedure, that any refinement of the simple kinetic theory (or at best Schrage's treatment including the effect of mass motion of the vapour) for analysis of experimental results is not yet justified.

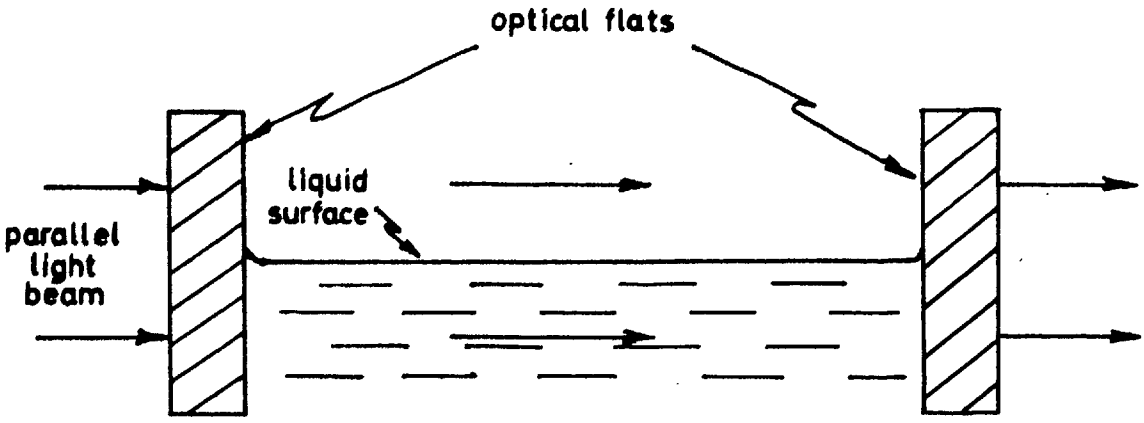

(a) INTERFEROMETER TEST CELL ARRANGEMENT

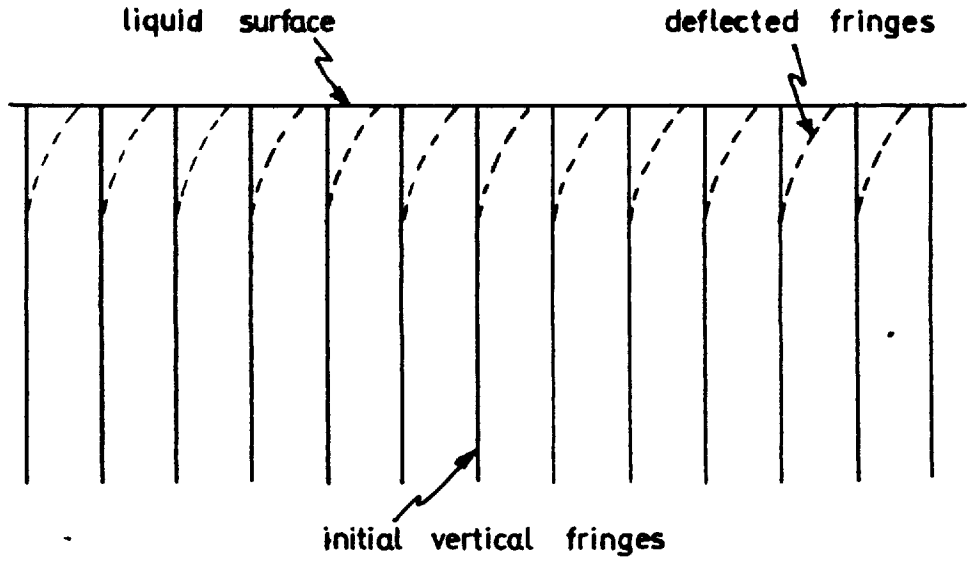

(b) FRINGE PATTERN OBTAINED

FIG 1 INTERFEROMETRIC TECHNIQUE

CHAPTER 2

INITIAL WORK - AN INTERFEROMETRIC TECHNIQUE.

2.1 The Apparatus.

The initial work done for this thesis followed on from the work of Johnstone[47] who designed and built the apparatus briefly described here. This apparatus was intended to overcome the problem of surface temperature measurement in experimental determinations of the evaporation coefficients of relatively high vapour pressure liquids (water being the one of chief interest). The centre piece of the equipment was a large Mach-Zehnder interferometer fitted with a test cell (and compensating cell) in the usual manner such that the evaporating liquid surface in question could be made parallel to light passing through the system normal to the test cell optical flats (see Fig. 1(a)). The basis of the method is that if the optical path length of one of the light beams in the interferometer set-up is changed, then any set of interference fringes being observed will be seen to shift across the field of view according to the following relationship:-

$$\text{N}^{\text{o}}\text{ fringe widths shift} = \frac{\Delta l}{\lambda}$$

where Δl = change in optical path length

λ = wavelength of light being used

During evaporation or condensation, the liquid in the test cell behaves as a two-dimensional system i.e.:- although the temperature will change at and near the surface it will be uniform in any given horizontal plane. This means that a light beam passing through the test cell will "see" liquid of a constant temperature, the value of this temperature being dependent only on the depth below the surface. Suppose

that a system of fringes is set up in the liquid phase field of view initially perpendicular to the surface (Fig. 1(b)) and that evaporation or condensation then takes place such that surface cooling or heating occurs. The change of temperature of the liquid will give rise to a corresponding change in refractive index and hence a change of optical path length. Over a small range of temperature, the refractive index can be considered to be proportional to temperature so that a sideways shift of the fringe pattern proportional to the temperature change will be observed. Since in fact there will be a temperature gradient set up at the liquid surface, the fringe pattern will be curved at the surface as shown in Fig. 1(b) and will remain unchanged in the bulk of the liquid where the temperature change has not penetrated. The relationship between optical path difference and change of refractive index is given by the following equation:-

$$\Delta l = L . \Delta \mu$$

where L = distance between optical flats of test cell

$\Delta \mu$ = refractive index change

Knowing the relationship between refractive index and temperature and having measured the temperature in the bulk liquid (unchanged) Johnstone was able to determine the temperature at any depth in the liquid by measuring the corresponding fringe shift (in terms of fringe widths).

The practical details were not as simple as this procedure suggests because the apparatus was designed to carry out unsteady-state evaporation or condensation experiments. Briefly, the initially perpendicular fringe pattern was set up whilst the liquid was in equilibrium

with its vapour (an evacuation and liquid degassing procedure was provided for) and then the vapour was quickly either rarified or compressed by the pneumatic operation of a set of bellows above the vapour space. It was necessary to film the resulting fringe pattern distortion with a cine-camera (64 frames per second) since the whole process was completed in a few seconds (in fact, in the analysis of results, only the first few frames of the film were used - corresponding to about 0.25 seconds). The temperature analysis was carried out by projecting the filmed fringe pattern on to a screen and making frame by frame measurements of fringe shift on the magnified image. For water at room temperature, a fringe shift equal to one fringe width corresponded to a temperature change of 0.053°C (mercury green was used as the light source) and since the overall magnification achieved was of the order of 90, Johnstone felt confident in quoting temperature changes to an accuracy of 0.001°C.

The pressure change in the vapour space during a run was detected by means of a pressure transducer in the floor of the test cell. This consisted of a thin copper-beryllium diaphragm on the underside of which was situated an adjustable probe which could be brought up to within a very short distance of the diaphragm to form an adjustable capacitance. Any change in pressure in the vapour was transmitted through the liquid to distort the diaphragm and hence change the capacity of the diaphragm-probe arrangement. This change of capacity upset the balance of a high frequency bridge circuit incorporated in a proximity meter. The signal representing the unbalance of the bridge was fed from the proximity meter to the y-gain input of a cathode ray oscilloscope so that a vertical trace was obtained, the height of which was proportional to the signal. This

trace was focussed on to a strip of light-sensitive paper in a rotating drum camera so that a continuous record of the trace height was made throughout a run.

Calibration of the pressure transducer was carried out by the addition or subtraction of known amounts of water to the test cell by means of a mercury column (the area of water surface in the cell was determined from full-scale design drawings of the cell). It was found that the transducer arrangement could be adjusted to give an oscilloscope trace satisfactorily proportional to pressure change.

2.2 Analysis of the Unsteady-State System.

Johnstone had at his disposal a continuous record of the pressure in the vapour space during an experiment and a virtually continuous record of the temperature profile at the liquid surface. No attempt had been made to measure directly the rate of evaporation or condensation, but the need to do this had been avoided by the use of a rather elegant mathematical treatment of the results which will now be briefly explained.

Johnstone assumed the mass transfer process to take place according to the following equation:-

$$\overline{N} = \alpha \phi (P_2 - P_1) \qquad (2.2\text{-}1)$$

where $\overline{N}$ = molar rate of transfer (condensation in this case)

$$\phi = (2\pi RMT)^{-\frac{1}{2}}$$

(Notice that equation (2.2-1) is equivalent to equation (1.1-6))

Because the experiments were carried out over very small pressure ranges, he was also able to assume the vapour pressure proportional to temperature in the following form:-

$$P = \beta T + \eta \qquad (2.2\text{-}2)$$

Incorporating this relationship in equation (2.2-1) gave the following equation:-

$$\bar{N} = \alpha \phi \beta (T^* - T_1)$$

where T^*= saturation temperature corresponding to the pressure in the vapour space

Calling the heat given up by each mole of condensing vapour H, Johnstone obtained the total heat flux per unit area as follows:-

$$Q = \alpha \phi \beta H.(T^* - T_1) \qquad (2.2\text{-}3)$$

If the heat released is considered to be removed from the surface wholly by conduction, the following equation holds:-

$$Q = - k\left|\frac{\partial T}{\partial x}\right|_s \qquad (2.2\text{-}4)$$

where k = thermal conductivity of the liquid

$\left|\frac{\partial T}{\partial x}\right|_s$ = temperature gradient at the surface

From equations (2.2-3) and (2.2-4) Johnstone obtained the following expression for the temperature gradient at the surface:-

$$\left|\frac{\partial T}{\partial x}\right|_s = - \gamma (T^* - T_1) \qquad (2.2\text{-}5)$$

where $\gamma = \frac{\alpha \phi \beta H}{k}$

(γ can be considered to be constant with respect to time and small temperature changes)

It was now necessary to solve the following differential equation describing the unsteady-state heat transfer into the liquid:-

$$\frac{\partial T}{\partial \Theta} = K. \frac{\partial^2 T}{\partial x^2} \qquad \left(K = \frac{k}{\rho C} \right)$$

Johnstone obtained a solution of this equation (from Carslaw and Jaeger[48]) which depends on the ability to express the surface temperature of the liquid in the form of a half-power series of time as follows:

$$T_1' = T_1 - T_o = \sum_n b_n \cdot \theta^{n/2} \qquad (2.2\text{-}6)$$

where b_n = constants (coefficients)

T_o = initial surface temperature

By using the solution mentioned, differentiating with respect to x, and applying surface boundary conditions, Johnstone was able to obtain the following expression for the temperature gradient at the surface:-

$$\left|\frac{\partial T}{\partial x}\right|_s = - \sum_n b_n \cdot f_n \cdot \theta^{n/2 - \frac{1}{2}} \qquad (2.2\text{-}7)$$

where $$f_n = \frac{\Gamma(n/2 + 1)}{\sqrt{K}\,\Gamma(n/2 + \frac{1}{2})}$$

$$\Gamma(n) = \int_0^\infty t^{n-1} e^{-t}\, dt$$

(values of the function $\Gamma(n)$ appropriate to this work are quoted by Johnstone[47], p.157)

He converted his vapour pressure measurements into terms of temperature by use of equation (2.2-2) and assumed that these also could be expressed in terms of a half-power series of time as follows:-

$$T^{*\prime} = T^* - T_o^* = \sum_n a_n \cdot \theta^{n/2} \qquad (2.2\text{-}8)$$

where T_o^* = temperature corresponding to the initial vapour pressure

Rearranging equation (2.2-5) Johnstone obtained the following:-

$$T^{*\prime} + T^{*}_{o} = T'_{1} + T_{o} - \frac{1}{\gamma}\left|\frac{\partial T}{\partial x}\right|_{s}$$

He pointed out that since initially the two phases are at equilibrium, $T^{*}_{o} = T_{o}$, and the above equation reduces to the following:-

$$T^{*\prime} = T'_{1} - \frac{1}{\gamma}\left|\frac{\partial T}{\partial x}\right|_{s}$$

Hence, substituting from equations (2.2-6), (2.2-7) and (2.2-8) he obtained the following:-

$$\sum_{n} a_{n} \cdot \theta^{n/2} = \sum_{n} b_{n} \cdot \theta^{n/2} + \frac{1}{\gamma} \sum_{n} b_{n} \cdot f_{n} \cdot \theta^{n/2 - \frac{1}{2}}$$

By comparing coefficients of like powers of θ he obtained the following general expression:-

$$\gamma = \frac{b_{n+1} \cdot f_{n+1}}{a_{n} - b_{n}}$$

or

$$\alpha_{n} = \frac{k}{\phi H \beta}\left(\frac{b_{n+1} \cdot f_{n+1}}{a_{n} - b_{n}}\right)$$

Johnstone pointed out that on the basis of his argument all values of α_{n} should be the same and equal to α, provided that the series representations of T'_{1} and T' are correct.

He also described an alternative method of analysis in which the time varying temperature profile under the liquid surface was used rather than the surface temperature. A similar expression for α in terms of power series coefficients was obtained.

2.3 Discussion of Johnstone's Results.

For some of his experimental data (e.g.:- Run 8) Johnstone

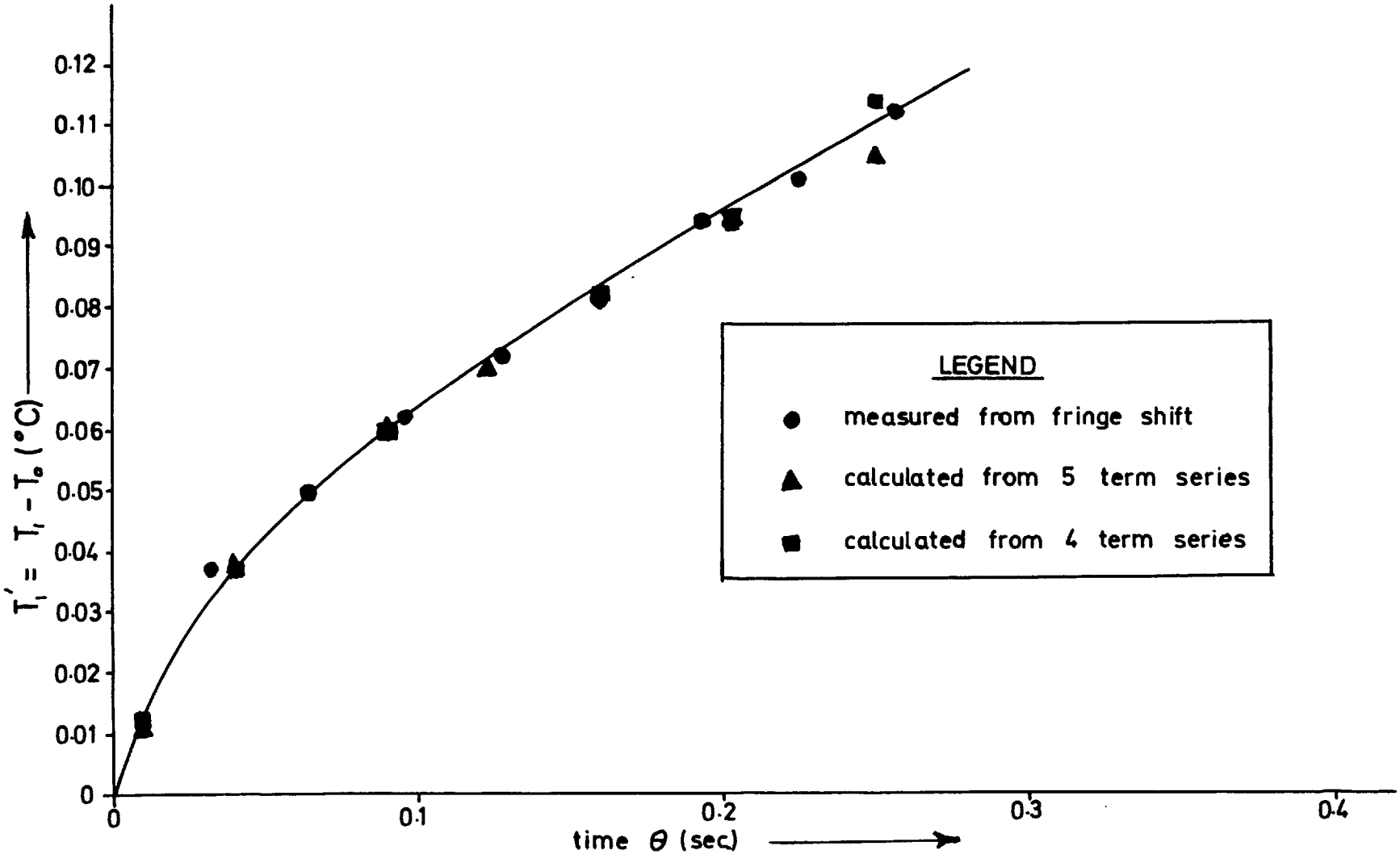

FIG 2 JOHNSTONE'S RUN 8 – MEASURED AND CALCULATED T_1'

used two, three, four and five term series to represent the surface temperature and vapour pressure as outlined in Section 2.2. He found that the values of α_n so obtained varied widely (including negative values) not only according to the number of terms used in the series representations but also according to which coefficients were used from any one pair of series. He concluded that the inconsistency in his calculated results was attributable to non-convergence of the half-power series used and the sensitivity of the values of the series coefficients to experimental error when longer series were employed.

It was decided in this work to take a closer look at the half-power series representations of surface temperature obtained by Johnstone. In particular the 4 and 5 term series for Run 8 were chosen for study. The coefficients obtained by Johnstone for these series are shown in Table 1, Appendix 2. By substituting these coefficients in equation (2.2-6) and using appropriate values of θ, the calculated variation of surface temperature (T_1') with time was obtained. The calculated results are given in Table 2, Appendix 2, together with the actual surface temperature data (obtained from fringe shift measurements) from which the series coefficients were derived. The data in Table 2 are plotted in Fig. 2 from which it is quite clear that the series approximations fit the observed data very well as might be expected.

However, it is clear from the outline of the theoretical treatment in Section 2.2 that it is not the actual surface temperature series alone which is used, but also the derived series for temperature gradient at the surface (equation (2.2-7)). Therefore, to further test the series coefficients given in Table 1, they were used to calculate

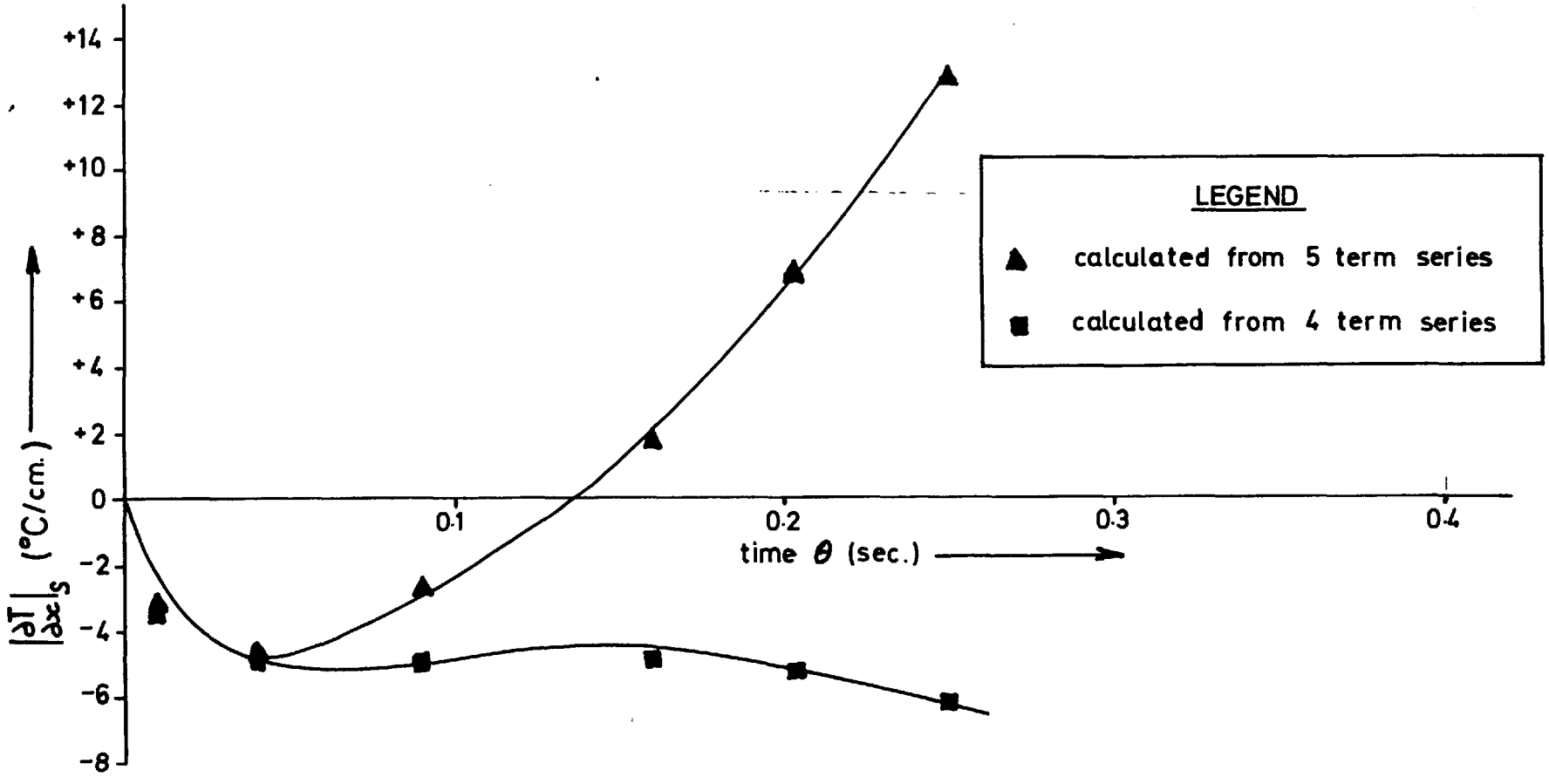

FIG 3 JOHNSTONES RUN 8 – CALCULATED SURFACE TEMPERATURE GRADIENT

temperature gradient as a function of time from equation (2.2-7). The results of these calculations are given in Table 3, Appendix 2 and are shown in Fig. 3 where the great difference in results for the 4 and 5 term series representations is evident. Since in fact Johnstone's Run 8 was a condensation run, the temperature gradient at the surface should be negative (positive net flow of heat into the bulk liquid) and on these ground it is clear from Fig. 3 that the 4 term series gives at least a feasible result whereas the 5 term series does not. It is easy to see why widely varying values of α_n (positive and negative) were obtained using the half-power series representations.

2.4 Practical Considerations.

Carslaw and Jaeger[48](p.70) describe the case for "radiation" from the surface of a semi-infinite solid into a medium at zero temperature, the initial temperature of the solid being constant. The "radiation" from the surface is defined to be governed by the following equation:-

$$-\frac{\partial T}{\partial x} + hT = 0 \text{ , when } x = 0.$$

i.e.:-

$$\left|\frac{\partial T}{\partial x}\right|_s = hT_1 \qquad (2.4\text{-}1)$$

where h = constant

We can now draw an analogy between this process and the process of evaporation of a liquid surface into its own vapour. Supposing a liquid is in equilibrium with its vapour initially and then the vapour pressure above the liquid is changed instantaneously and somehow maintained constant at the new value. Considering the relationship derived by Johnstone (equation (2.2-5)) the new vapour pressure would be represented

by t he quantity T*, its temperature "equivalent". If we now arbitrarily define the constant T* to be zero, equation (2.2-5) reduces to the following form:-

$$\left|\frac{\partial T}{\partial x}\right|_s = \gamma T_1$$

This expression is exactly equivalent to equation (2.4-1), γ (for all practical purposes a constant) being equivalent to the constant h. The solution for surface temperature under these conditions is given by Carslaw and Jaeger as follows:-

$$\frac{T_1}{T_o} = e^{h^2 Kt} \operatorname{erfc}\left(h\,(Kt)^{\frac{1}{2}} \right)$$

In the hypothetical situation described, T_1 is equal to T_o at zero time and thereafter will approach the value T* (zero) to restore equilibrium.

Values of the function $e^{z^2} \operatorname{erfc}(z)$ are tabulated by Carslaw and Jaeger and from these tables the value of the function was found to be 0.179 for $z = 3$.

Hence,
$$\frac{T_1}{T_o} = 0.179 \text{ for } h\,(Kt)^{\frac{1}{2}} = 3 \qquad (2.4\text{-}2)$$

Now
$$h = \gamma = \frac{\alpha \phi \beta H}{k}$$

Johnstone[47] (p.126) gives the value of $k/\phi\beta H$ for water at 20°C to be 0.000162 cm.. If for the purposes of this calculation we assume α to be unity, then for water at 20°C the following is obtained:-

$$h = \frac{1}{0.000162} = 6{,}170 \text{ cm.}^{-1}$$

Johnstone also gives the value of $(K)^{\frac{1}{2}}$ for water as 0.0385

cm. sec.$^{-\frac{1}{2}}$ (p.126). Hence, from equation (2.4-2):-

$$t^{\frac{1}{2}} = \frac{3}{6{,}170 \times 0.0385} \text{ sec.}^{\frac{1}{2}}$$

$$= 1.262 \times 10^{-2} \text{ sec.}^{\frac{1}{2}}$$

so that, $$t = 1.594 \times 10^{-4} \text{ sec.}$$

Hence, for the proposed hypothetical model, just over 80% of the initial driving force for mass transfer ($T_o - T^* = T_o$) at the surface has disappeared in an extremely short time. In the actual experiments carried out by Johnstone, it was not possible to produce an instantaneous change of pressure and thereafter maintain the pressure constant. In his experiments the pressure was increasing or decreasing continuously throughout the period used for analysis (about 0.25 seconds), but in view of the above argument the surface temperature would be expected to "follow" the pressure in the vapour space very closely. Under these conditions it is unreasonable to expect to measure these two quantities separately with an accuracy sufficient to obtain a satisfactory measure of driving force.

It should be noted that if the evaporation coefficient of water were 0.01 instead of 1.00, the time calculated above would become 1.594 seconds instead of 1.594×10^{-4} seconds. Under these conditions the unsteady-state process would become feasible. Hence, for relatively high vapour pressure liquids such as water (i.e.:- where β in equation (2.2-2) is relatively high) it is necessary to presuppose a low evaporation coefficient if step-change unsteady-state evaporation or condensation experiments are to be feasible.

Another practical point concerning the method of pressure measurement used by Johnstone is that the pressure change experienced by

the liquid surface (and then transmitted to the pressure transducer in the floor of the test cell) is not necessarily equal to the pressure change that would be experienced by a pressure sensing device situated in the vapour phase. This comes about because molecules striking the liquid surface are not necessarily reflected as they would be from a solid surface, and since the "pressure" on a surface is dependent on the change of momentum of molecules at the surface it is clear that the evaporation coefficient must be taken into account when considering the pressure exerted by a vapour on its parent material.

In view of the doubtful feasibility of the experimental method and also the inadequacy of the method of analysis described in Section 2.3, it was decided to abandon the use of the unsteady-state experimental system set up by Johnstone.

2.5 The Possibility of a Steady-State System.

Because of the basic merit in the idea of measuring the surface temperature interferometrically, and the time and effort which had been spent on building the interferometer and test cells, the possibility of adapting the apparatus for use in steady-state experiments was investigated.

A considerable amount of time was spent locating and eliminating leaks in the system, particularly around joints on the test cell (Johnstone has mentioned that he probably had air in the system during some of his runs). For this purpose, the original vacuum system associated with the test cell was dismantled and replaced by a simpler system incorporating a McLeod gauge and a Pirani gauge (only a mercury manometer was

available on the original rig) and including as little rubber or plastic tubing as possible. The "leak rate" was eventually reduced to a level which could feasibly be attributed to outgassing of the metal surfaces of the test cell (on standing, the pressure tended to level off at about 150 microns, indicating that outgassing was the problem).

At this stage it was possible to make a number of preliminary attempts to carry out steady-state experiments. A fringe pattern was set up in the liquid phase field of view in the usual way and vapour was bled from the system at a constant rate (via a needle valve). Under these conditions, the interference fringes at the surface of the liquid became inclined to the vertical in the usual way, but it was noticed that instead of being curved they were remarkably straight in the region of the surface, indicating the existence of a constant temperature gradient and hence steady-state conditions.

However, if these experiments were allowed to continue, the fringes at the surface of the liquid became progressively further deflected and the fringe deflection penetrated progressively deeper below the surface. Since the final steady-state would correspond to the existence of a uniform temperature gradient throughout the whole of the bulk liquid, the observed continued deflection corresponded to a slowly changing approach to this condition. It was evident that to set up a steady-state situation in a reasonably short time it would be necessary to provide a heat source or sink (e.g.:- a heated copper block) situated in the liquid fairly close to the surface. Although the temperature gradient (and hence mass transfer rate) could then be obtained directly from the slope ofthe fringes, to determine the surface temperature it would also be necessary

to measure the temperature independently at a point of reference below the liquid surface.

The most important observation made during these trial runs was that there was a limit to the fringe deflection (or slope) that could be tolerated before the fringes became indistinguishable. This meant that there was an upper limit of mass transfer rate tolerable in a steady-state evaporation or condensation experiment. One of the slowly changing unsteady-state trial runs was carried out to estimate this maximum tolerable rate for water. The evaporation rate was adjusted to give the limiting fringe pattern at the surface and then by photographing the pattern (single shot, 35 mm.) and projecting it on a screen it was possible to determine the fringe slope and hence calculate the limiting temperature gradient. The limiting condition corresponded to a fringe shift of about 12 fringe widths at the surface. The temperature gradient was calculated to be 3.33°C/cm. and using a value of 0.001418 cal./cm.sec.°C for the thermal conductivity of water, a corresponding heat transfer rate of 0.00472 cal./cm.^{2}sec. was obtained. A value of 585 cal./gm. for water at room temperature was used for the latent heat (Johnstone,p.126) and hence a limiting mass transfer rate of 8.06×10^{-6} g./cm.^{2}sec. was calculated.

Assuming the evaporation coefficient for water to be unity and substituting the above mass transfer rate in equation (1.1-6), the required pressure driving force, $(P_1 - P_2)$, was found to be 0.6 microns approximately. Even if the evaporation coefficient were taken to be 0.05, the required driving force was only 19 microns approximately. This means that the difference between the pressure in the vapour space and the

pressure corresponding to the liquid surface temperature (presumably obtained to an accuracy of 0.001°C) would be 19 microns. Measurement of the actual pressure change in the vapour space from the initial equilibrium value might be feasible, but since the pressure corresponding to the surface temperature changes in the same direction, the pressure driving force is obtained as the difference between these two changes. To measure such a difference of 19 microns at a pressure level of about 19 mm. Hg. (water at room temperature) would require extremely accurate measurement of the pressure change in the vapour space (measurement of surface temperature to an accuracy of 0.001°C gives the corresponding pressure to an accuracy of approximately 1 micron). This was clearly not feasible.

2.6 Conclusion.

It was now clear that temperature measurement with the interferometer arrangement was much too sensitive to allow measurable pressure driving forces to be used in steady-state evaporation or condensation experiments with relatively high vapour pressure liquids. For steady-state experiments, the system was suited only for use with liquids of low vapour pressure (perhaps up to 10 microns) and since for such materials the effect of surface cooling can usually be neglected, the purpose of using the interferometric techcique would be defeated.

The possibility of using Johnstone's apparatus for both unsteady-state and steady-state experiments had now been rejected and it was concluded that further attempts to use the apparatus should be abandoned. The design and construction of a completely new piece of apparatus was undertaken.

CHAPTER 3

EXPERIMENTAL.

3.1 Basis for Equipment Design.

The experimental technique was to be made as simple as possible (i) by eliminating the need to measure surface temperature by providing stirring of the evaporating liquid up to the liquid surface and assuming surface temperature equal to bulk temperature (ii) by eliminating the need for measurement of pressure in the vapour space by carrying out evaporation experiments from liquid at one temperature to the same liquid at a lower temperature.

Consider a liquid surface of area A_1 and temperature T_1 (corresponding to vapour pressure P_1) evaporating under steady-state conditions and condensing on a liquid surface of area A_2 and temperature T_2 ($T_2 < T_1$). The pressure in the vapour space will be some value lying between P_1 and P_2. If we assume no pressure drop in the system such that the pressure in the vapour space is uniform throughout and is denoted by P', and we assume that equation (1.1-6) applies, the following is true:-

Rate of evaporation from surface $A_1 = \alpha A_1 (M/2\pi RT_1)^{\frac{1}{2}} . (P_1 - P')$

Rate of condensation at surface $A_2 = \alpha A_2 (M/2\pi RT_2)^{\frac{1}{2}} . (P' - P_2)$

Since at steady-state these two rates are equal we obtain:-

$$\alpha A_1 (M/2\pi RT_1)^{\frac{1}{2}} . (P_1 - P') = \alpha A_2 (M/2\pi RT_2)^{\frac{1}{2}} . (P' - P_2)$$

from which

$$\frac{P_1 - P'}{P' - P_2} = \frac{A_2}{A_1} . (T_1/T_2)^{\frac{1}{2}}$$

Now $(T_1/T_2)^{\frac{1}{2}}$ will not vary greatly from unity under the

experimental conditions envisaged (in any case it will always be greater than unity) so that the governing factor in this equation is the ratio of the surface areas. It is clear that the larger A_2 is made with respect to A_1, the closer P' will approach P_2, so that if A_2 is larger than A_1 by a factor of several hundred most of the total pressure driving force, $(P_1 - P_2$ will exist between the evaporating surface A_1 and the vapour phase, and the approximation $(P_1 - P') = (P_1 - P_2)$ will not be in error by more than a fraction of a percent. It was decided on this basis to carry out experiments in which material is evaporated from the surface of a stirred liquid immersed in a constant temperature bath on to a relatively large condensing surface also immersed in a constant temperature bath. The pressure driving force was to be determined from the difference between the vapour pressures corresponding to the respective bath temperatures.

Apart from the area consideration outlined above, there are other approximations involved. Firstly, even assuming the stirred liquid to be of a uniform temperature right up to the surface, this temperature would have to be lower than that of the corresponding constant temperature bath to allow transfer of the necessary latent heat of vaporisation. The error involved in assuming liquid temperature equal to bath temperature is minimised (i) by having an area of heat transfer from the temperature bath to the liquid which is large relative to the area of the evaporating surface (ii) by choosing a test material for which a reasonably large temperature difference between the two temperature baths is feasible. Secondly, because of the absence of stirring in the condensing liquid, a certain amount of surface heating will inevitably be present. However, because of the difference in area, the mass flux will be

FIG 4 CONICAL STIRRING ARRANGEMENT WITH PULLEY DRIVE SYSTEM

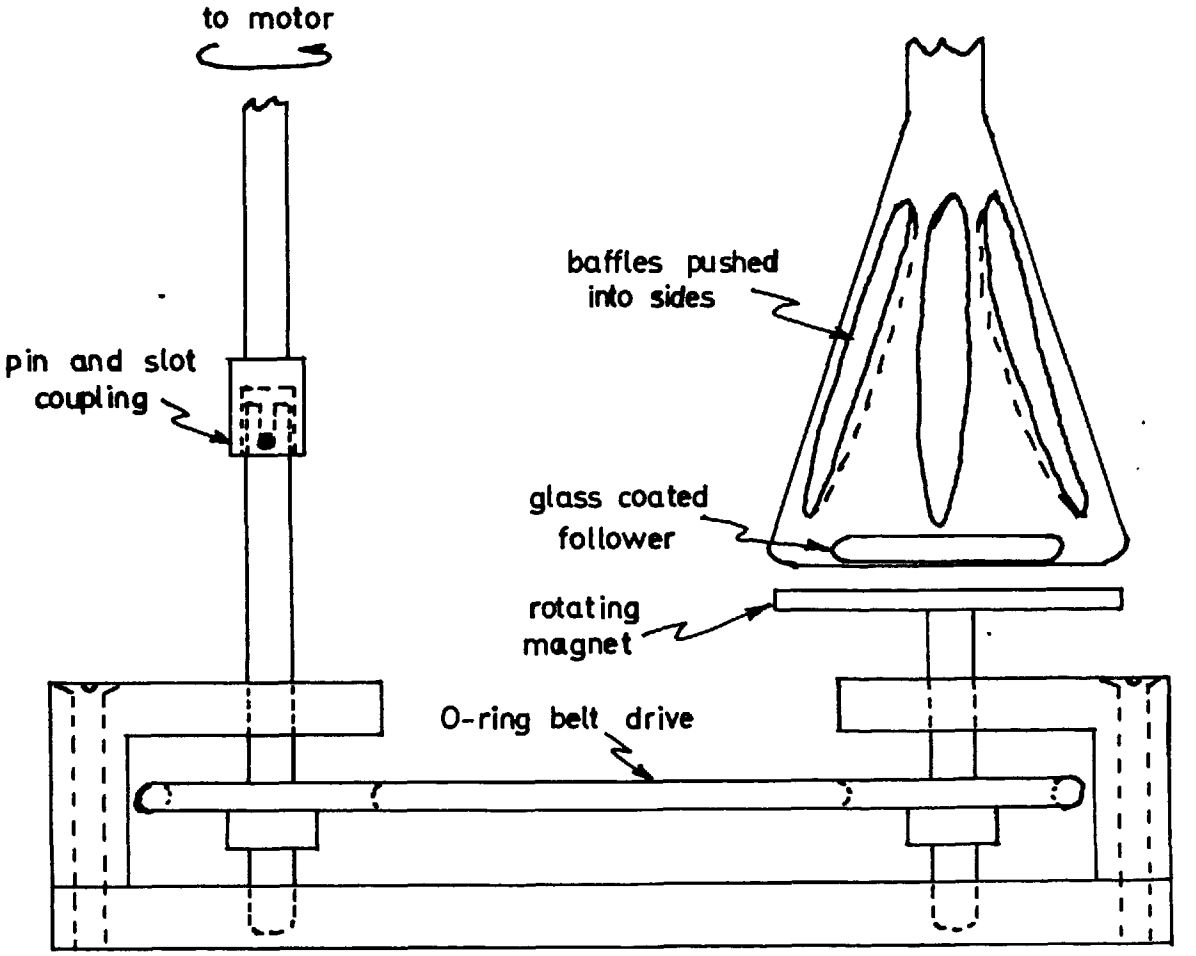

very low on the condensing surface compared with the flux from the evaporating surface and therefore it is assumed that the surface heating can be ignored, again particularly if a reaonably large overall temperature driving force can be used.

Notice that all approximations are such that the pressure driving force ($P_1 - P_2$) determined from the bath temperatures will always be nigher than the actual pressure driving force between the evaporating liquid and the vapour space, so that values of evaporation coefficient obtained using this method will, if anything, tend to be lower than the actual values.

3.2 Stirrer Design.

To comply with the requirements, outlined in Section 3.1, that the evaporating surface should be a great deal smaller than the condensing surface, it was envisaged that an evaporating area of about 1 $cm.^2$ should be used if the apparatus were to be kept to a resonable size. This raised the problem of stirring a very small area of liquid.

Since the apparatus was to be operated under vacuum tight conditions, magnetic stirring was the only acceptable method. Using a magnetic stirrer, it was found that if a normal 50 ml. conical flask was provided with baffles by having indentations pushed into the sloping sides (see Fig. 4) the normal vortex produced in a liquid by rapid stirring was eliminated (the test liquid was water). It appeared that the swirling motion was converted almost completely into vertical agitation such that when the liquid level was in the neck of the flask, vigorous stirring penetrated right up to the surface without actually "breaking"

or unduly distorting the surface. This was tested by placing drops of ink on to the liquid surface in the neck during stirring. The ink was found to disperse almost instantaneously into the bulk of the liquid. It was decided to use such an arrangement to provide a small stirred surface.

Since the whole of the stirred liquid arrangement was to be immersed in a constant temperature bath, it was necessary to provide some means of transmitting the drive from a motor to the immersed drive magnet. A pulley drive system was made from brass and stainless steel (see Fig. 4) and a synthetic rubber vacuum O-ring was used as the drive belt. To allow for the possible use of relatively high temperatures in the bath, a high temperature grease was used to lubricate the bearings of the pulley system. It was expected that the bearings would inevitably "dry up" during use, and the system was designed so that it could be dismantled in situ for greasing or for any other maintenance (e.g.:- replacement of the drive belt). Variation of the stirrer speed was provided for by connecting a variable resistance in series with the drive motor.

5.3 Description of the Apparatus.

One of the basic requirements from Section 3.1 was that there should be no pressure drop in the apparatus, so that it was necessary to use glassware with as large a bore as possible. The largest glass tubing readily available was 8 cm. bore, and a preliminary calculation of pressure drop, set out in Appendix 3, showed that this size was satisfactory for experimental conditions anticipated (both ordinary and Knudsen flow were considered).

The body of the equipment was made from 8 cm. bore glass

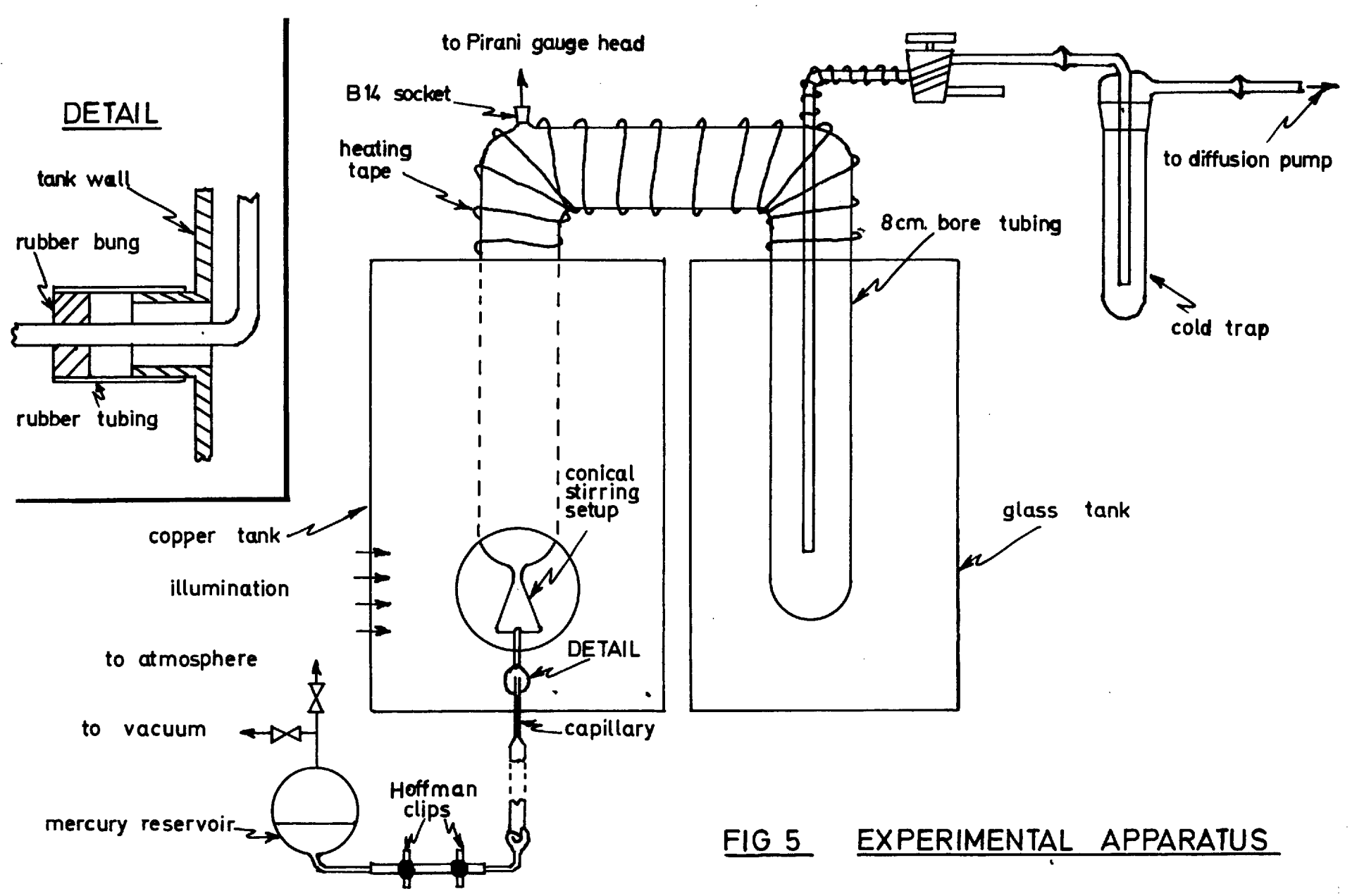

FIG 5 EXPERIMENTAL APPARATUS

tubing in the form of an inverted U - tube (see Fig. 5) one end of which was sealed (condensing leg). The other end (evaporating leg) had fused to it the conicalflask stirring arrangement described in Section 3.2 and shown in Fig. 4(for ease of cleaning and outgassing a glass coated magnetic follower was used). Each leg of the apparatus was immersed in a constant temperature bath.

The condensing leg bath (which was a glass tank) was fitted with a commercial on-off temperature control unit ("Tecam Tempunit" manufactured by Techne (Cambridge) Ltd., Duxford, Cambridge) employing a bimetallic strip sensing element. The whole of the inner surface of the immersed condensing leg provided the large condensing area to satisfy the area requirements outlined in Section 3.1. The evaporating leg bath was a copper tank with two glass windows (one used for illumination and the other for observation) and on-off temperature control was achieved using a mercury-toluene switch in conjunction with an electromagnetic relay. Both temperature control units were capable of controlling temperature within $\pm$ 0.05^{o}C.

When a temperature between 0^{o}C and room temperature was to be maintained in either bath, the temperature control unit could not be used (refrigerated cooling coils were not available). In such cases the temperature was maintained by appropriate addition of ice to the bath. In this way the temperature could easily be kept within a range of 0.1^{o}C and an average value was used in calculations.

The section of glassware exposed to ambient temperature was wound with a heating mantle ("Isotape" type ITW/240 made by Isopad Ltd., Boreham Wood, Herts.) the voltage to which could be regulated by means of

a "Variac" auto-transformer. This winding was necessary to warm the glassware in order to stop liquid condensation on parts other than the condensing leg whenever the condensing temperature was above ambient temperature. Ideally it should have been possible to heat the exposed glassware to a temperature just above the condensing temperature, but because of the awkward shape of the surface on which the heating mantle was wound, it was necessary to overheat some parts considerably to ensure that all points were sufficiently warm. The possible effect of this heating on the pressure in the system is discussed in Appendix 4.

Measurement of evaporation rate was made directly by regularly replacing the evaporated material from a 10 cm. length of calibrated capillary fitted with a scale (the calibration was determined to be 2.64×10^{-2} cc./cm. by weighing measured lengths of mercury thread). The capillary constituted the upper end of a mercury column of approximately barometric height. The bottom of the mercury column was fitted with an air trap which in turn was connected to a mercury reservoir via a short length of flexible P.V.C. tubing. The mercury reservoir was fitted with vacuum taps connecting it to the vacuum backing pump and atmosphere respectively, so that by suitable manipulation of the pressure in the reservoir the mercury level could be raised or lowered at will. When altering the mercury level, the flow was controlled with a Hoffman clip on the flexible P.V.C. tubing. To carry out a measurement of evaporation rate, the mercury level was adjusted to the bottom end of the capillary and the control clip closed tight. A second Hoffman clip was fitted to the P.V.C. tubing (nearer to the column than the control clip) so that mercury could be pushed into the capillary at the desired rate by closing the clip

on the P.V.C. tubing. At the commencement of this procedure, the cross-wires of a vernier microscope (Model 13, made by Precision Tool and Instrument Co., Thornton Heath, Surrey.) were fixed on the bottom of the meniscus of the evaporating liquid, and thereafter the observed level was restored regularly by replenishment with liquid from the capillary. The vernier microscope was supported on a rigid plywood platform.

To avoid surface contamination, the possibility of any greased joints coming into contact with the test liquid could not be permitted and therefore it was necessary to fuse the liquid stirring section and the capillary section in one piece. The capillary section and the tube connecting it to the conical section were quite fragile so that rigid fastening at the point where the connecting tubing was passed through the wall of the copper tank was undesirable. Hence, a watertight seal which still allowed a certain degree of flexibility was devised and used at this point (Detail, Fig. 5).

Provision was made for introducing the test material into the apparatus through a B-14 ground glass socket fitting situated vertically above the neck of the conical section. This fitting served two purposes in that it also allowed the installation of a Pirani gauge head in the system. This gauge head was normally connected to the system via a vacuum tap so that it could be isolated when the experimental conditions were such that there was danger of liquid condensation inside the gauge.

Evacuation of the apparatus was provided for via 10 mm. bore tubing fused vertically into the system along the axis of the condensing leg. The vacuum line was fitted with a 10 mm. bore double oblique tap so that the apparatus could be isolated or connected to either vacuum

or atmosphere. The vacuum line downstream of this point passed through a liquid nitrogen cold trap (this could be dismantled and cleaned) to a mercury diffusion pump which in turn was connected to the backing pump.

3.4 Liquids Investigated.

It was thought that to establish the experimental method, the first liquid to be used should be a low vapour pressure material for which evaporating flux and hence surface cooling could be anticipated to be small. Under these conditions the surface cooling could perhaps be considered to be negligible, and certainly easy to eliminate by stirring. Advancement to successively higher vapour pressure materiols was envisaged thereafter.

Glycerol was the first choice of material largely because of the considerable amount of work already carried out on this liquid in the past. (The size of capillary chosen for the apparatus was based on an anticipated evaporation rate of glycerol from equation (1.1-6) using an evaporation coefficient of unity.) Unfortunately glycerol proved to be a bad choice because its high viscosity prevented stirring at a sufficiently high rate to affect the liquid in the neck of the conical section. Above a certain stirring rate (quite slow) the magnetic follower was no longer able to follow the rotating magnet. The viscosity was reduced by operating at an evaporating temperature of about 80°C, but even under these conditions, although a faster stirring rate was obtainable it was still not sufficient. In addition, at this temperature considerable cavitation occurred i.e.:- bubbles of vapour were formed behind the rotating magnetic follower. These vapour bubbles tended to break away from the

stirrer and "explode" from the surface of the liquid such that liquid was spattered over the inner walls of the evaporating leg above the level of the neck of the conical section. The use of glycerol was abandoned.

It was now clear that the requirements were for a low viscosity transparent liquid having a reasonably low vapour pressure and being readily available at a reasonable price. It was also desirable that work had previously been carried out with the material chosen, but unfortunately no such material existed to fit the above requirements. The material finally chosen was benzyl alcohol which has a vapour pressure of 1 mm. Hg. at 58°C and a viscosity of 5.8 cp. at 20°C.

In the first series of runs, General Purpose Reagent grade benzyl alcohol obtained from Hopkin and Williams Ltd. was used without any further purification. The vapour pressure of this material was obtained from the following relationship given in Landolt-Börnstein[51] (p.118) for the pressure range 1-10 mm. Hg.:-

$$\log P \text{ (mm. Hg.)} = 10.597 - 3509. \frac{1}{T}$$

This equation is based on mean data from several sources.

In accordance with the desired increase of vapour pressure of successive materials used, the second material chosen for study was n-butyric acid which has a vapour pressure of 1 mm. Hg. at about 25°C. Again in this series of runs, General Purpose Reagent grade n-butyric acid obtained from Hopkin and Williams Ltd. was used without further purification. A linear regression analysis was carried out using the vapour pressure data quoted by Perry[49](p.154) for n-butyric acid (again mean data from several sources) and the following relationship was obtained for use in the calculations:-

$$\log P \text{ (mm. Hg.)} = 9.247 - 2761. \frac{1}{T}$$

In view of the changes made to the apparatus after the first series of runs with benzyl alcohol (see Section 3.6) it was decided to extend the work on this material by doing a new series of runs in the modified apparatus. This was also regarded as an opportunity to check the possible effect on the results of purifying the material before use.

The benzyl alcohol as received from Hopkin and Williams Ltd. was fractionated at almost total reflux conditions in a 1 inch diameter glass column about 4 feet high and packed with $\frac{1}{4}$ inch lengths of glass tubing. The ground glass joints of the still-head condenser and overhead product tap were lubricated with benzyl alcohol itself, thereby avoiding contact of the product liquid with grease. An initial fraction of milky consistency came off at about 100°C indicating the presence of water in the feedstock. Thereafter the column conditions became extremely steady and the cut to be used in the third series of runs was collected dropwise over a period of 2-3 hours during which time the still-temperature remained absolutely steady at 207.8°C (fractionation carried out at atmospheric pressure). Vapour pressure was again determined from the equation quoted above from Landolt-Börnstein.

3.5 Initial Experimental Procedure.

The main glassware, the glass coated magnetic follower, and the mercury column and reservoir (including the P.V.C. tubing) were cleaned thoroughly with sulphuric/chromic cleaning solution, rinsed and dried. After placing the magnetic follower in position in the conical section, the main glassware was clamped in place and the flexible water-

tight seal was made around the connecting tubing protruding through the opening in the copper bath (Detail, Fig. 5). At this stage the mercury column was fixed in position and fused to the connecting tubing at a point just above the capillary. Mercury was admitted to the mercury reservoir and allowed to fill the P.V.C. tubing section but was not at this stage permitted to fill the air trap. Ground glass joints were now greased (for temperature resistance, silicone grease was used on joints and taps in the vicinity of the heating mantle) and the system was evacuated. After a short period of evacuation mercury was permitted to fill the air trap and flow a few centimetres into the column (by use of the Hoffman clip control) The system was now degassed for a period of days until no change in Pirani gauge reading was observed after overnight standing. Since the system was to be opened to atmosphere for introduction of the test liquid, the degassing procedure was not primarily intended to remove air but rather to evaporate any remaining volatile materials in the system which might have contaminated the test liquid.

Mercury was now allowed to fill completely the mercury column, capillary and connecting tubing to a point just below the junction of the connecting tubing with the bottom of the conical section. The Hoffman control clip was closed tightly and the system opened to atmosphere Grease was cleaned from the B-14 socket directly above the conical section and a clean funnel carefully placed through the opening (great care was taken not to allow grease to come in contact with the test liquid). The test liquid was poured through the funnel until the liquid level was somewhat above the neck of the conical section. Sufficient liquid above the conical section was provided to fill the connecting tubing and cap-

illary and also to provide a 2 or 3 cm. depth of liquid in the condensing leg.

The system was resealed and a preliminary evacuation carried out until bubbling of air from the test liquid ceased. During this period the rate of pumping was regulated by means of the double oblique tap to avoid excessive splashing as the air bubbles were released from the surface of the liquid. When bubbling had ceased, the system was isolated from the vacuum pump and the temperature of the evaporating leg bath was raised to about 70°C and maintained at this level until all of the test liquid had evaporated over into the condensing leg. During this transfer, the heating mantle was used to prevent condensation on the glassware exposed to ambient temperature. When the transfer of material was complete, the system was allowed to cool and was then opened to vacuum for a short period to purge out any non-condensibles left behind in the vapour phase during the transfer process. The system was once more isolated, the test liquid was evaporated back from the condensing leg to the evaporating leg and, after cooling, another brief period of purging was carried out. At this stage the liquid was considered to have been satisfactorily degassed, but as a precautionary measure, frequent purges of the vapour phase were subsequently carried out, particularly after overnight standing.

The mercury level was now withdrawn to a position at the bottom of the capillary such that the capillary and connecting tubing were now filled with the test liquid. The level in the evaporating leg was adjusted to the desired position in the neck of the conical section by evaporating the excess liquid back into the condensing leg. During this process it was arranged that the desired experimental conditions were

established (i.e.:- the bath temperatures were set at the desired values) by the time the level of the evaporating surface had reached its position in the neck. It was now possible to commence an experimental run.

The evaporating surface area was to be estimated by assuming the liquid meniscus in the neck to be part of the surface of a sphere (see Appendix 5) and therefore a systematic error was anticipated. During a number of preliminary experiments with benzyl alcohol it was found that the apparent evaporation flux for a given set of experimental conditions varied according to the position of the evaporating surface in the neck of the conical section. It was concluded that this was a direct result of the systematic error in estimation of area being different for different parts of the neck (this would be caused by unavoidable distortion of the neck during fusion of the conical section to the main body of the apparatus). It was therefore necessary to carry out all experiments with the liquid level at a single chosen position in the neck. To avoid the possibility of a pressure drop being set up in the restriction of the neck, the position chosen was the top of the neck.

For calculation of surface area, vernier microscope readings were taken on the horizontal scale for the extreme right and left points of contact of the liquid surface with the glass, and on the vertical scale for the "top" and "bottom" of the meniscus (see Fig. 27, Appendix 5). The dimensions of the liquid surface were obtained with the stirrer operating at the speed to be used during the experiment.

With the microscope cross-wires now fixed on the "bottom" of the meniscus, the reading on the capillary scale was noted and timing of the run was commenced. The bottom surface of the meniscus was restored

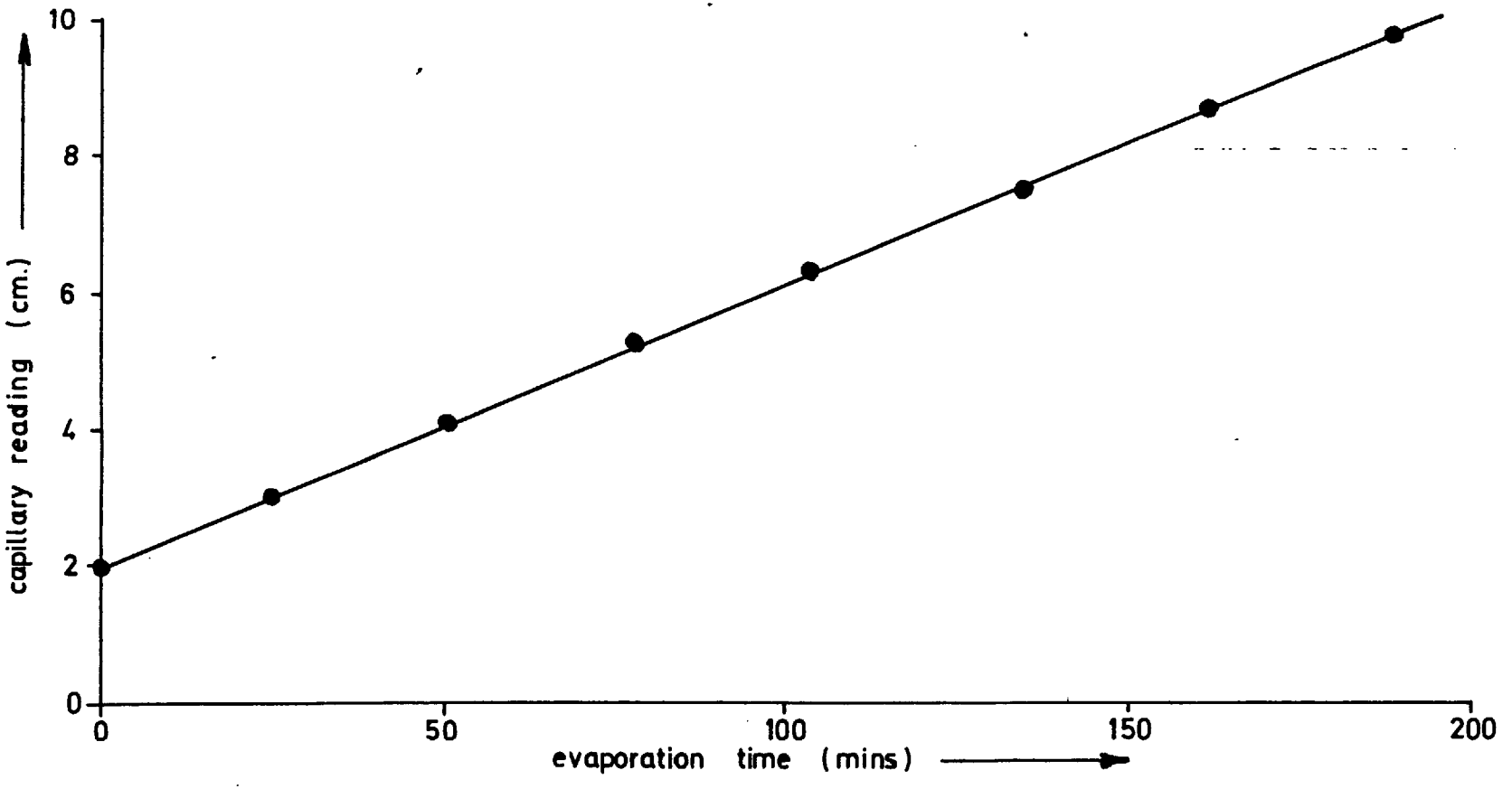

FIG 6 RUN 3 — A CHECK FOR CONSTANT EVAPORATION RATE

to its position at the cross-wires at intervals as required throughout the run by forcing mercury into the capillary as described in Section 3.3. The temperatures of the evaporating leg and condensing leg temperature baths were noted (measured by mercury-in-glass thermometers). Completion of the run was reached by making a final adjustment of the meniscus level and noting the final capillary reading and the time of completion. The stirring speed was measured during the run using a stroboscope on the drive shaft of the motor. From the data obtained, it was now possible to calculate the evaporation coefficient from equation (1.1-6).

It was to be assumed that the rate of evaporation throughout a run was constant so that it could be determined from knowledge of the initial and final capillary readings and the total time of evaporation. This assumption was tested in one of the early runs with benzyl alcohol (Run 3) during which capillary readings and corresponding times were noted at frequent intervals (immediately after adjustment of the meniscus level in each case). The results obtained are given in Table 4, Appendix 6 and are shown in Fig. 6. It is clear from the linear relationship obtained in Fig. 6 that the assumption of constant evaporation rate throughout a run was valid.

To replenish the material in the evaporating leg in preparation for a further run, it was necessary to reverse the direction of the evaporation procedure as previously described. Since, during this process, the liquid condensed on the walls of the evaporating leg, it was necessary to transfer material in excess of the actual amount required so that when the process was again reversed, it was possible to evaporate material for a sufficient time to dry the walls without the liquid level

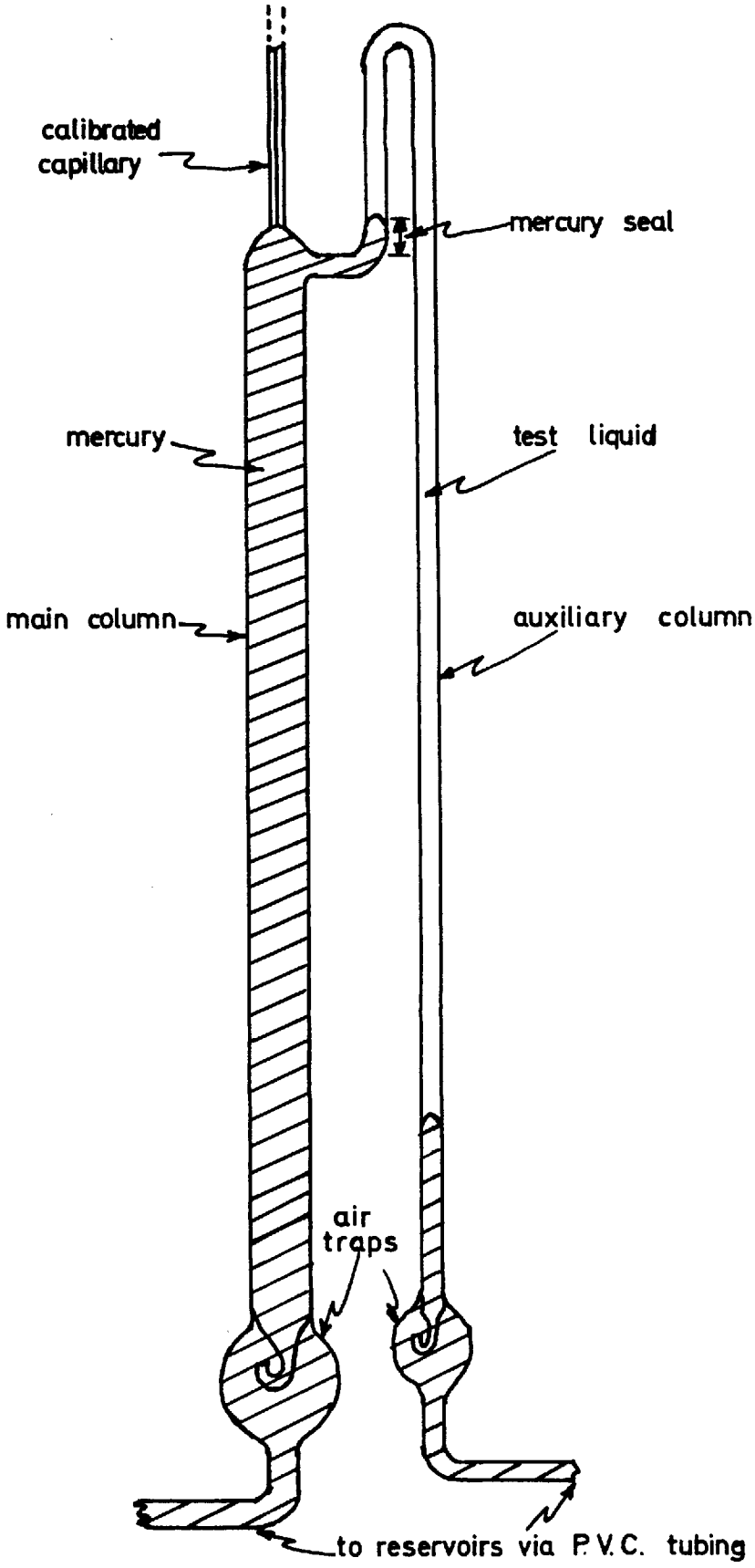

FIG 7 AUXILIARY COLUMN ARRANGEMENT

dropping below the desired position in the neck. The overall procedure required between runs proved to be very time consuming.

3.6 Improvement of the Apparatus.

On the basis of the experience gained during the first series of runs with benzyl alcohol, it was concluded that some means was needed for quicker replenishment of material in the evaporating leg between runs. This was provided for by adding an auxiliary column to the existing mercury column (see Fig. 7) such that the point of junction was below the level of the measuring capillary. This particular arrangement was used to avoid the possibility of error being incurred as a result of expansion or contraction of the liquid in the auxiliary column (due to ambient temperature changes). It is clear that any expansion or contraction was automatically registered as a change in level of mercury in the capillary, thereby avoiding error in measurement of evaporation rate.

Provision was also made for liquid nitrogen cooling of the condensing leg. This required that the condensing leg temperature bath could be removed without dismantling the apparatus (a vacuum flask large enough to contain the condensing leg was available). For this purpose the whole of the experimental rig was moved to a position where the condensing leg was overhanging the edge of the bench so that the temperature bath could be supported on a removable platform.

3.7 Revised Experimental Procedure.

The apparatus was cleaned, assembled and degassed as described in Section 3.5. For introduction of the test liquid, the mercury

level was taken up into the connecting tubing as described in Section 3.5 such that the main mercury column and the auxiliary column were both completely filled with mercury.

At this point, the procedure for degassing the liquid was greatly improved. After the preliminary evacuation (bubbling ceased) a vacuum flask of liquid nitrogen was placed in position around the condensing leg so that pumping could be continued throughout the transfer of the test liquid from the evaporating leg to the condensing leg. When all of the material had been frozen out in the condensing leg, the system was shut off from the vacuum and the material allowed to thaw. After replacing the condensing leg temperature bath in position, the test liquid was evaporated back into the evaporating leg as previously described. When this outgassing procedure had been carried out twice, the liquid was considered ready for experimental runs.

The mercury level was now lowered and the auxiliary column was filled with degassed material as shown in Fig. 7. Care was taken to establish a mercury seal at the point of junction with the main mercury column to avoid the possibility of test material escaping into the working section during the course of an experiment. Replenishment of material between runs could now be made from the auxiliary column by suitable manipulation of mercury levels.

To carry out experimental runs with the condensing leg cooled by liquid nitrogen it was necessary first to transfer all the test liquid into the evaporating leg, because any liquid remaining in the condensing leg might have expanded on freezing and smashed the glassware. The rates of evaporation in these experiments were in some cases quite high so

that the run duration was small (of the order of 1 minute). A technique had to be developed for obtaining all the necessaryreadings in the time available. With the level of evaporating liquid above the neck of the conical section and the level of mercury in the main column slightly below the bottom of the capillary, a position in the neck was selected in the field of view of the vernier microscope. Horizontal vernier readings were taken for the extreme left and extreme right liquid/glass boundaries visible, and the corresponding reading for the vertical position of the microscope was taken. The liquid surface was now observed through the microscope as it evaporated into the field of view. When the "top" of the meniscus was level with the horizontal cross-wire, the vertical position of the microscope was quickly changed by means of the screw adjustment so that the cross-wires coincided with the bottom of the meniscus. The vertical vernier reading for this position was taken so that now the four required vernier readings described in Section 3.5 had been obtained.

The level of mercury in the main column was now quickly raised to position at the bottom of the capillary so that now the evaporating liquid surface had been restored to a position higher in the neck. The surface was once more observed as it again evaporated through the field of view. Timing of the run was commenced and the initial capillary reading was taken as the "bottom" of the meniscus reached the cross-wires. Complete attention could now be devoted to the virtually continuous adjustment of meniscus level required during these fast runs.

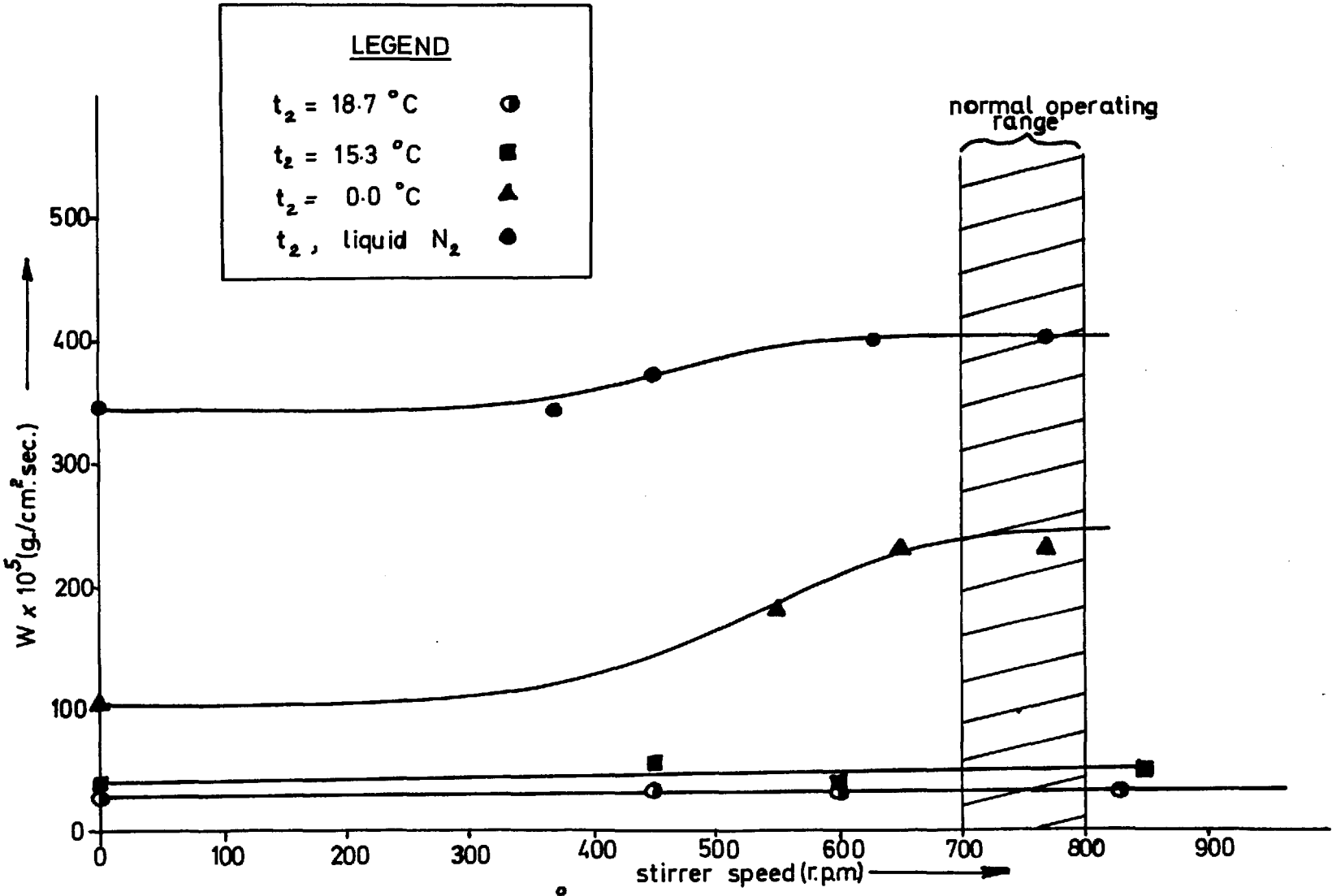

FIG 8 n-BUTYRIC ACID, t_1 = 30·1 °C — EFFECTIVENESS OF STIRRING AT DIFFERENT FLUX LEVELS

CHAPTER 4

EXPERIMENTAL RESULTS

4.1 Effectiveness of Stirring.

To test the effectiveness of stirring for experiments using n-butyric acid, the evaporating temperature was maintained constant at 30.1°C and a series of stirred runs was carried out for each of four sets of conditions established by fixing the condensing temperature at four successively lower values (viz.:- 18.7°C, 15.3°C, 0.0°C and liquid N_2). Within each series, the stirring speed was varied from zero to the normal operating range (700-800 r.p.m.) or slightly beyond. The principle used was that , for a given set of temperature conditions, as long as increase of stirring speed caused a corresponding increase of mass flux, then the level of stirring was considered to be inadequate to make surface temperature equal to bulk temperature. The stirring was considered to be adequate when a speed was reached such that further increase no longer caused a corresponding increase in the mass flux.

The results of these series of runs are given in Table 5, Appendix 6 and are shown in Fig. 8, from which it can be seen that for the lower flux conditions stirring had no significant effect over the whole range of speeds, indicating that surface cooling under these conditions was a negligible factor. It is also clear from Fig. 8 that at the higher flux conditions, no further increase of flux was obtained above a stirring speed of about 650 r.p.m.. It was therefore concluded on the basis of the principle outlined above, that stirring in the normal operating range was adequate for experiments with n-butyric acid involving a mass flux up to at least 4×10^{-3} g./cm.^{2}sec..

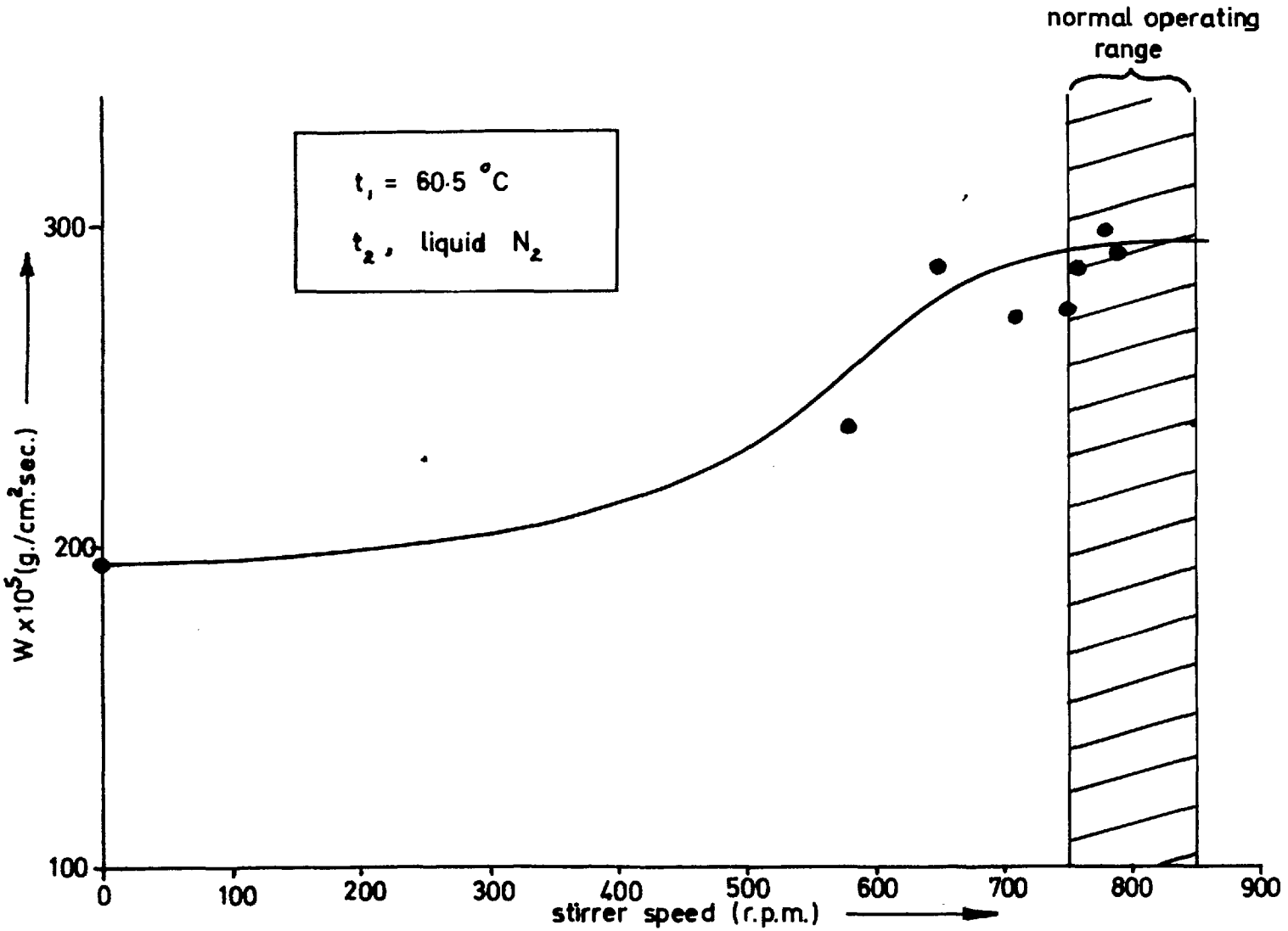

FIG 9 FRACTIONATED BENZYL ALCOHOL – EFFECTIVENESS OF STIRRING AT MAXIMUM FLUX CONDITIONS

A similar stirring test was carried out for evaporation of Benzyl alcohol at a single set of conditions corresponding to the maximum mass flux used ($t_1 = 60.5^{\circ}C$, t_2 liquid N_2). Fractionated benzyl alcohol was used and the results obtained are given in Table 6, Appendix 6 and shown in Fig. 9 from which it is clear that stirring in the normal operating range could be considered adequate for this material for mass flux up to 3×10^{-3} g./cm.^{2} sec..

It was not possible to operate the stirrer in the low speed range, but the data shown in Figs 8 and 9 indicates that stirring had little effect in the speed range up to about 400 r.p.m.. This is consistent with the physical situation, since it is reasonable to suppose that at lower stirring speeds, the agitation would not be sufficiently vigorous to penetrate fully into the neck of the conical section.

Referring to Fig. 8, it seemed strange that the increase of mass flux caused by stirring was greater for the medium range of mass flux ($t_2 = 0.0^{\circ}C$) than for the high range (t_2 liquid N_2). It would be expected that surface cooling under the higher flux conditions would be more severe, so that the effect of stirring would be correspondingly more marked. It was thought, however, that the contribution of natural convection to the elimination of surface cooling might be sufficiently greater in the high mass flux runs to account for the apparently anomolous results.

This idea is supported by the fact that streams of cooled liquid could actually be seen falling from the liquid surface under the high flux conditions. Surprisingly, this situation persisted in stirred runs even in the normal operating speed range where adequacy of stirring was verified. In this case, however, the streams of cooled liquid did not

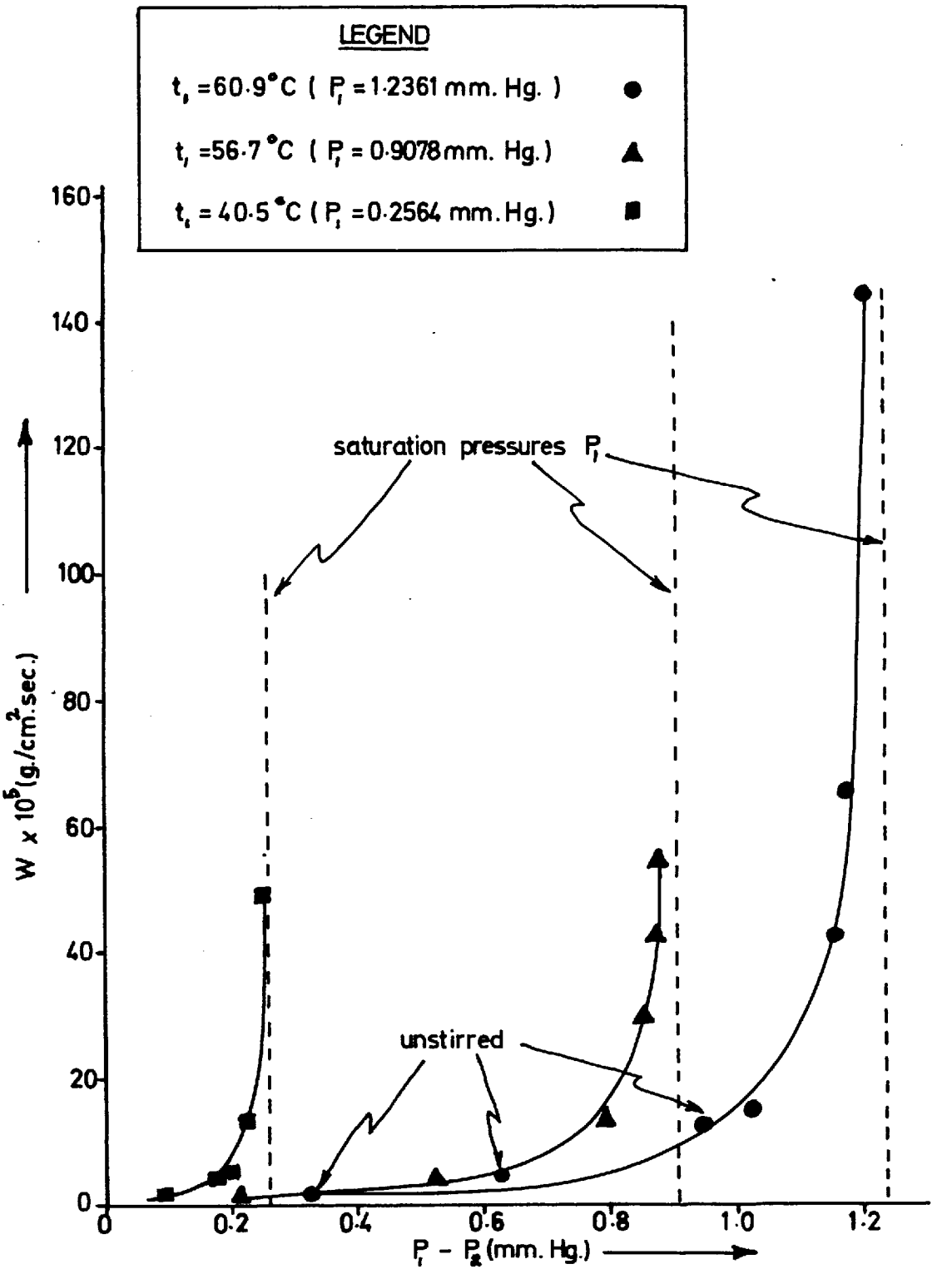

FIG 10 UNTREATED BENZYL ALCOHOL— RELATIONSHIP BETWEEN MASS FLUX AND PRESSURE DRIVING FORCE

persist to any depth below the surface, but rapid dissipation of optical density differences near the surface could be seen. It was clear that if the procedure described in this section for verification of effectiveness of stirring was valid, the observed optical effects must have been caused by relatively small temperature differences at the evaporating surface (smallenough to cause a negligibly small change in the corresponding vapour pressure).

4.2 Untreated Benzyl Alcohol.

It is clear from equation (1.1-6) that, since $(M/2\pi RT)^{\frac{1}{2}}$ is a constant for a given material and evaporating temperature, information concerning the evaporation coefficient, α , is best obtained by graphing experimental mass flux,W, as a function of the pressure driving force,$(P_1 - P_2)$, with evaporating temperature,t_1, as parameter. Accordingly, three series of experiments were carried out using untreated benzyl alcohol evaporating at 60.9°C, 56.7°C and 40.5°C respectively. The results obtained are given in Tables 7, 8 and 9, Appendix 6 and the relationship between mass flux and pressure driving force is shown for each evaporating temperature in Fig. 10.

The unstirred runs shown for t_1 = 60.9°C were used because no stirred runs were carried out at the lower flux levels for this evaporating temperature. Their inclusion is justified since the mass flux involved was low enough for stirring to have no effect (see Section 4.1).

If α were constant over the range of conditions used, a linear relationship between W and $(P_1 - P_2)$ would be expected for each of the evaporating temperatures used. It is therefore clear from Fig. 10

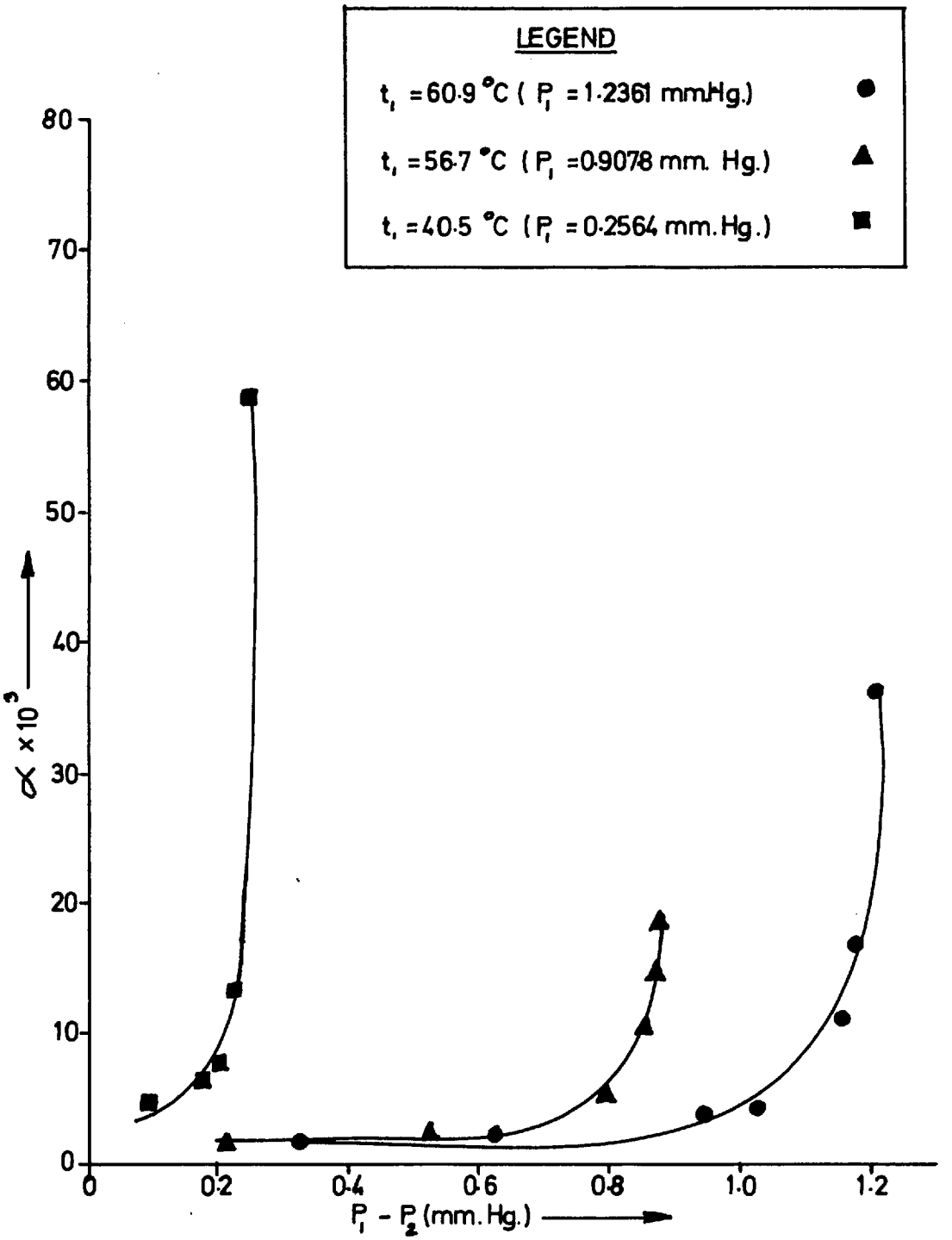

FIG 11 UNTREATED BENZYL ALCOHOL—RELATIONSHIP BETWEEN EVAPORATION COEFFICIENT AND PRESSURE DRIVING FORCE

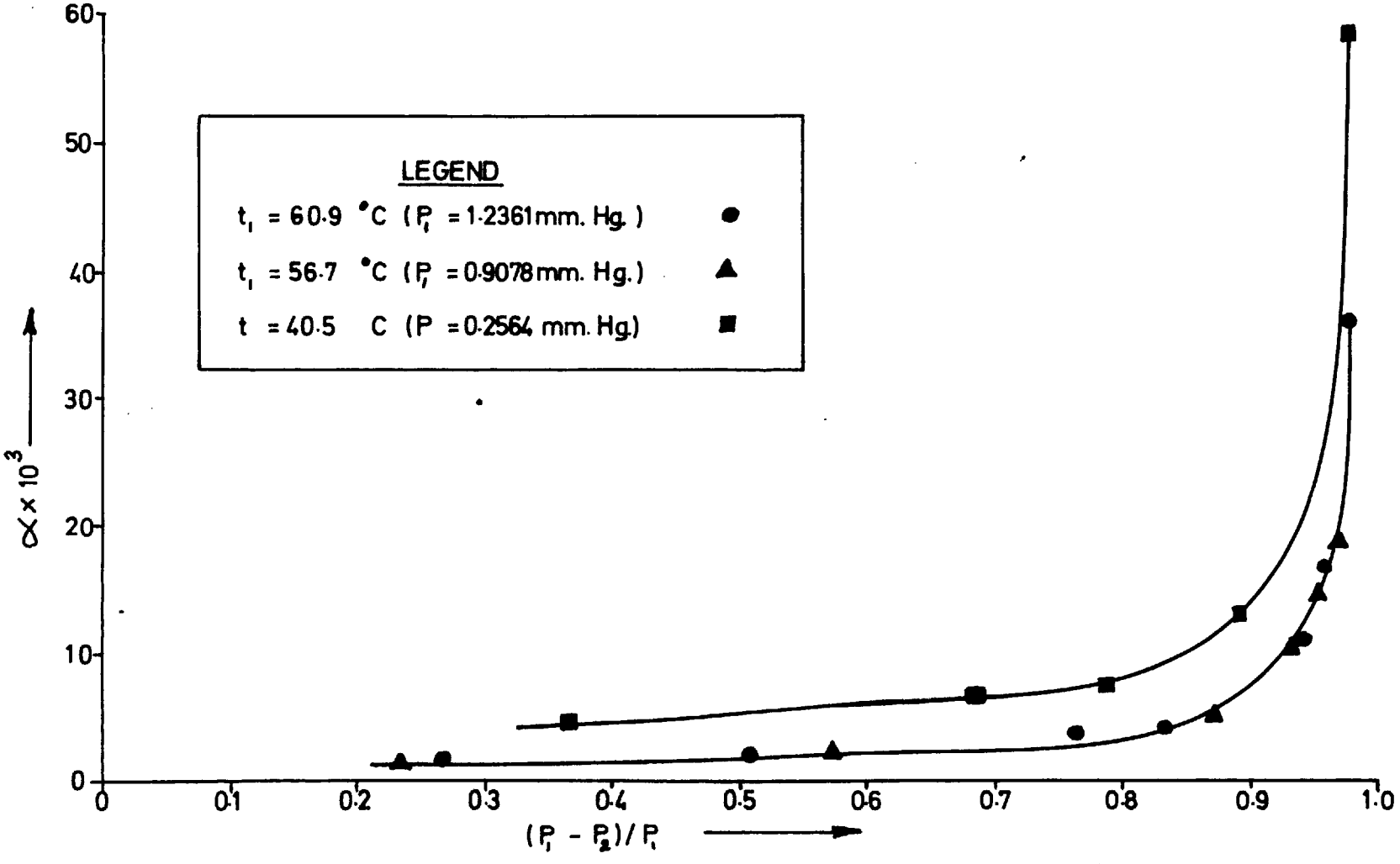

FIG 12 UNTREATED BENZYL ALCOHOL—RELATIONSHIP BETWEEN EVAPORATION COEFFICIENT AND RELATIVE UNDERSATURATION IN THE VAPOUR

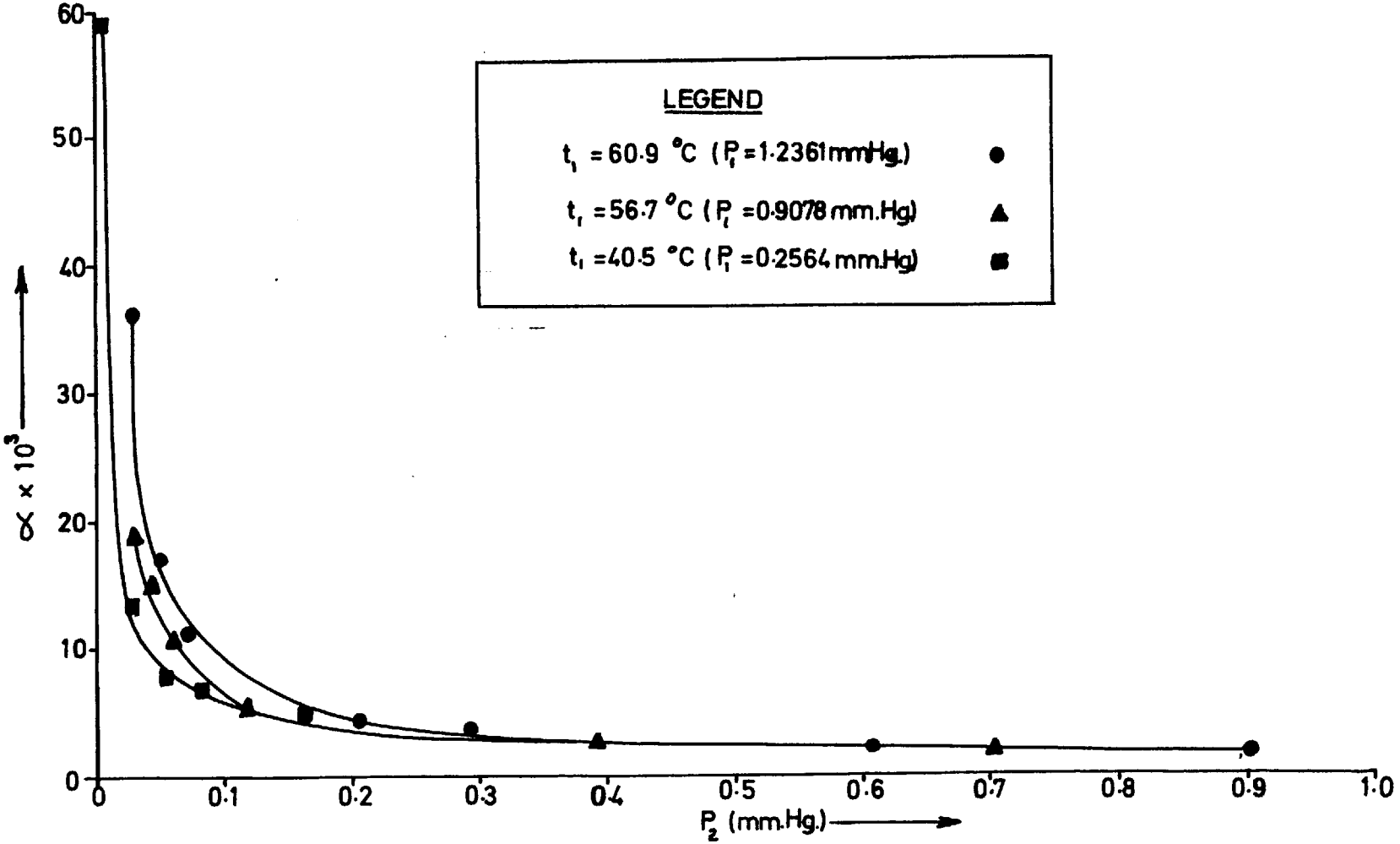

FIG 13 UNTREATED BENZYL ALCOHOL – RELATIONSHIP BETWEEN EVAPORATION COEFFICIENT AND VAPOUR PRESSURE ABOVE SURFACE

that α did not remain constant over the range of conditions used.

A number of possibilities was considered in seeking a variable with which the observed variation of α might be connected. The values of α obtained were graphed in turn as a function of pressure driving force, $(P_1 - P_2)$, relative undersaturation in the vapour, $(P_1 - P_2)/P$ and the vapour pressure above the evaporating surface, P_2 (evaporating temperature was again used as parameter in each case). The data are given in Tables 7, 8 and 9, Appendix 6 and the resulting graphs are shown in Figs 11, 12 and 13 respectively. Inspection of these graphs shows that α was best expressed as a function of P_2 (Fig. 13) since in this way the apparent dependence of α on evaporating temperature was minimised.

It can be seen from Fig. 13 that the values of α increased gradually at first as the vapour pressure above the evaporating surface was decreased (from about 0.7 mm. Hg.) and then rapidly as the pressure was reduced below a value of about 0.1 mm. Hg.. Also, in the region of rapid increase of α, it appeared that for a given value of P_2 the values of α corresponding to the three evaporating temperatures increased in order of increase of evaporating temperature. This phenomenon is discussed in Section 5.4.

4.3 n- Butyric Acid.

Two series of runs similar to those reported in Section 4.2 were carried out using n-butyric acid as the test material. Liquid nitrogen cooling of the condensing leg was now available and it was therefore possible to reduce the vapour pressure above the evaporating surface to approximately zero (i.e.:- "free evaporation" conditions could be approx-

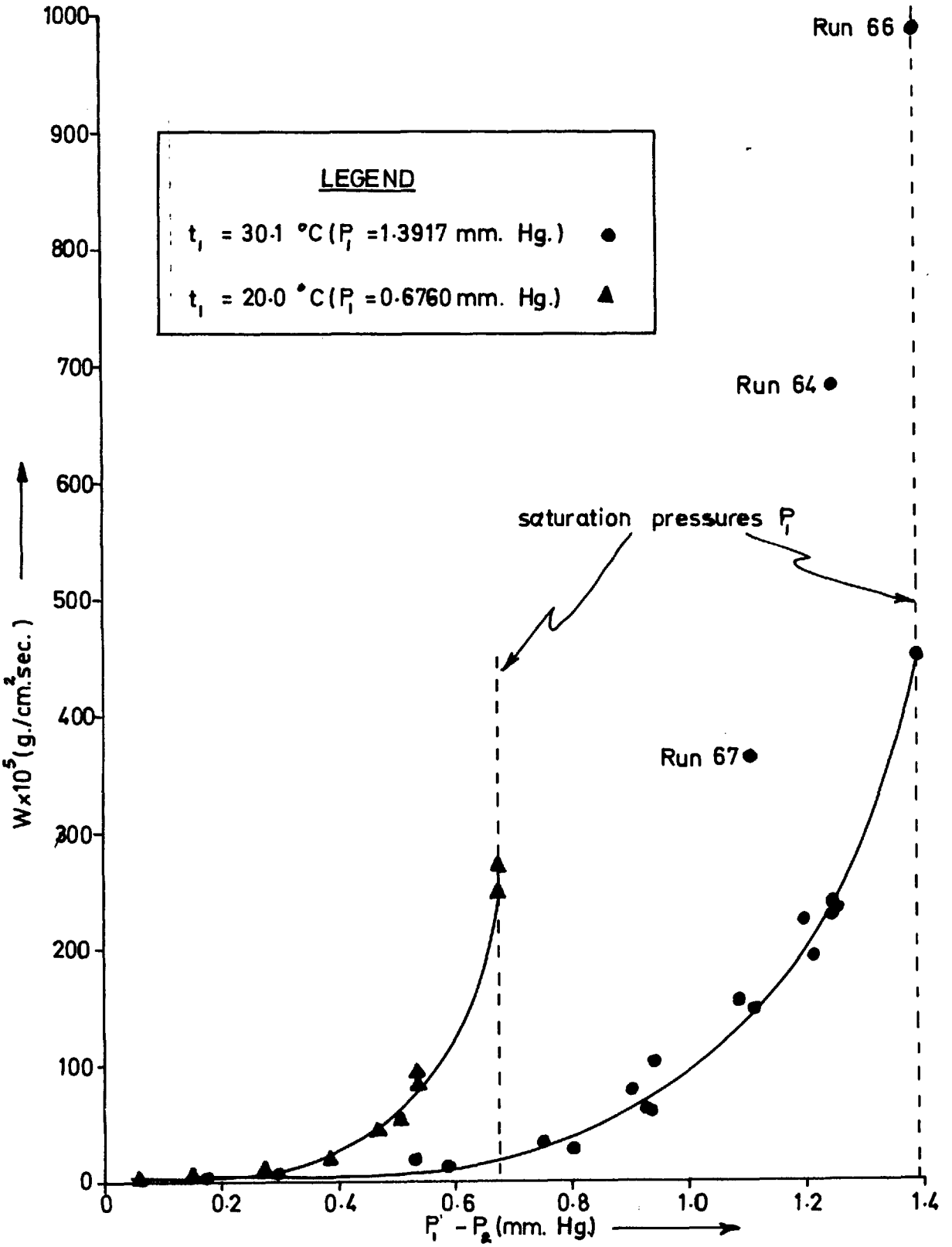

FIG 14 n-BUTYRIC ACID – RELATIONSHIP BETWEEN MASS FLUX AND PRESSURE DRIVING FORCE

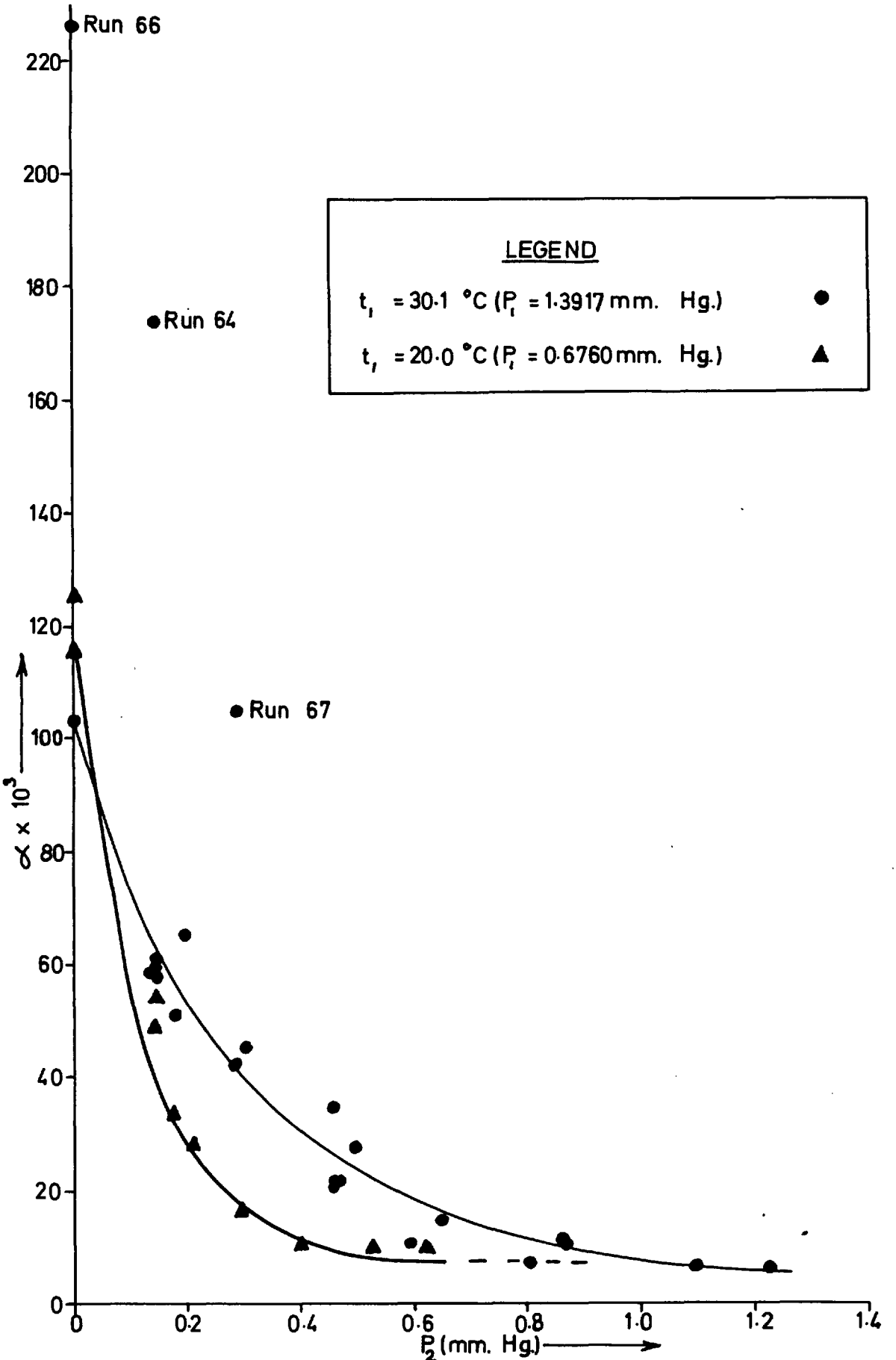

FIG 15 n-BUTYRIC ACID – RELATIONSHIP BETWEEN EVAPORATION COEFFICIENT AND VAPOUR PRESSURE ABOVE SURFACE

imated). The evaporating temperatures used were 30.1°C and 20.0°C respectively. The results obtained are given in Tables 10 and 11, Appendix 6, and for each evaporating temperature the mass flux is shown as a function of pressure driving force in Fig. 14, from which it is again clear that α was not constant over the range of conditions used. In Fig. 15, the values of α are shown as a function of P_2 with t_1 as parameter. It is clear that these results showed the same trend as the results for benzyl alcohol shown in Fig. 13, although the increase of α with decrease of P_2 was more gradual.

The three high values of α marked in Fig. 15 (Runs 64, 66 and 67) were obtained during the first few runs with this material and thereafter could never be reproduced. It can be seen that a considerable number of subsequent runs carried out under approximately the same conditions consistently and reproducibly gave lower values of α, so that the three high values can be disregarded.

The reasonfor the three high values of α obtained was not clear, the only clue being that during the three runs concerned, the liquid was observed to "creep" up the walls of the glass neck apparently under the influence of the relatively high mass flux involved (as if being "blown' up the glass walls by the evaporating material). The normal meniscus was considerably deepened and became almost U-shaped. This situation was an unstable one and the resulting meniscus oscillation made estimation of surface area less reliable than usual. However, it was not considered likely that the estimated area was in error (on the low side) by a factor of 2 or 3 as would be required to explain the high results. A possible explanation of these results is suggested in Section 4.5 as part of the

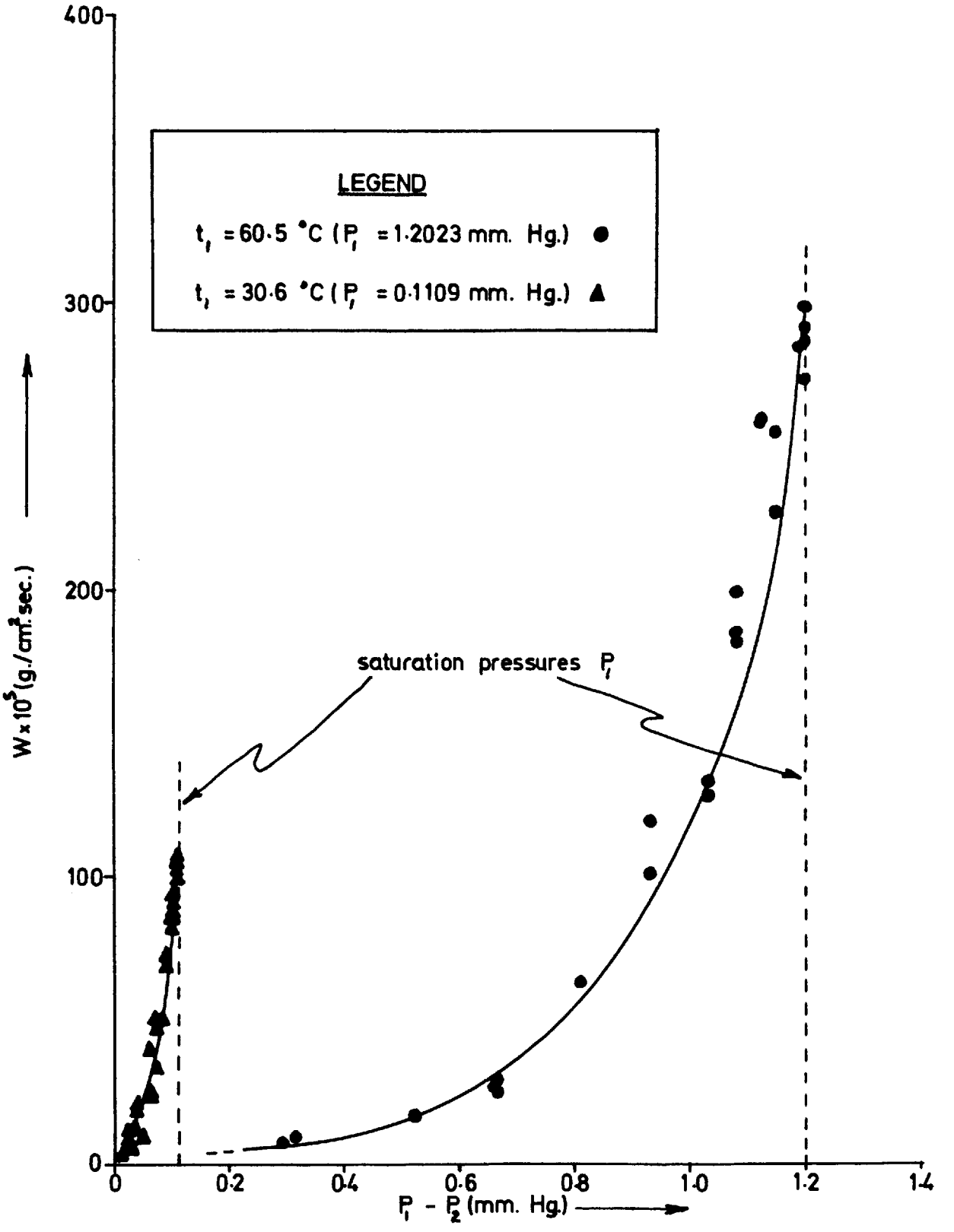

FIG 16 FRACTIONATED BENZYL ALCOHOL—RELATIONSHIP BETWEEN MASS FLUX AND PRESSURE DRIVING FORCE

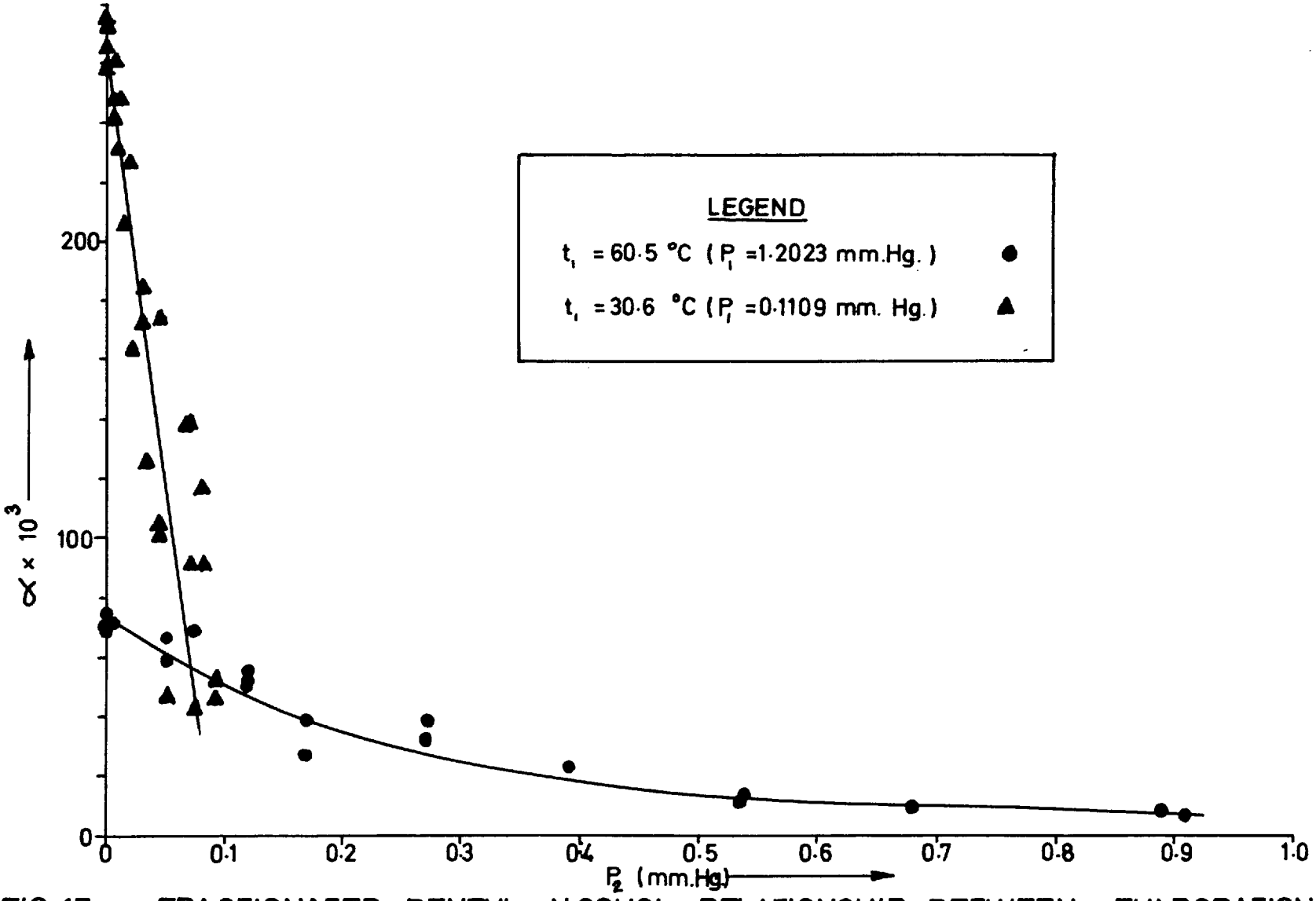

FIG 17 FRACTIONATED BENZYL ALCOHOL—RELATIONSHIP BETWEEN EVAPORATION COEFFICIENT AND VAPOUR PRESSURE ABOVE SURFACE

discussion of the possible existence of surface cooling.

4.4 Fractionated Benzyl Alcohol.

Two series of evaporation runs were carried out using fractionated benzyl alcohol, the evaporating temperatures being 60.5°C and 30.6°C respectively. The results obtained are given in Tables 12 and 13, Appendix 6, and are shown in Fig. 16 where mass flux is shown as a function of pressure driving force for each evaporating temperature. It is clear from Fig. 16 that α was again not constant over the range of conditions used. The values of α obtained are also shown in Fig. 17 as a function of P_2 with t_1 as parameter.

It is clear from a comparison of the results in Fig. 17 with those in Fig. 13 that the values of α obtained for fractionated benzyl alcohol were considerably greater than the corresponding values for the untreated material, indicating that purification of the test material might be a vital factor in this work. However, unlike the fractionated benzyl alcohol, the untreated material could not be outgassed by the improved procedure described in Section 3.7, and this might also be a contributing factor towards the difference obtained between the results for these two materials.

The main feature of the results in Fig. 17 is that α again increased with decrease of P_2 as was observed for both untreated benzyl alcohol and n-butyric acid. However, it is clear that the increase of α as P_2 approached zero was much more rapid when the evaporating temperature was 30.6°C than when it was 60.5°C, such that the respective values of α obtained at "free evaporation" conditions ($P_2 = 0$) were 0.27

and 0.07 approximately. It can be seen from Fig. 14 that the same trend was obtained to a lesser extent in the results for n-butyric acid (the difference between the two evaporating temperatures was considerably smaller than in experiments with fractionated benzyl alcohol). These observations led to the consideration, in Section 4.5, of the possibility of the existence of surface cooling.

4.5 Surface Cooling Considerations.

The main feature of the results presented above is the fact that α was not constant but increased steeply as P_2 approached zero. This is a surprising result and difficult to account for on a rational physical basis. Every effort was therefore made to criticise the experimental procedure to make sure that the effect was not due to some shortcoming of the method which had been overlooked.

One such possibility was indicated by the fact that a higher value of α was obtained at "free evaporation" conditions for the lower evaporating temperature, both for n-butyric acid and fractionated benzyl alcohol (Figs 15 and 17). It was clear that this trend of results was consistent with the existence of surface cooling (since the mass flux at "free evaporation" conditions is higher for the higher evaporating temperature, the surface cooling must also be higher and hence the depression of the true value of α will be greater. Thus, if surface cooling is present, the apparent value of α would be expected to be lower for the higher evaporating temperature). Furthermore, the existence of optical effects at the liquid surface during high flux experiments (as mentioned in Section 4.1) indicated that there was some degree of surface cooling.

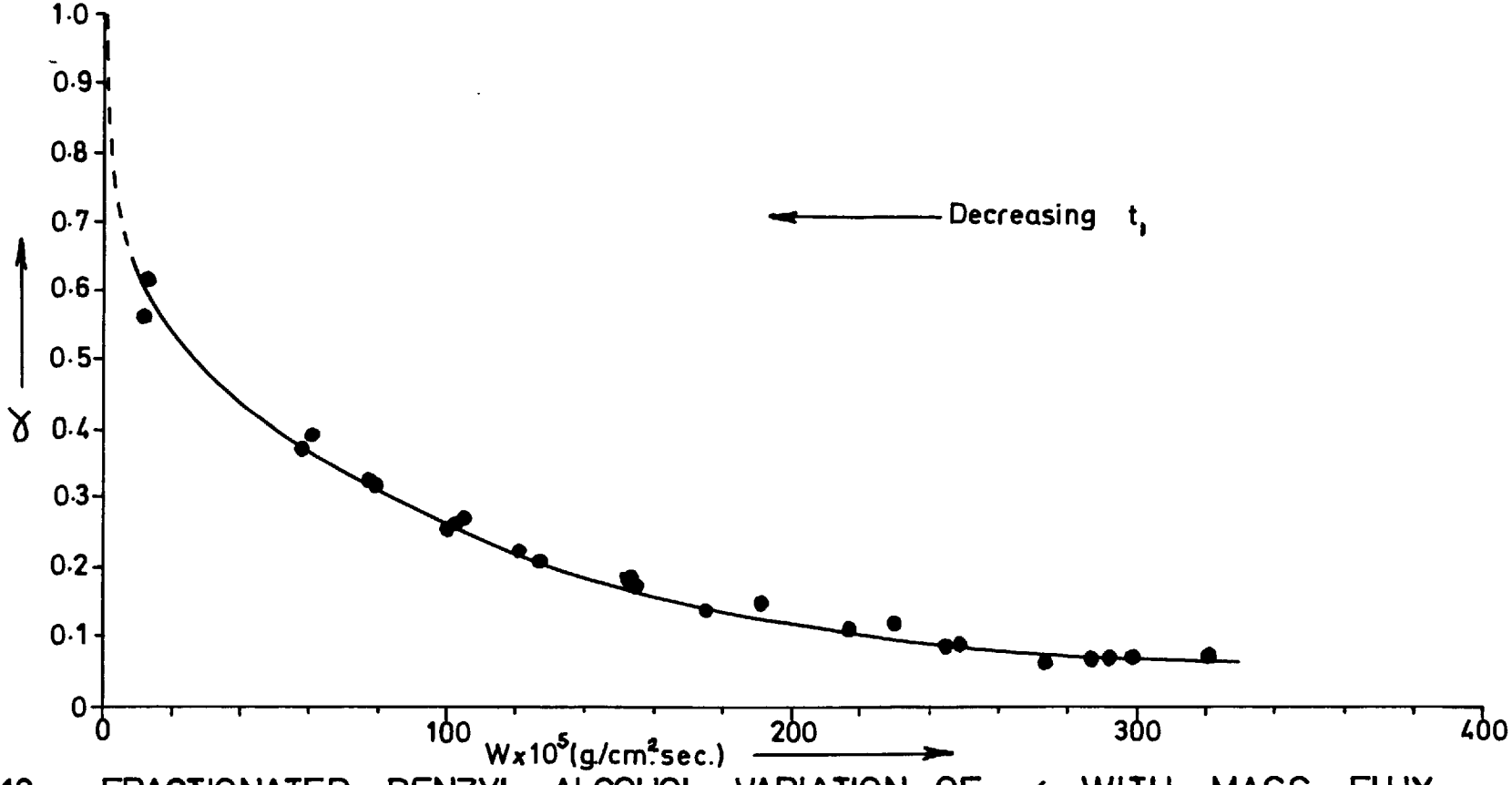

FIG 18 FRACTIONATED BENZYL ALCOHOL – VARIATION OF α WITH MASS FLUX AT "FREE EVAPORATION" CONDITIONS

It is also possible to interpret the anomolously high values of α obtained for n-butyric acid (see Section 4.3) in terms of the existence of surface cooling during normal operation. Under such conditions, the observed meniscus oscillations would provide surface agitation in excess of the normal agitation, thereby giving rise to the observed higher evaporation flux and consequent higher values of α.

In the light of the above evidence, it was considered necessary to investigate the possibility of the existence of surface cooling, despite the evidence described in Section 4.1 verifying the effectiveness of stirring. For this purpose, a series of "free evaporation" runs was carried out with fractionated benzyl alcohol such that the evaporating temperature was fixed at values ranging from 0°C to 60°C. The relationship between the values of α obtained and the corresponding values of mass flux was then considered. The results of these runs are given in Table 14, Appendix 6 and are shown in Fig. 18, where α is plotted as a function of W (the results given in Table 14 include "free evaporation" runs already reported for this material in Section 4.4). It is clear from Fig. 18 that α did increase with decrease of mass flux as would be expected if surface cooling were present.

It is true that the increase of α also corresponded to a decrease in evaporating temperature, but on the basis of results of experiments so far carried out at different evaporating temperatures (Figs 13 and 15), a temperature dependence of α large enough to account for this increase is not likely.

It seemed that the most likely explanation of the results shown in Fig. 18 was that surface cooling was present despite stirring.

If this was the case it remained to explain why the increase of W with stirring rate levelled off in the manner shown in Figs 8 and 9. This matter is discussed in Section 5.1.

4.6 Estimation of Surface Cooling.

In the following pages a description is given of an attempt to make surface cooling corrections for experiments carried out with fractionated benzyl alcohol. In the course of this procedure, a correction factor was also deduced to account for the anticipated systematic error in estimation of surface area of the liquid. These corrections were based on assumptions which have certain logic to support them but they may well be considered invalid. The calculations however are considered worthwhile as explaining the consequences which would result if the assumptions were correct.

As a starting point it was considered not unreasonable to conclude from Fig. 18 that as mass flux approached zero the value of α approached unity. Since zero mass flux corresponds to the absence of surface cooling, the true value of α for fractionated benzyl alcohol at "free evaporation" conditions was assumed to be unity. On the basis of this assumption, it was possible to calculate for each "free evaporation" run the surface cooling that would be required to depress the true value of α (unity) to the value shown in Fig. 18 (see Sample Calculations, Appendix 9).

The surface cooling estimated in this way represented the worst possible case (the true value of α could presumably not be greater than unity) so that the corrections subsequently made on the basis of

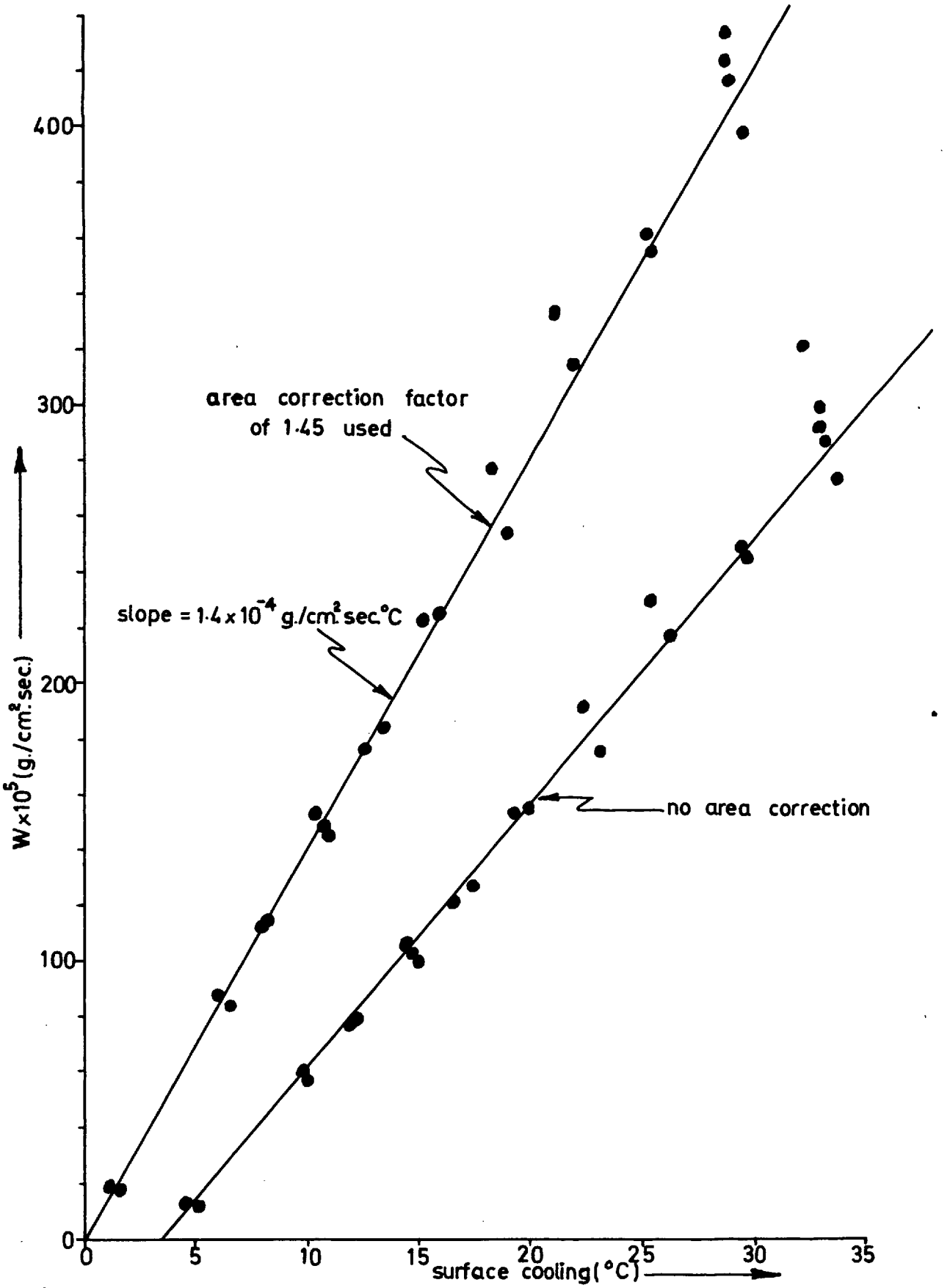

FIG 19 FRACTIONATED BENZYL ALCOHOL—SURFACE COOLING FOR "FREE EVAPORATION" CONDITIONS ASSUMING $\alpha = 1$

this estimation would be as drastic as they could possibly be. Results of the surface cooling calculations are given in Table 15, Appendix 6 and are shown in Fig. 19 from which it can be seen that a good linear relationship existed between the estimated surface cooling and the corresponding mass flux (the data from Table 15 is plotted on the line labelled "no area correction").

It is obvious that surface cooling must be zero when mass flux is zero so that the initially calculated data shown in Fig. 19 (marked "no area correction") should have passed through the origin. However, it was realised that a systematic error in the calculation of the area of the evaporating surface could account for the failure of the data to pass through the origin (because of the consequent errors in both the calculated mass flux and the derived value of α).

A trial-and-error procedure was used to determine an area correction factor which would adjust the surface cooling data to pass through the origin as shown in Fig. 19. The corrected surface cooling data is given in Table 16, Appendix 6. The area correction factor used was as follows:-

$$\frac{\text{Area used in original calculation}}{\text{True area}} = 1.45$$

If this factor were correct, it meant that the original estimation of area differed from the true area by considerably more than had originally been anticipated. Nevertheless it can be seen that the factor could arise because of the assumption that the liquid surface was part of a sphere (including the assumption that the cross-section of the neck was circular) and because of a possible magnification effect due to the thick curved glass walls of the neck of the conical section.

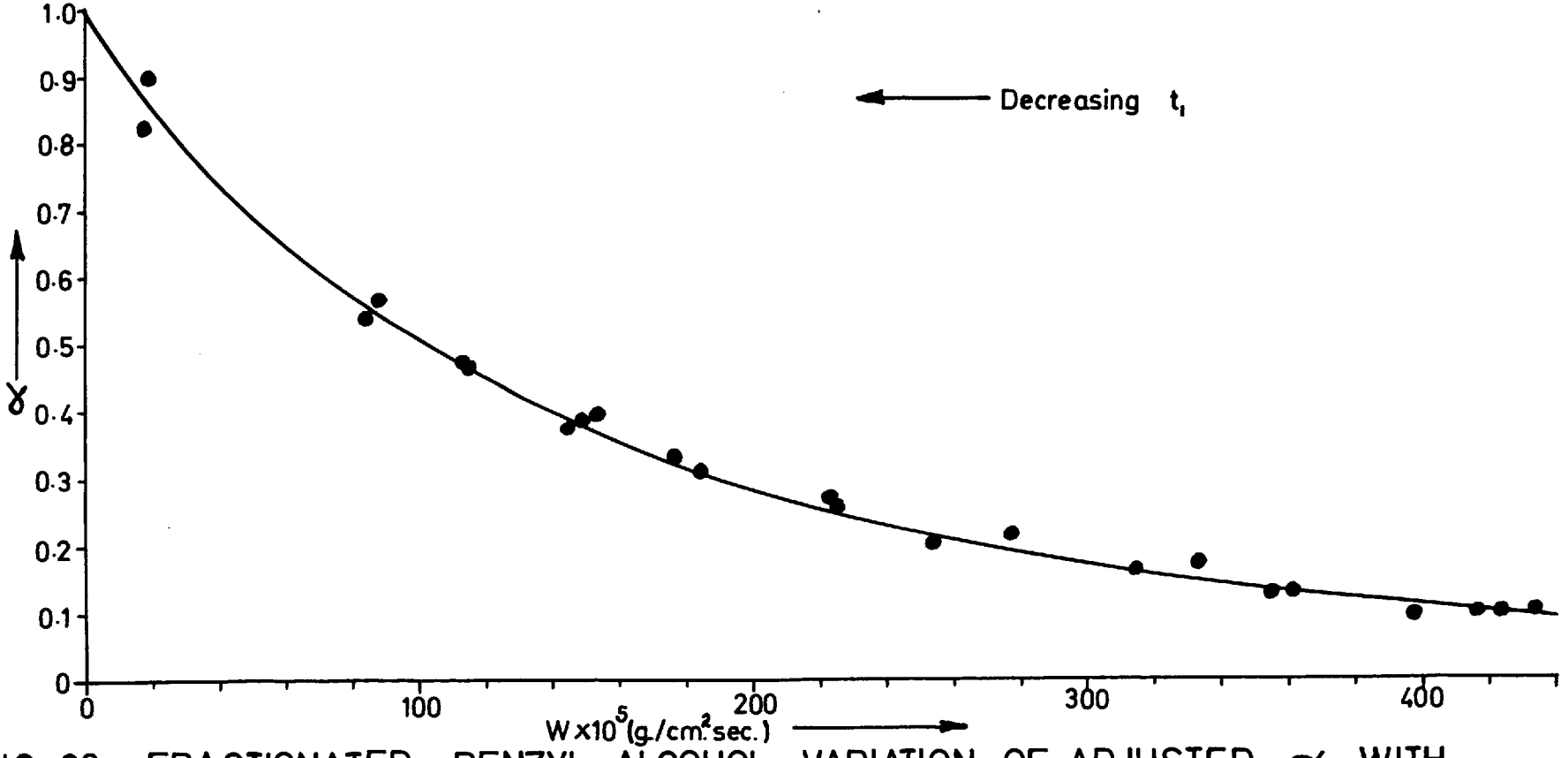

FIG 20 FRACTIONATED BENZYL ALCOHOL—VARIATION OF ADJUSTED α WITH ADJUSTED MASS FLUX AT "FREE EVAPORATION" CONDITIONS

The deduced area correction factor was applied to the corresponding values of W and α for the series of "free evaporation" runs shown in Fig. 18. The adjusted values are given in Table 16, Appendix 6 and the relationship between them is shown in Fig. 20 from which it is clear that after applying the area correction factor, the extrapolation to $\alpha = 1$ for "free evaporation" conditions in the absence of surface cooling(i.e.:- for $W = 0$) was more strongly supported than in the original results shown in Fig. 18.

The area correction factor was now applied to the corresponding values of W and α for the original series of experiments with fractionated benzyl alcohol (Tables 12 and 15, Appendix 6). Using the adjusted values of W, the surface cooling was estimated for each run by assuming the relationship between W and surface cooling to be given by the straight line drawn through the adjusted data in Fig. 19 (i.e.:- it was assumed Surface Cooling ($^{\circ}C$) = 1.4×10^{-4}.W ($g./cm.^2 sec.$)).

In this way, the true surface temperature was estimated so that the corresponding value of P_1 could be used in equation (1.1-6) and an estimate of the true value of α obtained (see Sample Calculations, Appendix 9). Because of the widely differing values of surface cooling involved in the corrections, evaporating temperature could no longer be used as parameter in the graphical representation of the results. However, to maintain the same form as previously used, the results were presented using the temperature of the bulk liquid as parameter (i.e.:- the temperature of the evaporating leg bath).

The corrected results are given in this form in Tables 17 and 18, Appendix 6 and are shown separately for the two bulk temperatures

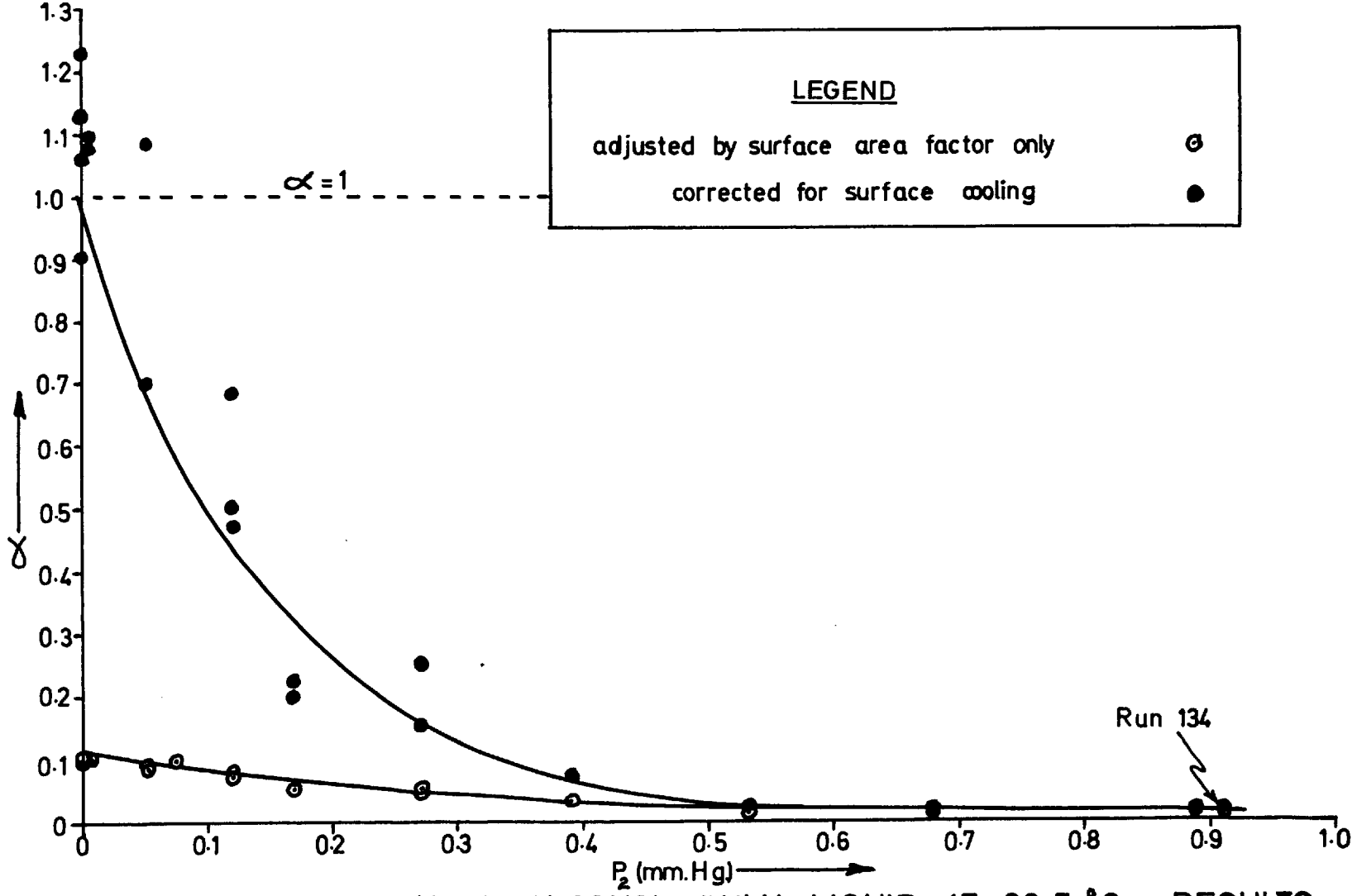

FIG 21 FRACTIONATED BENZYL ALCOHOL, BULK LIQUID AT 60·5 °C — RESULTS CORRECTED FOR SURFACE COOLING

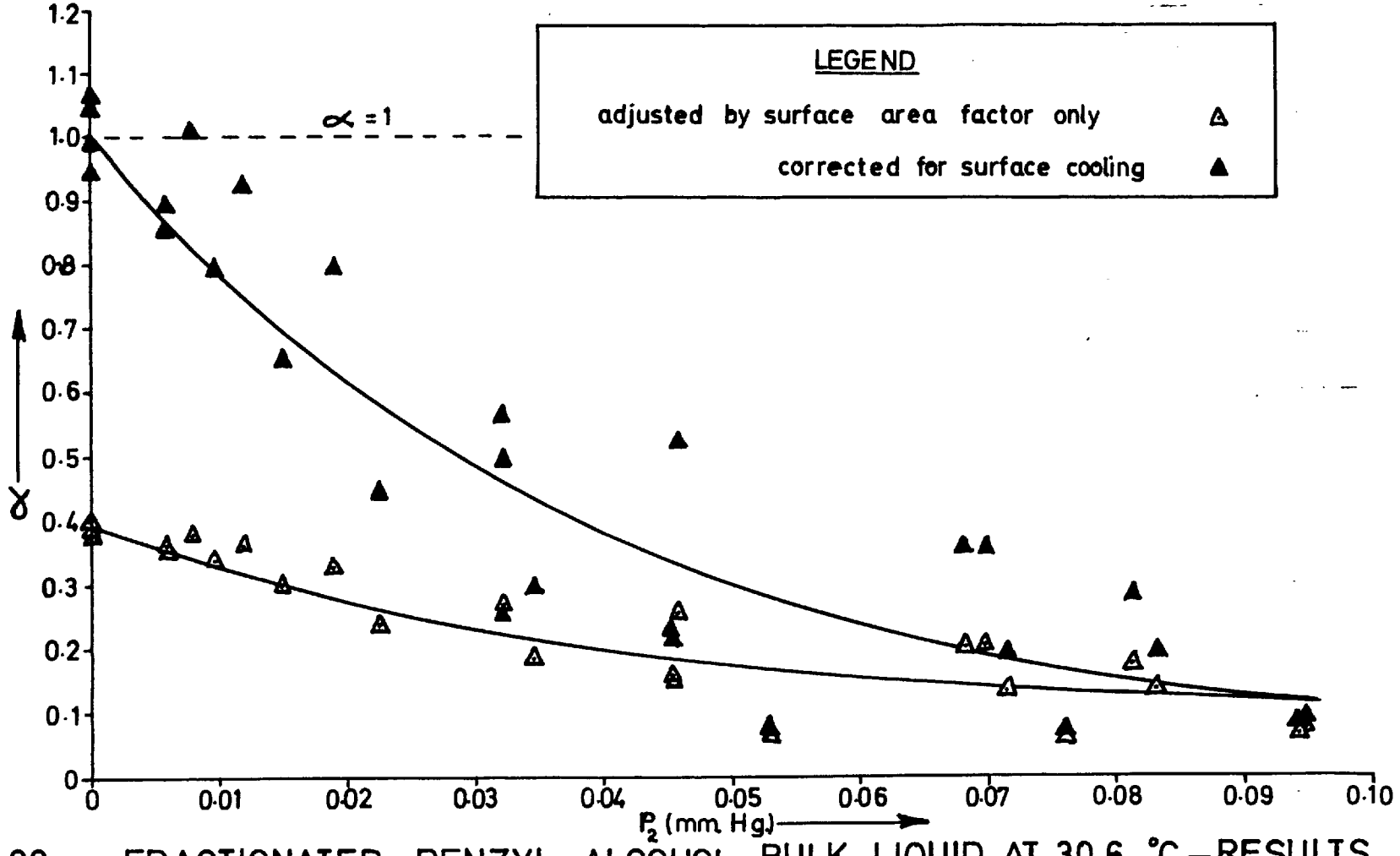

FIG 22 FRACTIONATED BENZYL ALCOHOL, BULK LIQUID AT 30·6 °C – RESULTS CORRECTED FOR SURFACE COOLING

in Figs 21 and 22 respectively, in which values of α corrected only with the surface area factor can be compared with those also corrected for surface cooling (notice that the P_2 scale in Fig. 22 has been considerably expanded compared with the original scale used in Fig. 17). It is clear for the runs with lower mass flux (in the higher P_2 region) that the values of α corrected for surface cooling were increased only slightly compared with the corresponding uncorrected values, whereas for runs with higher mass flux (in the low P_2 region) the increase was quite considerable.

Thus, allowance for the worst possible surface cooling has served only to accentuate the phenomenon observed throughout this work whereby the evaporation coefficient was observed to increase markedly as the vapour pressure above the evaporating surface approached zero.

It is true that the estimation of surface cooling is likely to be in error to some degree and it might be argued that if the true surface temperature were known, the corrected values of α would be found to be constant and equal to unity in this case. However, if we consider for example Run 134 (Table 17, Fig. 21) the surface cooling that would be required to make the corrected value of α unity in this case is about $3.8^{\circ}C$ (see Sample Calculations, Appendix 9). The correction estimated from the data in Fig. 19 was $0.75^{\circ}C$ (corresponding to $W = 10.4 \times 10^{-5}$ g./cm.^{2}sec.) and an error of the order of $3^{\circ}C$ is most unlikely.

Unfortunately, the only way to check the estimated surface cooling would be to devise a satisfactory method of measuring surface temperature directly, and this problem at the present time seems to be insurmountable.

CHAPTER 5

DISCUSSION OF RESULTS.

5.1 The Existence of Surface Cooling Despite Stirring.

The most striking feature of the surface cooling data shown in Fig. 19 was that there was a surprisingly good linear relationship between mass flux (hence heat flux) and the estimated surface cooling. Since the surface cooling gives the driving force for heat transfer from the bulk liquid to the surface, a linear relationship between mass flux (heat flux) and surface cooling indicates that the heat transfer coefficient at the liquid surface was constant over the range of conditions used. This in turn is consistent with a situation where all of the heat transfer resistance at the surface is confined to a layer of liquid of constant thickness through which heat is transferred solely by conduction. Such a model is considered in Appendix 7, where it is calculated from the (corrected) data in Fig. 19 that the thickness of the hypothetical surface layer would be about 0.2mm. in this case.

It was thought that the apparent adequacy of stirring as deduced from the data shown in Figs 8 and 9 (Section 4.1) could be explained in terms of the existence of such a thin layer. Since the stirring arrangement was designed not to "break" the actual liquid surface, it is possible that the stirring maintained a uniform temperature in the liquid only to within a short distance of the surface. The increase of W with stirring rate shown in Figs 8 and 9 would then correspond to the stirring range over which agitation became sufficient to reach fully into the neck of the conical section and up to within a short distance of the liquid surface. It is possible that further increase in stirring would then have

no further effect until a high enough speed was reached to distort and "break" the liquid surface.

5.2 Reliability of Vapour Pressure Data.

Having considered the question of surface cooling in Section 4.6, it seemed clear that the observed rapid increase of α with decrease of vapour pressure above the evaporating surface could not be accounted for in terms of experimental error. It remained only to consider the method of analysis of results.

It was first considered possible that the vapour pressure data used in the calculations might be in error in such a way as to give rise to the pattern of results obtained. In particular, Skylarenko et al.[54] have reported experimental vapour pressure data for n-butyric acid which differs quite markedly from the data used in the present work. Instead of measuring the vapour pressure by means of a mercury manometer of one form or another (this was the basis for the data used here), Skylarenko et al. designed an apparatus using a membrane manometer which, after calibration with a M^{c}Leod gauge, was used either for direct pressure measurement or as a zero instrument. They determined the saturated vapour pressure of n-butyric acid in the range 15^{o}C - 40^{o}C and were able to express their results in the following form:-

$$\log P \text{ (mm. Hg.)} = 13.068 - 3799.36 . \frac{1}{T} \qquad (5.2\text{-}1)$$

The vapour pressureequation used in this work has been given in Section 3.4 as follows:-

$$\log P \text{ (mm. Hg.)} = 9.247 - 2761 . \frac{1}{T} \qquad (5.2\text{-}2)$$

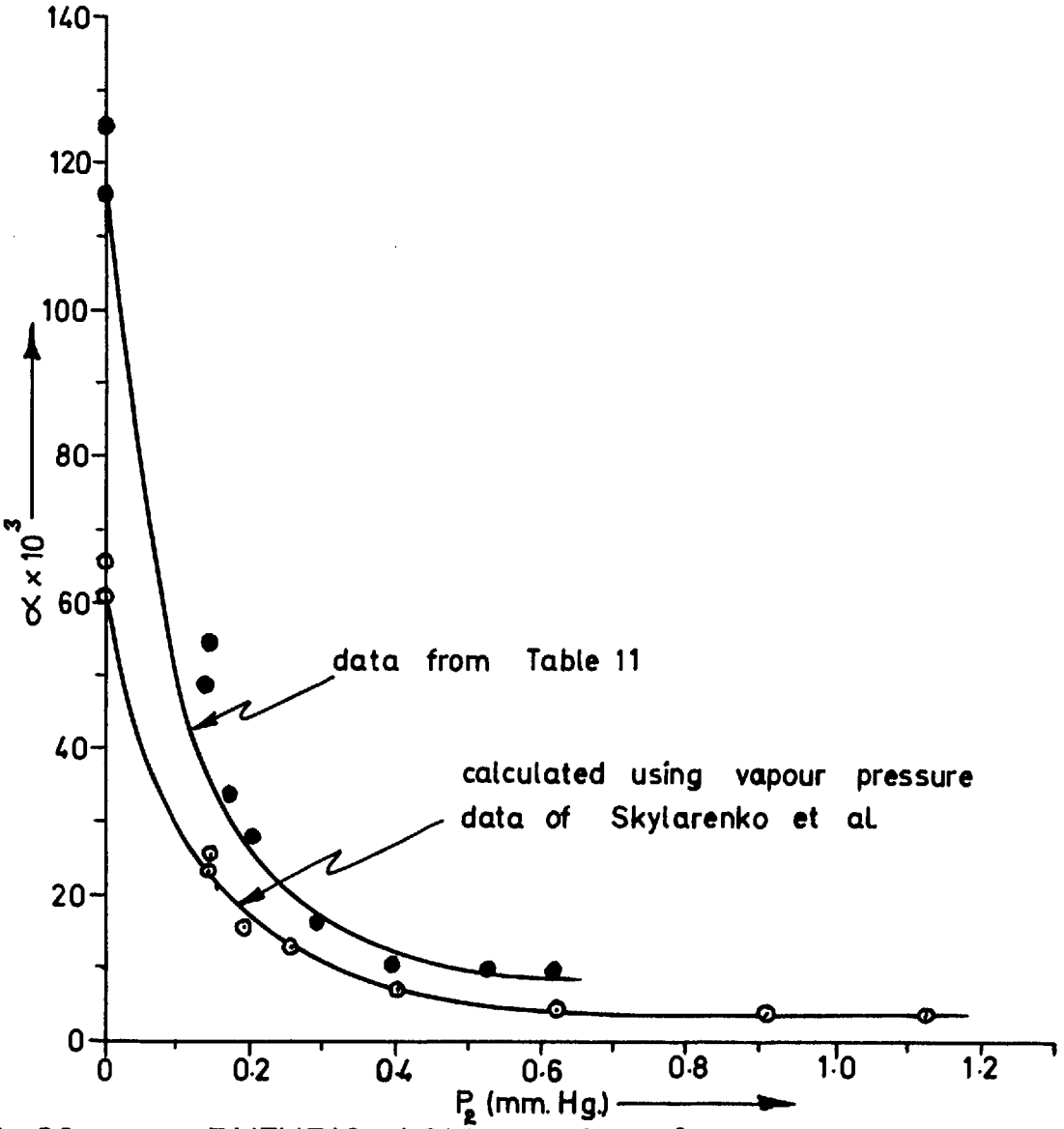

FIG 23 n-BUTYRIC ACID, $t_1 = 20{\cdot}0$ °C – EFFECT OF USING VAPOUR PRESSURE DATA OF SKYLARENKO ET AL.

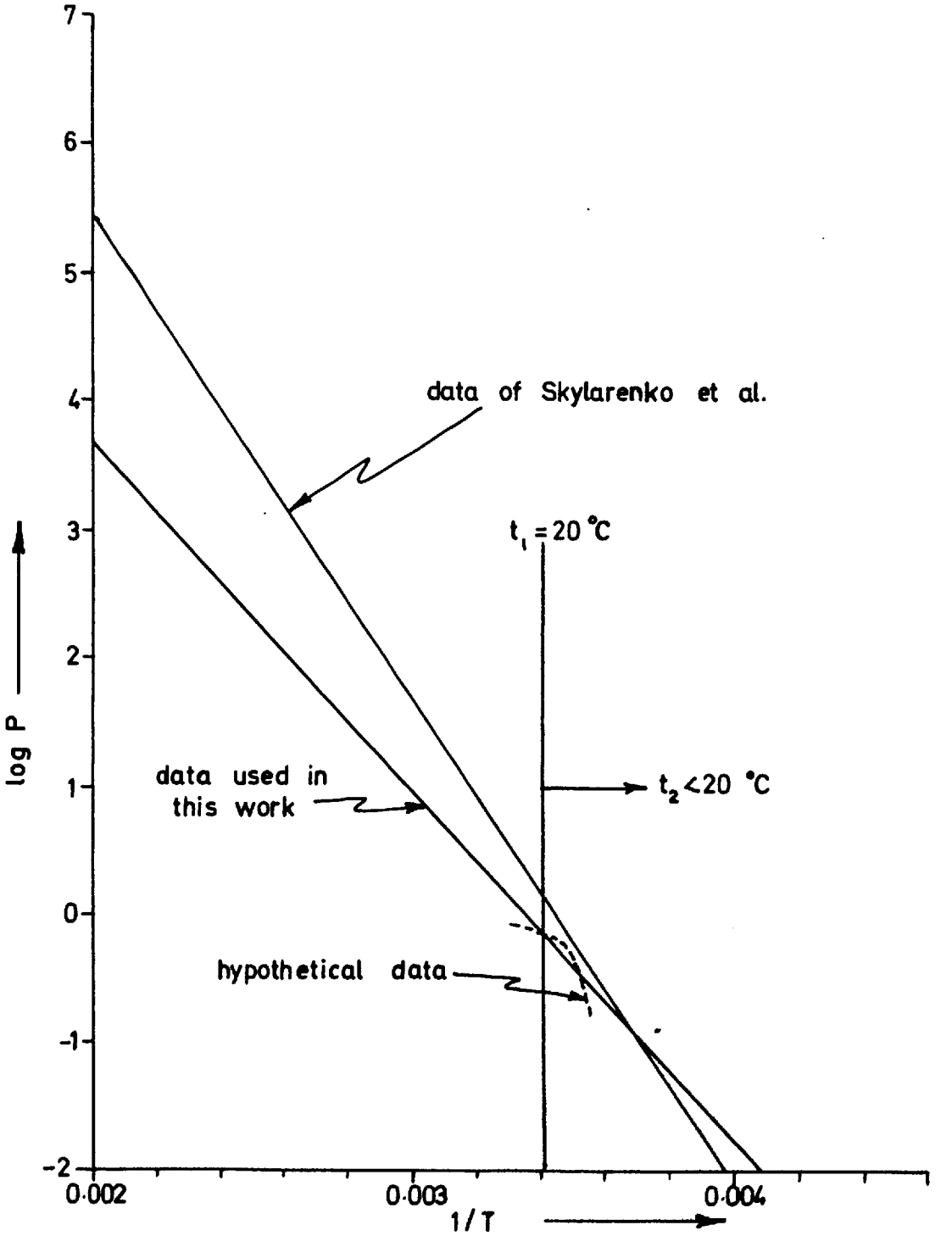

FIG 24 n-BUTYRIC ACID — CONSIDERATION OF VAPOUR PRESSURE DATA

To check the possible effect of the vastly different data of Skylarenko et al. on the results, equation (5.2-1) was used in the recalculation of the results for n-butyric acid evaporating at 20°C (Table 11, Appendix 6). The recalculated data is given in Table 19, Appendix 6 and is shown in Fig. 23, where the original data from Table 11 is also shown for the purpose of comparison. It is clear from Fig. 23 that use of the vapour pressure data of Skylarenko et al. has merely shifted the curve representing the relationship between α and P_2, so that the pattern of results is preserved.

The possibility was now considered that both vapour pressure equations ((5.2-1) and (5.2-2)) might be wrong and that if the true vapour pressure was known and was used in the calculations, α would not be found to vary according to the value of P_2. To give some idea of the nature of the vapour pressure data required to give this result, consider Fig. 24 on which the lines representing equations (5.2-1) and (5.2-2) are drawn. For a given value of t_1 (20°C in this case), the temperature dependence of vapour pressure would have to be lower in the region of t_1 and become higher at temperatures less than t_1. The type of vapour pressure relationship described is shown as a dotted line in Fig. 24. In this situation it would be possible to obtain lower values of pressure driving force for the low flux experiments(t_2 approaching t_1) whilst obtaining disproportionately higher values of pressure driving force for the higher flux experiments (larger $(t_1 - t_2)$). Hence, considering now Fig. 23, the values of α in the high P_2 region would tend to be increased by virtue of the use of the new lower driving force, and similarly the values in the low P_2 region would tend to be decreased because of the new higher

driving force. Presumably a hypothetical vapour pressure / temperature relationship such as the one shown in Fig. 24 could be determined such that the resulting values of α were constant over the whole range of P_2.

However, on the basis of experience it is clear that a curved relationship between log P and 1/T such as shown in Fig. 24 cannot possibly exist over the small range of temperatures concerned in this work. (It can be seen from the Clausius-Clapeyron equation, on which this representation of vapour pressure data is based, that a sharply curved relationship between log P and 1/T would require a corresponding rapid change of the latent heat of vaporisation with temperature. In practice this does not occur.) It was therefore possible to conclude that it would be unrealistic to consider errors in vapour pressure data as a possible explanation of the observed increase of α with decrease of P_2.

5.3 Effect of "Velocity of Approach" Factor.

The assumptions made in the derivation of the kinetic equation were now considered. As pointed out by Schrage[44], (discussed in Section 1.4) the assumption that the evaporating surface and the vapour in contact with it are at the same temperature is not a bad one, provided that all the energy transfer necessary for condensation or evaporation occurs through the liquid rather than through the vapour phase. This was the situation existing in the experiments reported here and hence the assumption $T_1 = T_2$ was reasonably justified.

However, it was thought possible that inclusion of the "velocity of approach" factor introduced by Schrage might make a significant difference to the results. To test this possibility, again the res-

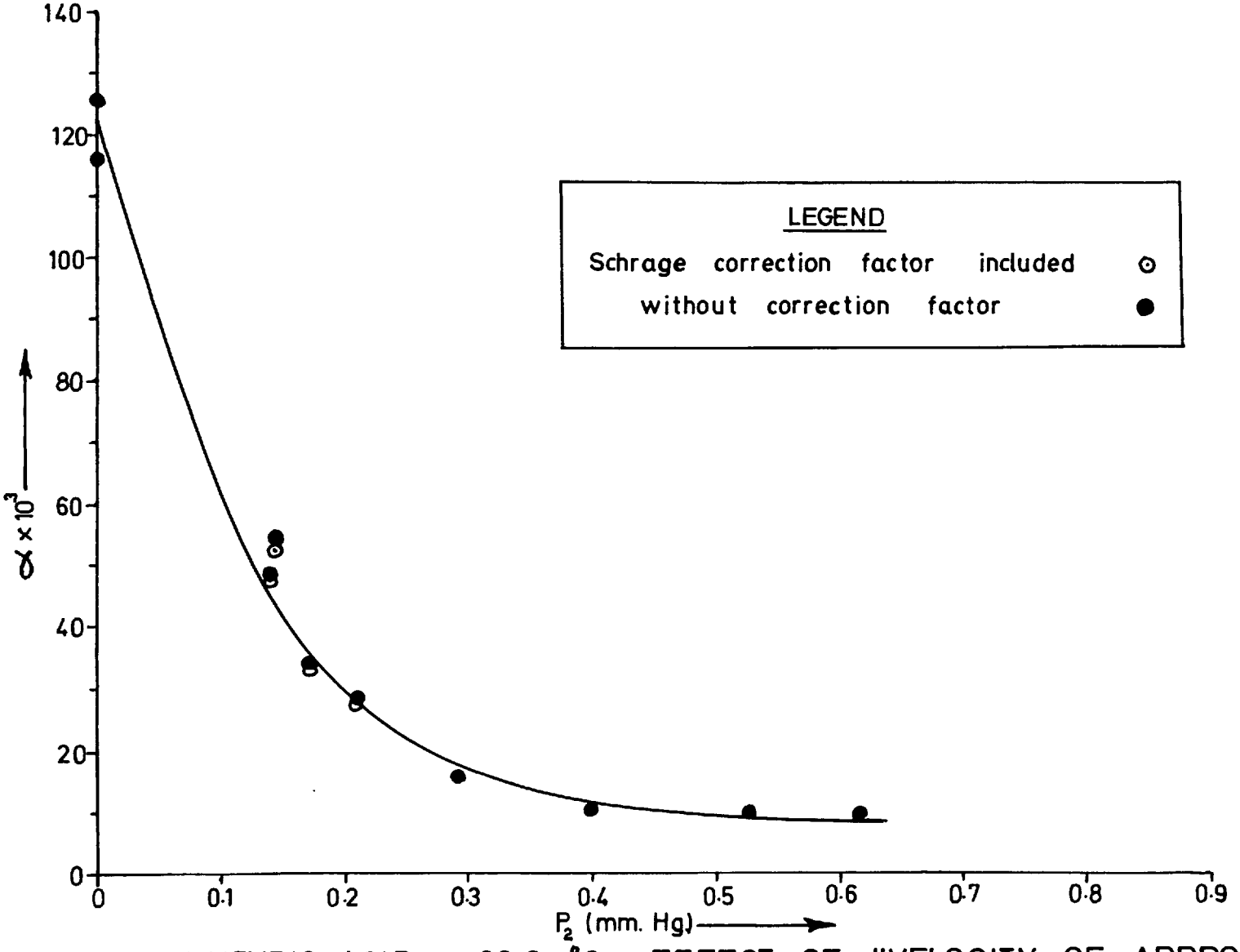

FIG 25 n-BUTYRIC ACID, t_1 = 20·0 °C – EFFECT OF "VELOCITY OF APPROACH" FACTOR

ults for evaporation of n-butyric acid at 20°C (Table 11, Appendix 6) were recalculated with the inclusion of the appropriate values of Γ (see equation (1.4-1)) obtained from the graph of this function presented by Schrage[44](p.35). The results so obtained (see Sample Calculations, Appendix 9) are given in Table 20, Appendix 6 and are shown in Fig. 25 where the original results from Table 11 are also shown for the purpose of comparison. It is clear from Fig. 25 that, for the experimental conditions used here, the two sets of results are almost inseparable. Thus, it can be concluded that the effect of bulk motion in the vapour is not sufficient to explain the increase of α obtained with decrease of vapour pressure above the evaporating surface.

5.4 A Qualitative Interpretation.

It has commonly been assumed that the evaporation coefficient, α, defined in terms of the net mass flux by equation (1.1-6) can be applied separately to the kinetic expressions for gross evaporation rate and gross condensation rate. In other words it has been assumed that a true picture of the physical process involved is obtained when equation (1.1-6) is rewritten in the following form:-

$$W_{net} = \alpha \chi P_1 - \alpha \chi P_2$$

where

$$\chi = (M/2\pi RT_1)^{\frac{1}{2}}$$

As mentioned in Section 1.4, Wilhelm[46] has pointed out that there appear to be no supportingreasons for this assumption. Suppose that the factors applying to the two gross processes are considered separately such that equation (1.1-6) is rewritten as follows:-

$$W_{net} = \alpha_e \chi P_1 - \alpha_c \chi P_2 = \alpha \chi (P_1 - P_2) \qquad (5.4\text{-}1)$$

where α_e = factor applying to gross evaporation rate

α_c = factor applying to gross condensation rate

From equation (5.4-1), α can be expressed as follows:-

$$\alpha = \frac{\alpha_e P_1 - \alpha_c P_2}{P_1 - P_2} \qquad (5.4\text{-}2)$$

At equilibrium it is clear that $\alpha_e = \alpha_c = \alpha$, but if the vapour pressure above the liquid surface is reduced so that evaporation takes place, it is possible that the value of α_e increases because of the lower density of molecules in the vapour at the surface and the consequent lower probability of an evaporating molecule being reflected back into the surface by collision with other molecules.

In addition, because of the net flux of material away from the surface, it is possible that the value of α_c is either reduced or increases more slowly than α_e by virtue of the fact that fewer molecules are able to reach the surface from the vapour than would be the case under zero net flux conditions (this is related to Schrage's "velocity of approach" factor discussed in Section 1.4). It can be seen from equation (5.4-2) that the net result of these two changes would be to tend to increase the value of α at a greater rate than if α_c remained equal to α_e. This would then possibly account for the very rapid increase of α with decrease of P_2 observed at higher flux conditions (in the region of low P_2).

This qualitative picture tends to fit some of the experimental data obtained. Considering the results for fractionated benzyl alcohol corrected for surface cooling (Figs 21 and 22), it can be seen that

for any given value of P_2 in the region where α is increasing, the value of α for the lower bulk temperature (Fig. 22) is lower than the corresponding value for the higher temperature (Fig. 21). (This is the same phenomenon as observed in the initial series of runs with untreated benzyl alcohol (Fig. 13) and in the runs with n-butyric acid (Fig. 15)).

Inspection of Tables 17 and 18, Appendix 6, will show that mass flux was considerably greater for the higher bulk temperature (at a given value of P_2) so that the postulated reduction or depression of α_c could account for the observed difference in values of α for the two bulk temperatures.

At higher values of P_2 (where α was not changing rapidly with P_2) the disparity between values of α obtained for different evaporating temperatures (i.e.:- flux levels) became small and this could be explained in terms of the flux level under these conditions being insufficient to cause any significant reduction or depression of α_c. The value of α expressed by equation (5.4-2) would then be expected to be approximately the same at a given value of P_2 for each evaporating temperature used.

5.5An Alternative Interpretation.

The interpretation described above in Section 5.4 takes into consideration a possible mechanism in the vapour phase whereby the results obtained might be explained. In this section, a possible mechanism of mass transfer from the liquid phase is considered.

Variation of the evaporation coefficient in the way found

in this work (as shown by the non-linearity of the relationship between W and $(P_1 - P_2)$ in Figs 10, 14 and 16) has been reported in the literature[10,12,15] for work on the evaporation of solids. The evaporation of a solid into its vapour is considered to take place via a mobile layer of adsorbed molecules at the solid surface (see Section 1.3). The present day view on the structure of a liquid is that at least short range order of molecules exists at the surface (compared with the long range order in the lattice of a solid) so that some similarity to a solid surface might be expected. It therefore seems quite possible that a mobile layer of adsorbed molecules might exist at a liquid surface.

It is proposed to investigate the consequences of assuming Langmuir adsorption at the liquid surface. At the same time it is assumed that the adsorbed molecules pass into the bulk liquid at a rate proportional to the density of adsorbed molecules at the surface and that molecules pass from the bulk liquid into the adsorbed layer at a rate proportional to the free surface available.

Assume that the fraction of the surface occupied by adsorbed molecules is σ (the fraction of free surface is then $(1 - \sigma)$). The transfer processes at the surface are then governed by the following set of equations:-

Rate of transfer from adsorbed layer to bulk liquid $= k_1 . \sigma$

Rate of transfer from bulk liquid to adsorbed layer $= k_2 . (1 - \sigma)$

Rate of evaporation into gas phase $= k_3 . \sigma$

Rate of condensation from gas phase into adsorbed layer $= k_4 . (1 - \sigma) . P_2$

where k_1, k_2, k_3 and k_4 are rate constants.

For steady-state:-

Rate of transfer into adsorbed layer = Rate of transfer from adsorbed layer

i.e.:- $k_2 \cdot (1 - \sigma) + k_4 \cdot (1 - \sigma) \cdot P_2 = k_1 \cdot \sigma + k_3 \cdot \sigma$

from which

$$\sigma = \frac{k_2 + k_4 \cdot P_2}{k_1 + k_2 + k_3 + k_4 \cdot P_2} \qquad (5.5\text{-}1)$$

Now, net evaporation flux is given by:-

$$W = k_3 \cdot \sigma - k_4 \cdot (1 - \sigma) \cdot P_2$$
$$= k_4 \cdot P_2 + (k_3 + k_4 \cdot P_2) \cdot \sigma$$

Substituting for σ from equation (5.5-1) and simplifying we obtain:-

$$W = \frac{k_2 \cdot k_3 - k_1 \cdot k_4 \cdot P_2}{k_1 + k_2 + k_3 + k_4 \cdot P_2}$$

Now, $W = 0$ when $P_2 = P_1$ (equilibrium)

Hence $$k_2 \cdot k_3 = k_1 \cdot k_4 \cdot P_1$$

so that

$$W = \frac{k_1 \cdot k_4 \cdot (P_1 - P_2)}{k_1 + k_2 + k_3 + k_4 \cdot P_2}$$

Let $$k_1 \cdot k_4 = k_a$$

$$k_1 + k_2 + k_3 = k_b$$

$$k_4 = k_c$$

then

$$W = \frac{k_a \cdot (P_1 - P_2)}{k_b + k_c \cdot P_2} \qquad (5.5\text{-}2)$$

Now, since P_1 is a constant for a given evaporating temperature, we can define a new constant, k_d, such that:-

$$k_b = k_d - k_c \cdot P_1$$

Substituting for k_b in equation (5.5-2) we obtain:-

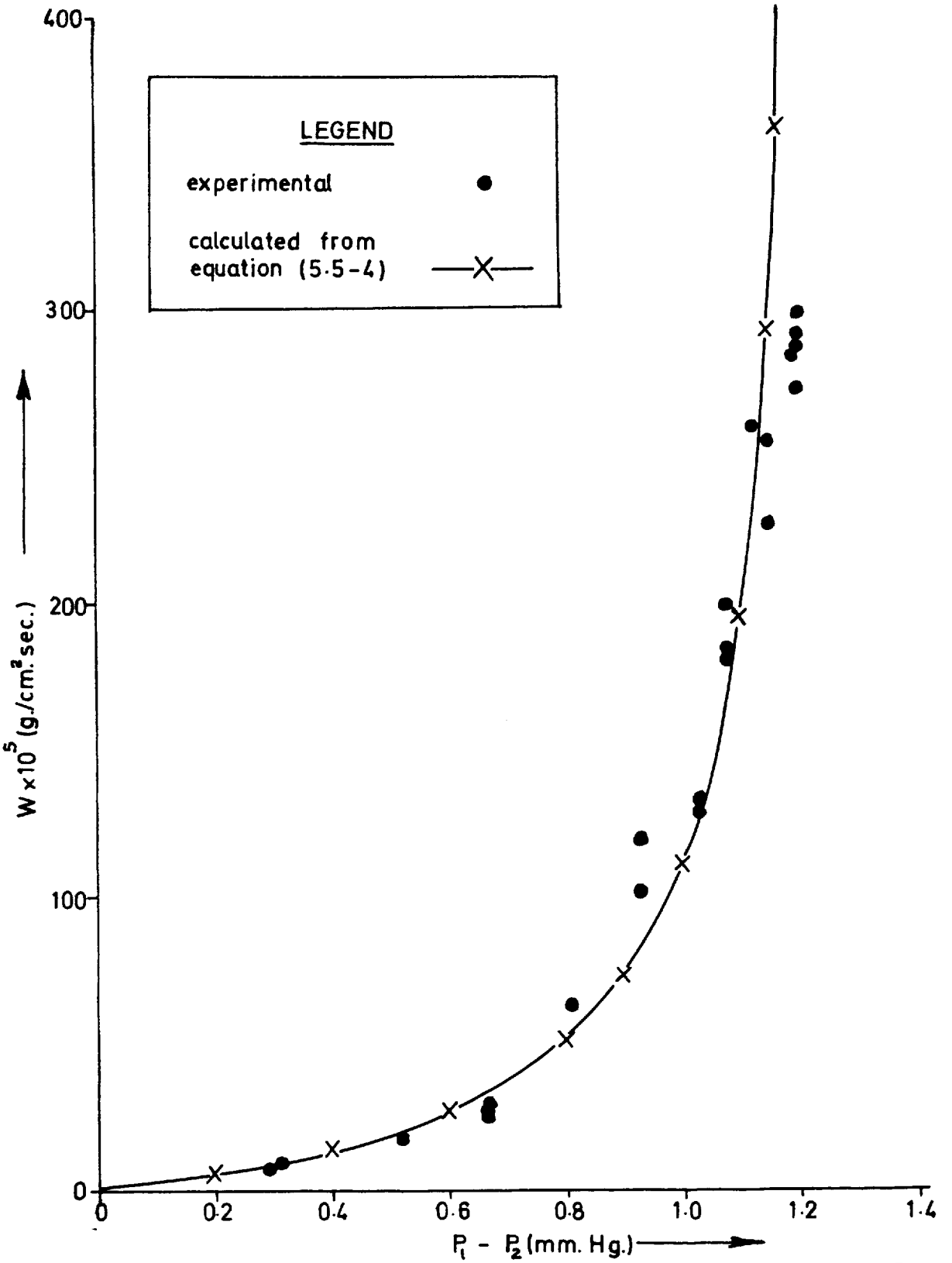

FIG 26 FRACTIONATED BENZYL ALCOHOL, t_1 = 60·5 °C — COMPARISON OF EXPERIMENTAL AND CALCULATED RESULTS

$$W = \frac{k_a \cdot (P_1 - P_2)}{k_d - k_c \cdot (P_1 - P_2)}$$

i.e.:-

$$W = \frac{(k_a/k_d) \cdot (P_1 - P_2)}{1 - (k_c/k_d) \cdot (P_1 - P_2)} \qquad (5.5\text{-}3)$$

It was found that values of the constants (k_a/k_d) and (k_c/k_d) could be chosen such that equation (5.5-3) was a satisfactory representation of the experimentally determined relationship between mass flux and pressure driving force.

This is demonstrated in Fig. 26 where the results for fractionated benzyl alcohol evaporating at 60.5°C (Table 12, Appendix 6) are shown together with the curve representing the following form of equation (5.5-3):-

$$W = \frac{2.32 \times 10^{-4}(P_1 - P_2)}{1 - 0.79(P_1 - P_2)} \qquad (5.5\text{-}4)$$

i.e.:- where $(k_a/k_d) = 2.32 \times 10^{-4}$

and $(k_c/k_d) = 0.79$

It is clear that if surface cooling were not present, the experimental results shown in Fig. 26 would form an even steeper curve, but it is equally clear that suitable values of the constants in equation (5.5-3) could be found to fit such data. However, a different set of constants would be required for each evaporating temperature used, and interpretation of this in terms of the individual rate constants concerned is not clear. Despite this, the mechanism outlined above is of interest since it does predict the nature of the relationship obtained between experimental values of mass flux and pressure driving force.

5.6 Conclusions.

(1) For the liquids investigated, the evaporation coefficient (as defined by equation (1.1-6)) appears to be dependent on the undersaturation in the vapour above the evaporating surface. This dependence is such that the evaporation coefficient increases with decrease of vapour pressure above the surface and, in particular, the increase becomes very rapid as the vapour pressure approaches zero (i.e.:- as "free evaporation" conditions are approached). It is believed that this is the first time that this phenomenon has been noted for liquids.

As mentioned in Section 1.2, similar behaviour has been reported in the literature[15,10,12] for work on the evaporation of solids. Also, in the work of Alty and Mackay[19] on the evaporation of water, it is true that the lower values of α obtained corresponded to experiments carried out with the higher vapour pressures above the evaporating surface, although the authors make no mention of this.

(2) Assuming that the above phenomenon is true of all liquids (or solids) it is clear that experimentally determined evaporation coefficients reported in the literature cannot be compared without due regard for the conditions under which the experiments were carried out.

It is also clear that the analysis of unsteady-state evaporation experiments by integration (as used by Johnstone[47], Bogdandy et al.[24] and Heideger and Boudart[35]) becomes invalid since α can no longer be regarded as a constant.

(3) The explanation of the nature of the increase of α with

decrease of vapour pressure above the surface might involve abandoning the use of the commonly made assumption that α (as defined in terms of the net mass flux in equation (1.1-6)) can be applied separately to the kinetic expressions for gross evaporation rate and gross condensation rate. (Wilhelm[46] has pointed out that there appear to be no supporting reasons for this assumption.)

This would mean that separate factors (α_e and α_c in equation (5.4-1)) would have to be assigned to the two gross processes.

(4) There was evidence that elimination of surface cooling at an evaporating liquid surface cannot be achieved by stirring the bulk liquid if the stirring is such that it does not "break" or distort the surface. In the present work it seemed possible that a high temperature gradient existed over a small distance at the surface (estimated to be about 0.2 mm.) despite stirring. This coincides with the findings of Prüger[21] for unstirred boiling liquids (see Section 1.2).

The problem of finding a satisfactory method of measuring surface temperature under these conditions remains unsolved. In view of this, some of the results of other workers in this field must be even less reliable than they might otherwise appear to be.

(5) For benzyl alcohol and n-butyric acid, it seems possible that the evaporation coefficient is unity under "free evaporation" conditions.

APPENDIX 1

THE SIGNIFICANCE OF THE CONDENSATION COEFFICIENT IN ENGINEERING.

Silver and Simpson[37] eliminated the velocity of approach factor, Γ, from equation (1.4-1) by use of an approximation given by Schrage[44] ($\Gamma = 1 - 1.85\,\phi$, $0.1 \geqslant \phi \geqslant 0.001$) and obtained an expression for net mass flux in the following form:-

$$m = \frac{1}{\frac{1}{\alpha} - 0.523} \cdot (M/2\pi R)^{\frac{1}{2}} \cdot \left[\frac{P^*_{ls}}{T_{ls}^{\frac{1}{2}}} - \frac{P_{vs}}{T_{vs}^{\frac{1}{2}}} \right] \qquad \text{(A1-1)}$$

where m = net mass flux from the surface

P^*_{ls}, T_{ls} relate to the liquid surface

P_{vs}, T_{vs} relate to the vapour at the interface

In connection with their study of the condensation of steam they defined an "interfacial" heat transfer coefficient, h_i, as follows:-

$$h_i = \frac{m.l}{T_{ls} - T_{vs}} \qquad \text{(A1-2)}$$

where l = latent heat (per unit mass) of condensing steam

By assuming $T_{ls} = T_{vs}$ in equation (A1-1), and then substituting for m in equation (A1-2), the following expression was obtained:-

$$h_i = \frac{1}{\frac{1}{\alpha} - 0.523} \cdot (M/2\pi RT_{vs})^{\frac{1}{2}} \cdot \left[\frac{P^*_{ls} - P_{vs}}{T_{ls} - T_{vs}} \right] \qquad \text{(A1-3)}$$

Using the Clapeyron equation to estimate small differences in vapour pressure, $P^*_{ls} - P_{vs}$, the final equation for h_i was obtained as follows:-

$$h_i = \frac{1}{\frac{1}{\alpha} - 0.523} \cdot (M/2\pi RT_{vs})^{\frac{1}{2}} \cdot \left[\frac{Ml^2 P_{vs}}{RT_{vs}^2} \right]$$

This expression was used by Silver and Simpson to calculate the interfacial heat transfer coefficient for saturated steam at various pressure levels (α was taken to be 0.036 as reported by Alty and Mackay[19]). The calculations showed that h_i increased markedly with increase in pressure e.g.:- at atmospheric pressure (14.7 p.s.i.) the value of h_i was calculated to be 49,000 B.T.U./ft.^{2}hr.$^\circ$F whereas at a pressure of 0.5 p.s.i. the value was 3,200 B.T.U./ft.^{2}hr.$^\circ$F. (If a value of α higher than 0.036 were assumed, the corresponding calculated values of h_i would be higher.)

In practice, the overall heat transfer coefficient in steam condensers is of the order of 1,000 B.T.U./ft.^{2}hr.$^\circ$F so that for condensation at near vacuum conditions, the calculated value of h_i given above is comparable with th e heat transfer coefficients through the other resistances (condensate film, condenser tube, water side). Since h_i is dependent on the condensation coefficient, it is under conditions of condensation at low pressures that α becomes important from an engineering point of view.

It has been mentioned in Section 1.2 that Nabavian and Bromley[36] have used the principle outlined above to determine the condensation coefficient for water.

APPENDIX 2

SOME CALCULATIONS USING JOHNSTONE'S DATA

Table 1. Johnstone's Run 8 - Coefficients for Surface Temperature Half-Power Series.

5 term series	4 term series
$b_2 = +\ 0.507$	$b_2 = +1.614$
$b_3 = +\ 11.38$	$b_3 = -3.883$
$b_4 = +\ 73.72$	$b_4 = +1.517$
$b_5 = +161.2$	$b_5 = +3.227$
$b_6 = -120.0$	

Table 2. Surface Temperature as a Function of Time.

θ	Calculated T_1' (°C)		Measuredfrom Fringe Shift	
(sec.)	5 term series	4 term series	θ (sec.)	T_1' (°C)
0.000	0.0000	0.0000	0.000	0.000
0.010	0.0106	0.0124	0.032	0.037
0.040	0.0373	0.0370	0.064	0.050
0.090	0.0600	0.0605	0.096	0.062
0.123	0.0698	-	0.128	0.072
0.160	-	0.0816	0.160	0.081
0.203	0.0948	0.0948	0.193	0.094
0.250	0.1043	0.1137	0.225	0.101
			0.257	0.112

Table 3. Temperature Gradient at the Surface as a Function of Time.

θ	Calculated $\left\lvert \frac{\partial T}{\partial x} \right\rvert_s$ (°C/cm.)	
(sec.)	5 term series	4 term series
0.010	- 3.16	-3.50
0.040	- 4.62	-4.86
0.090	- 2.74	-4.92
0.160	+ 1.76	-4.86
0.205	+ 6.88	-5.24
0.250	+12.82	-6.18

APPENDIX 5

ESTIMATION OF PRESSURE DROP IN APPARATUS.

Case 1. High Vapour Pressure Material.

Consider the case of water evaporating at a temperature corresponding to 20 mm. Hg. vapour pressure (i.e.:- room temperature) and a condenser temperature corresponding to 19 mm. Hg. vapour pressure.

The pressure in the vapour space is assumed to be uniform and equal to 19 mm. Hg. so that the pressure driving force, $(P_1 - P_2)$, is 1 mm. Hg..

If the pressure driving force is expressed in terms of mm. Hg. and the mass flux is in terms of g./cm.^{2}sec., it can be shown that equation (1.1-6) becomes:-

$$W = 5.83 \times 10^{-2} \alpha (M/T)^{\frac{1}{2}}.(P_1 - P_2) \qquad (A5\text{-}1)$$

At room temperature, $(M/T)^{\frac{1}{2}}$ for water is about 0.248 so that if the value of α is assumed to be unity for the purpose of this calculation, the mass flux is given by:-

$$W = 5.83 \times 10^{-2} \times 0.248 \times 1$$
$$= 1.445 \times 10^{-2} \text{ g./cm.}^2\text{sec.}$$

If the evaporating surface is assumed to have an area of 1 cm.^{2}, the total mass flowrate is 1.445×10^{-2} g./sec..

The density of the vapour is given by $\rho = \frac{MP}{RT}$.

where $R = 82.06$ cm.^{3}atm./g. mole $^\circ$K

$T = 298^\circ$K approx.

$P = 19/760 = 2.5 \times 10^{-2}$atm.

$M = 18$

Hence $\rho = \frac{18 \times 2.5 \times 10^{-2}}{82.06 \times 298}$ g./cc.

$$= 1.84 \times 10^{-5} \text{ g./cc.}$$

and the volumetric flowrate is given by:-

$$\frac{1.445 \times 10^{-2}}{1.84 \times 10^{-5}} = 7.86 \times 10^{2} \text{ cc./sec.}$$

Cross-sectional area of 8 cm. diam. tubing is given by:-

$$\frac{\pi (8)^2}{4} = 50.3 \text{ cm.}^2$$

Hence, velocity of vapour in tubing is given by:-

$$\frac{7.86 \times 10^{2}}{50.3} = 15.6 \text{ cm./sec.}$$

In the absence of exact data, take the viscosity of water vapour to be 0.008 centipoise (Perry[49], p.371).

i.e.:- $\mu = 8 \times 10^{-5}$ poise

Reynolds' No. $= \frac{vD\rho}{\mu}$

$$= \frac{15.6 \times 8 \times 1.84 \times 10^{-5}}{8 \times 10^{-5}}$$

$$= 29$$

The flow is well inside the laminar region so that the Poiseuille equation can be used to calculate pressure drop:-

$$\Delta P = \frac{V.128 \mu l}{\pi D^4}$$

where V = volumetric flowrate (cc./sec.)

l = length of tubing (estimated in this case to be 60 cm.)

Hence, $\Delta P = \frac{7.86 \times 10^{2} \times 128 \times 8 \times 10^{-5} \times 60}{(8)^4}$

$$= 3.76 \times 10^{-2} \text{ dynes/cm.}^2$$

Since 1 mm. Hg. = 1,331 dynes/cm.^{2}, it can be seen that

the pressure drop in the system is negligible compared with the pressure driving force.

Case 2. Low Vapour Pressure Material - Knudsen Flow Applicable.

Consider glycerol evaporating at a temperature corresponding to 2 microns vapour pressure (estimated from the data of Trevoy[33] to be 48°C) and a condensing temperature corresponding to 1 micron vapour pressure.

The vapour pressure is assumed to be equal to 1 micron throughout the vapour space so that the pressure driving force is 1 micron. Assuming α to be unity we obtain from equation (A3-1):-

$$W = 5.83 \times 10^{-2} \times (92/321)^{\frac{1}{2}} \times 10^{-3}$$

$$= 3.12 \times 10^{-5} \text{ g./cm.}^2\text{sec.}$$

Again assuming the evaporating area to be 1 cm.^{2}, the total mass flowrate is 3.12×10^{-5} g./sec..

A form of the Knudsen flow equation is given in terms of mass flowrate by Newman and Searle[50](p.263) as follows:-

$$Q = \frac{\pi r^3 b}{1.41} \cdot (2\pi M/RT)^{\frac{1}{2}} \cdot \Delta P \qquad \text{(A3-2)}$$

A value of b derived by Knudsen is given by Newman and Searle as $2.88/\pi$. If this value is substituted in equation (A3-2) the following approximate equation is obtained:-

$$Q = \frac{2 r^3}{1} \cdot (2\pi M/RT)^{\frac{1}{2}} \cdot \Delta P$$

Substituting $D/2 = r$,

$$Q(\text{g./sec.}) = \frac{D^3}{41} \cdot (2\pi M/RT)^{\frac{1}{2}} \cdot \Delta P \text{ (dynes/cm.}^2\text{)}$$

so that, $$\Delta P = \frac{41Q}{D^3} \cdot (RT/2\pi M)^{\frac{1}{2}}$$

$$= \frac{4 \times 60 \times 3.12 \times 10^{-5}}{(8)^3} \cdot \left[\frac{8.315 \times 10^{-3} \times 321}{2\pi \times 92}\right]^{\frac{1}{2}}$$

$$= 9.87 \times 10^{-2} \text{ dynes/cm.}^2$$

1 mm. Hg. = 1,331 dynes/cm.^{2}

hence, $$P = \frac{9.87 \times 10^{-2}}{1,331} \text{ mm. Hg.}$$

$$= 7.4 \times 10^{-5} \text{ mm. Hg.}$$

$$= 7.4 \times 10^{-2} \text{ microns}$$

i.e.:- Pressure drop / Pressure driving force

$$= 7.4\%$$

The pressure drop appears to be a more serious problem for low pressure, low driving force experiments but even so it is not prohibitive.

Since it was anticipated that conditions more closely approaching those in Case 1 would be used, the 8 cm. bore glass tubing was considered to be satisfactory.

APPENDIX 4

EFFECT OF VAPOUR HEATING ON PRESSURE DRIVING FORCE.

Consider equation (1.1-1). Assuming unit evaporation or condensation coefficient, the mass flux evaporating from the condensing surface at temperature T_2 is given by:-

$$W_e = (M/2\pi RT_2)^{\frac{1}{2}}.P_2$$

If, as explained in Section 3.1, the pressure in the vapour space is P' and the temperature is T', then the mass flux condensing at the condensing surface is given by:-

$$W_c = (M/2\pi RT')^{\frac{1}{2}}. P'$$

The net rate of condensation is then given by:-

$$W_c - W_e = (M/2\pi RT')^{\frac{1}{2}}. P' - (M/2\pi RT_2)^{\frac{1}{2}}. P_2$$

If, as put forward in Section 3.1, the ratio of evaporating and condensing areas is such that the net condensing flux is comparatively small, then as an approximation we assume $W_c = W_e$ (i.e.:- equilibrium at the condensing surface).

Hence we assume,

$$(M/2\pi RT')^{\frac{1}{2}}.P' = (M/2\pi RT_2)^{\frac{1}{2}}. P_2$$

and therefore, $\frac{P'}{P_2} = (T'/T_2)^{\frac{1}{2}}$

It is clear that the additional assumption made in Section 3.1 was that $T' = T_2$, making $P' = P_2$. This assumption might possibly be justified in the case where condensation coefficient was less than unity, since after several collisions with the condensing surface the vapour molecules could be assumed to have attained the temperature of the surface.

If this were not the case, and because of the heating mantle the temperature of the vapour was higher than that of the condensing surface, the actual pressure driving force would be lower than the value, $(P_1 - P_2)$, used in the calculations. Hence values of evaporation coefficient lower than the true value would be obtained.

However, from a practical point of view, the factor $(T'/T_2)^{\frac{1}{2}}$ could never be a great deal more than unity under the experimental conditions used here. Hence, any error from this source incurred in assuming $P' = P_2$ would be small and would become significant only in experiments carried out near equilibrium conditions. This is so because under conditions of small $(P_1 - P_2)$, a small error in P_2 might become significant compared with $(P_1 - P_2)$.

During the course of the experimental runs, a test of this possibility was carried out. For Runs 157 and 158 (Table 13, Appendix 6) the evaporation was carried out under conditions such that the pressure driving force was 0.017 mm. Hg. approx. whilst the pressure corresponding to condensing temperature was 0.094 mm. Hg. approx.. Run 157 was carried out with the input to the heating mantle set at 110 volts (warm to the touch - sufficient to prevent condensation on the glassware) whereas Run 158 was carried out with the heating mantle input at its 240 volt maximum (glassware much too hot to touch). The values of evaporation coefficient obtained from these runs were 4.68×10^{-2} and 5.28×10^{-2} respectively. The trend obtained was in fact opposite to the one expected from the above argument but in any case this variation could not be considered significant since it was within the limits of reproducibility normally obtainable for consecutive runs under identical conditions.

It could be concluded that overheating of the glassware by the heating mantle had no significant effect on the values of evaporation coefficient obtained.

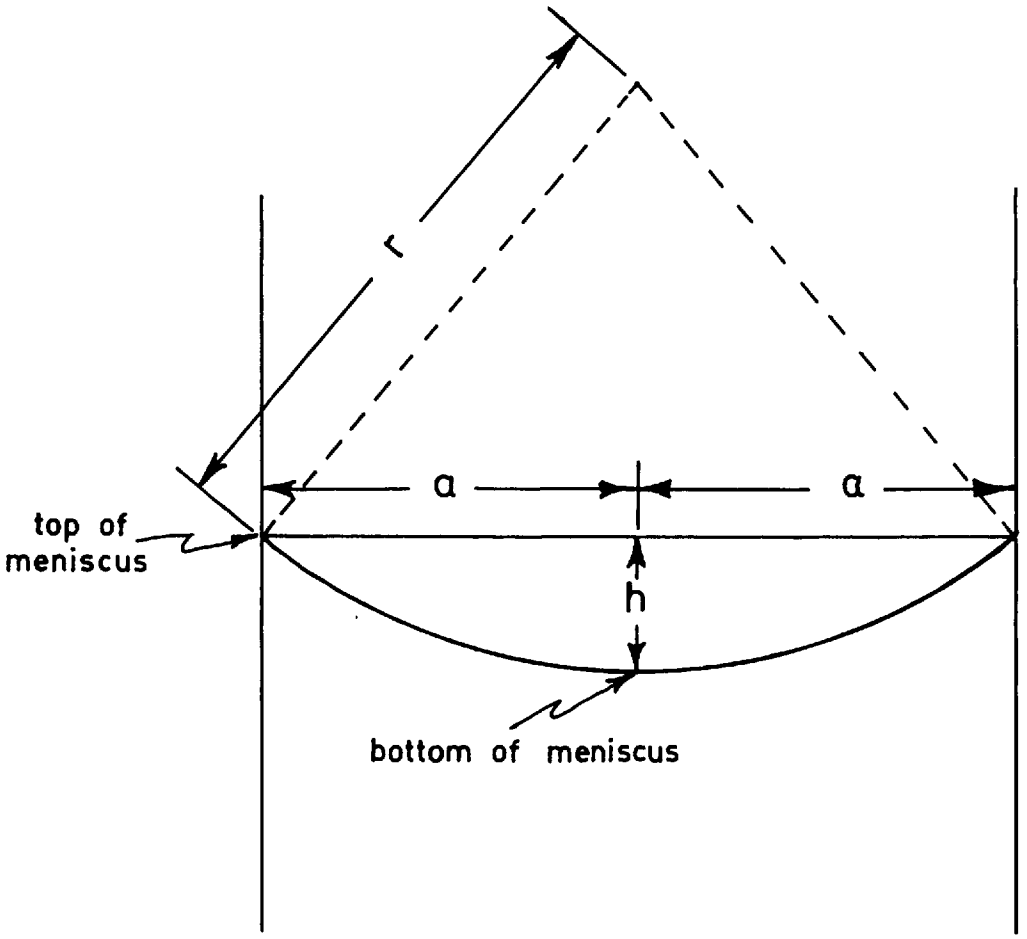

FIG 27 ESTIMATION OF EVAPORATING SURFACE AREA

APPENDIX 5

ESTIMATION OF EVAPORATING SURFACE AREA

The surface area of a segment of a sphere (see Fig. 27) is given by the following expression (Perry[49], p.58).

$$A = 2\pi rh \qquad \text{(A5-1)}$$

It is clear from Fig. 27 that the following is true:-

$$r^2 = a^2 + (r - h)^2$$

i.e.:- $$r^2 = a^2 + r^2 - 2rh + h^2$$

so that $$r = \frac{a^2 + h^2}{2h}$$

Substituting this expression for r in equation (A5-1) we obtain:-

$$A = 2\pi h \left(\frac{a^2 + h^2}{2h}\right)$$

$$= \pi (a^2 + h^2)$$

If we assume the liquid meniscus to be part of the surface of a sphere, then the width of the "top" of the meniscus becomes 2a and the depth of the meniscus becomes h.

Hence, Surface Area $= \pi \left[\left(\frac{\text{width of meniscus}}{2}\right)^2 + (\text{depth of meniscus})^2\right]$

APPENDIX 6

EXPERIMENTAL RESULTS.

Table 4. Run 5 - A Check for Constant Evaporation Rate.

Time Recorded	Evaporation Time (min.)	Capillary Reading (cm.)
1:00	0	2.0
1:25	25	3.0
1:51	51	4.1
2:18	78	5.3
2:44	104	6.3
3:15	135	7.5
3:42	162	8.7
4:09	189	9.8

Table 5. n-Butyric Acid - $t_1 = 30.1^{\circ}C$ ($P_1 = 1.5917$ mm. Hg.)

Effectiveness of Stirring at Various Flux Levels.

Run N°	t_2 ($^{\circ}C$)	Mass Flux, $W \times 10^5$ ($g./cm.^2 sec.$)	Stirrer Speed (r.p.m.)	$\alpha \times 10^3$
86	18.7	29.1	zero	11.9
87	"	31.4	450	12.8
88	"	31.3	600	12.8
89	"	30.9	850	12.6
90	15.3	40.3	zero	13.8
91	"	52.5	450	18.0
92	"	38.2	600	13.2
93	"	49.4	850	17.1

Table 5 cont^{d}

Run N^{o}	t_2 (^{o}C)	Mass Flux, W x 10^5 (g./cm.^{2}sec)	Stirrer Speed (r.p.m.)	α x10^3
94	0.0	104.6	zero	26.3
95	"	178.9	550	45.3
96	"	228.6	770	57,9
97	"	229.8	650	57.9
98	liquid N_2	345.6	zero	73.5
99	"	343.2	370	77.9
100	"	370.8	450	84.3
101	"	399.0	630	90.6
102	"	402.0	770	91.3

Table 6. Fractionated Benzyl Alcohol - t_1 = 60.5^{o}C (P_1 = 1.2023 mm. Hg.)

Effectiveness of Stirring at Maximum Flux Conditions (P_2 = 0)

Run N^{o}	t_2	Mass Flux, W x 10^5 (g./cm.^{2}sec.)	Stirrer Speed (r.p.m.)	α x10^3
146	liquid N_2	194.9	zero	48.8
147	"	237.0	580	59.4
148	"	287.6	650	72.2
149	"	271.8	710	68.2
150	"	273.6	750	68.7
151	"	292.0	790	73.2
144	"	298.8	780	74.9
145	"	286.6	760	71.9

Table 7. Untreated Benzyl Alcohol - t_1 = 60.9°C (P_1 = 1.2361 mm. Hg.)

Run N°	t_2 (°C)	P_2 (mm. Hg.)	$P_1 - P_2$ (mm. Hg.)	$\frac{P_1 - P_2}{P_1}$	Mass Flux, W ×10^5 (g./cm.^{2}sec.)	α ×10^3
15*	42.10	0.2917	0.9444	0.764	12.47	3.99
35*	56.60	0.9016	0.3258	0.266	1.92	1.78
36*	51.40	0.6081	0.6280	0.508	4.55	2.19
39	16.25	0.0296	1.2065	0.977	144.10	36.10
40	25.50	0.0703	1.1571	0.943	42.50	11.10
41	37.80	0.2051	1.0223	0.833	15.00	4.43
42	22.10	0.0514	1.1760	0.957	65.65	16.90

*Unstirred

Table 8. Untreated Benzyl Alcohol - t_1 = 56.7°C (P_1 = 0.9078 mm. Hg.)

Run N°	t_2 (°C)	P_2 (mm. Hg.)	$P_1 - P_2$ (mm. Hg.)	$\frac{P_1 - P_2}{P_1}$	Mass Flux, W ×10^5 (g./cm.^{2}sec.)	α ×10^3
45	16.30	0.0297	0.8781	0.967	54.30	18.53
46	24.00	0.0612	0.8550	0.933	29.92	10.48
47	20.20	0.0431	0.8751	0.953	42.80	14.70
48	31.40	0.1186	0.7976	0.871	13.73	5.17
49	45.75	0.3917	0.5245	0.572	4.04	2.31
50	53.30	0.7031	0.2131	0.233	1.12	1.58

Table 9. Untreated Benzyl Alcohol - $t_1 = 40.5^{\circ}C$ ($P_1 = 0.2564$ mm. Hg.)

Run N°	t_2 (°C)	P_2 (mm. Hg.)	$P_1 - P_2$ (mm. Hg.)	$\frac{P_1 - P_2}{P_1}$	Mass Flux, W $\times 10^5$ (g./cm.^{2}sec.)	α $\times 10^3$
51	15.70	0.0281	0.2283	0.891	10.54	13.23
52	22.70	0.0543	0.2021	0.788	5.20	7.52
53	27.05	0.0807	0.1757	0.685	4.15	6.91
54	35.05	0.1626	0.0938	0.366	1.49	4.66
55	0.60	0.0060	0.2504	0.977	49.55	58.80

Table 10. n-Butyric Acid - $t_1 = 30.1^{\circ}C$ ($P_1 = 1.3917$ mm. Hg.)

Run N°	t_2 (°C)	P_2 (mm. Hg.)	$P_1 - P_2$ (mm. Hg.)	Mass Flux, W $\times 10^5$ (g./cm.^{2}sec.)	α $\times 10^3$
61	14.85	0.4587	0.9284	60.8	20.9
62	18.20	0.5912	0.8005	26.1	10.4
63	22.35	0.8052	0.5885	12.9	7.0
64	0.30	0.1418	1.2499	682.0	173.8
65	26.65	1.0935	0.2982	6.0	6.4
66	liquid N_2	zero	1.3917	988.0	226.0
67	8.80	0.2857	1.1060	364.0	104.8
68	4.10	0.1950	1.1967	223.9	65.1
69	8.60	0.2811	1.1106	146.9	42.1
70	15.10	0.4676	0.9241	61.6	21.2
71	0.45	0.1436	1.2481	227.2	57.9
72	3.00	0.1779	1.2138	194.7	51.0
73	0.15	0.1400	1.2517	233.0	59.2
74	liquid N_2	zero	1.3917	450.0	103.0

Table 10 cont[d]

Run N°	t_2 (°C)	P_2 (mm. Hg.)	$P_1 - P_2$ (mm. Hg.)	Mass Flux, $W \times 10^5$ ($g./cm.^2 sec.$)	$\alpha \times 10^3$
75	0.20	0.1438	1.2479	239.6	61.1
76	9.52	0.3026	1.0891	154.7	45.2
77	14.80	0.4570	0.9395	102.3	34.7
78	14.85	0.4587	0.9349	62.0	21.2
79	23.30	0.8605	0.5312	18.8	11.3
80	0.20	0.1438	1.2479	230.8	58.9
81	15.85	0.4951	0.9014	78.8	27.8
82	0.10	0.1394	1.2571	232.0	58.8
83	23.40	0.8667	0.5298	17.6	10.6
84	28.25	1.2237	0.1728	3.4	6.2
85	19.40	0.6466	0.7499	34.6	14.7

Table 11. n-Butyric Acid - $t_1 = 20.0°C$ ($P_1 = 0.6760$ mm. Hg.)

Run N°	t_2 (°C)	P_2 (mm. Hg.)	$P_1 - P_2$ (mm. Hg.)	Mass Flux, $W \times 10^5$ ($g./cm.^2 sec.$)	$\alpha \times 10^3$
103	16.67	0.5269	0.1501	4.8	10.0
104	18.75	0.6160	0.0600	1.9	9.9
105	0.20	0.1438	0.5322	92.1	54.3
106	4.85	0.2074	0.4686	42.2	28.2
107	9.05	0.2914	0.3846	19.6	16.0
108	13.05	0.3993	0.2767	9.1	10.3
109	0.07	0.1390	0.5370	85.9	48.9
110	2.50	0.1707	0.5055	54.6	33.8

Table 11 cont^{d}

Run N^{o}	t_2 (^{o}C)	P_2 (mm. Hg.)	$P_1 - P_2$ (mm. Hg.)	Mass Flux, W $\times 10^5$ (g./cm.^{2}sec.)	α $\times 10^3$
111	liquid N_2	zero	0.6760	270.0	125.2
115	"	"	0.6760	249.8	115.7

Table 12. Fractionated Benzyl Alcohol - t_1 = 60.5^{o}C (P_1 = 1.2023 mm. Hg.)

Run N^{o}	t_2 (^{o}C)	P_2 (mm. Hg.)	$P_1 - P_2$ (mm. Hg.)	Mass Flux, W $\times 10^5$ (g./cm.^{2}sec.)	α $\times 10^3$
120	22.05	0.0514	1.1509	226.8	59.4
124	22.00	0.0512	1.1511	255.4	66.8
126	31.50	0.1200	1.0823	181.7	50.6
127	31.50	0.1200	1.0823	199.4	55.6
128	31.50	0.1200	1.0823	184.7	51.4
129	41.15	0.2710	0.9313	119.2	38.6
130	49.65	0.5333	0.6690	25.0	11.2
132	49.70	0.5358	0.6665	26.3	11.9
133	49.70	0.5358	0.6665	28.7	13.0
134	56.70	0.9099	0.2924	7.2	7.4
135	45.70	0.3908	0.8115	63.0	23.4
136	35.50	0.1694	1.0329	133.0	38.8
137	26.20	0.0750	1.1273	259.6	69.4
138	35.40	0.1679	1.0344	128.0	37.3
139	56.40	0.8892	0.3131	9.0	8.6
140	41.10	0.2698	0.9325	101.3	32.8
141	52.80	0.6792	0.5231	17.2	9.9

Table 12 cont[d]

Run N°	t_2 (°C)	P_2 (mm. Hg.)	$P_1 - P_2$ (mm. Hg.)	Mass Flux, W x 10^5 (g./cm.^{2}sec.)	α x 10^3
142	0.30	0.0058	1.1965	284.2	71.7
143	0.05	0.0057	1.1966	285.4	72.0
144	liquid N_2	zero	1.2023	298.8	74.9
145	"	"	1.2023	286.6	71.9
150	"	"	1.2023	273.6	68.7
151	"	"	1.2023	292.0	73.2

Table 13. Fractionated Benzyl Alcohol - t_1 = 30.6°C (P_1 = 0.1109 mm. Hg.)

Run N°	t_2 (°C)	P_2 (mm. Hg.)	$P_1 - P_2$ (mm. Hg.)	Mass Flux, W x 10^5 (g./cm.^{2}sec.)	α x 10^3
153	20.70	0.0453	0.0656	23.0	100.9
154	20.70	0.0453	0.0656	24.2	105.8
155	23.35	0.0530	0.0530	8.6	46.4
156	26.35	0.0760	0.0349	5.2	43.1
157	28.75	0.0942	0.0167	2.7	46.8
158	28.80	0.0946	0.0163	3.0	52.8
159	0.05	0.0057	0.1052	90.8	248.0
160	0.05	0.0057	0.1052	88.6	242.0
161	5.00	0.0096	0.1013	81.4	230.8
162	9.25	0.0149	0.0960	68.9	206.2
163	13.35	0.0224	0.0885	50.4	163.6
164	17.05	0.0321	0.0788	47.4	172.9
165	20.75	0.0455	0.0654	23.1	101.6

Table 13 cont[d]

Run N°	t_2 (°C)	P_2 (mm. Hg.)	$P_1 - P_2$ (mm. Hg.)	Mass Flux, W x 10^5 (g./cm.^{2}sec.)	α x 10^3
166	liquid N_2	zero	0.1109	99.8	258.6
167	"	"	0.1109	102.3	265.4
168	25.65	0.0715	0.0394	12.5	91.3
169	27.35	0.0832	0.0277	8.8	91.7
170	17.85	0.0346	0.0763	33.4	126.0
171	17.05	0.0321	0.0788	50.7	185.1
172	11.65	0.0189	0.0920	72.6	226.8
173	6.95	0.0118	0.0991	85.5	248.0
174	2.95	0.0077	0.1032	93.9	261.4
175	25.15	0.0682	0.0427	20.6	138.1
176	25.40	0.0698	0.0411	19.9	139.0
177	27.10	0.0813	0.0296	12.1	117.9
178	20.80	0.0457	0.0652	39.5	173.8
179	liquid N_2	zero	0.1109	105.3	273.4
180	"	"	0.1109	106.2	275.4

Table 14. Fractionated Benzyl Alcohol - "Free Evaporation" Experiments.

Run N°	t_1 (°C)	Mass Flux, W x 10^5 (g./cm.^{2}sec.)	α
144	60.50	298.8	0.075
145	"	286.6	0.072
150	"	273.6	0.069
151	"	292.0	0.073

Table 14 cont^{d}

Run N^{o}	t_1 (^{o}C)	Mass Flux, W x 10^5 (g./cm.^{2}sec.)	α
166	30.60	99.8	0.259
167	"	102.3	0.265
179	"	105.3	0.273
180	"	106.2	0.275
181	60.70	320.6	0.079
182	20.30	60.6	0.392
183	20.30	57.8	0.374
184	0.20	13.1	0.621
185	- 0.10	11.9	0.568
186	25.00	77.5	0.328
187	35.65	126.8	0.214
188	40.35	155.0	0.179
189	45.10	190.9	0.151
190	50.10	229.6	0.123
191	25.35	78.8	0.323
192	34.35	121.4	0.229
193	39.55	153.2	0.188
194	44.85	175.0	0.141
195	50.30	216.6	0.115
196	55.10	248.8	0.092
197	55.10	244.6	0.091

Table 15. Fractionated Benzyl Alcohol - "Free Evaporation" Experiments

Surface Cooling Calculated Assuming $\alpha = 1$.

Run N°	Mass Flux, W x 10^5 (g./cm.^{2}sec.)	Surface Cooling ($^\circ$C)
184	13.1	4.5
182	60.6	9.8
180	106.2	14.4
181	320.6	32.3
179	105.3	14.4
166	99.8	15.0
167	102.3	14.7
183	57.4	10.3
144	298.8	33.1
145	286.6	33.3
150	273.6	33.8
151	292.0	33.1
185	11.9	5.1
186	77.5	12.0
187	126.8	17.4
188	155.0	20.0
189	190.0	22.5
190	229.6	25.4
191	78.8	12.2
192	121.4	16.6
193	153.2	19.3
194	175.0	23.2

Table 15 cont[d]

Run N°	Mass Flux, W x 10^5 (g./cm.^{2}sec.)	Surface Cooling (°C)
195	216.6	26.3
196	248.8	29.5
197	244.6	29.8

Table 16. Fractionated Benzyl Alcohol - "Free Evaporation" Experiments

Surface Cooling Calculated Assuming $\alpha = 1$ after Area Correction Factor of 1.45 Applied.

Run N°	Adjusted Mass Flux, W x 10^5 (g./cm.^{2}sec.)	Adjusted α	Adjusted Surface Cooling (°C)
144	433.5	0.109	28.8
145	416.0	0.104	29.0
150	396.8	0.100	29.6
151	423.5	0.106	28.8
166	144.7	0.375	11.0
167	148.4	0.385	10.8
179	152.7	0.396	10.4
180	154.0	0.399	10.4
181	465.0	0.115	28.0
182	87.8	0.568	6.0
183	83.8	0.542	6.5
184	19.0	0.900	1.1
185	17.5	0.823	1.6
186	112.3	0.476	8.1

Table 16 cont[d]

Run N°	Adjusted Mass Flux, W x 10^5 ($g./cm.^2 sec.$)	Adjusted α	Adjusted Surface Cooling (°C)
187	183.8	0.311	13.4
188	224.8	0.259	15.9
189	276.8	0.219	18.3
190	332.8	0.179	21.2
191	114.2	0.468	8.3
192	176.2	0.332	12.6
193	222.2	0.273	15.2
194	253.6	0.205	19.0
195	314.4	0.166	22.1
196	361.0	0.134	25.3
197	354.8	0.131	25.5

Table 17. FractionatedBenzyl Alcohol - Bulk Liquid at 60.5°C

Results Corrected for Surface Cooling.

Run N°	Temperature (°C)		Pressure (mm. Hg.)		Mass Flux, W x 10^5 ($g./cm.^2 sec.$)	α	
	t_1	t_2	P_1	P_2		Before Correction	After Correction
120	36.98	22.05	0.1919	0.0514	329.2	0.086	0.701
124	34.06	22.00	0.1496	0.0512	370.0	0.097	1.087
126	41.69	31.50	0.2831	0.1200	263.5	0.073	0.473
127	39.84	31.50	0.2432	0.1200	289.4	0.081	0.685
128	41.38	31.50	0.2761	0.1200	267.6	0.075	0.502
129	48.16	41.15	0.4742	0.2710	172.8	0.056	0.251

Table 17 cont^{d}

Run N^{o}	Temperature (°C)		Pressure (mm. Hg.)		Mass Flux, W x 10^{5} (g./cm.^{2}sec.)	α	
	t_1	t_2	P_1	P_2		Before Correction	After Correction
130	57.92	49.65	0.9954	0.5333	36.2	0.016	0.024
132	57.78	49.70	0.9863	0.5558	38.2	0.017	0.025
133	57.52	49.70	0.9683	0.5358	41.7	0.019	0.029
134	59.75	56.70	1.1403	0.9099	10.4	0.011	0.014
135	53.98	45.70	0.7430	0.3908	91.3	0.034	0.077
136	46.72	35.50	0.4236	0.1694	192.9	0.056	0.224
137	33.62	26.20	0.1442	0.0750	576.4	0.101	1.572
138	47.23	35.40	0.4416	0.1679	185.7	0.054	0.200
139	59.57	56.40	1.1246	0.8892	13.0	0.013	0.017
140	50.00	41.10	0.5483	0.2698	147.0	0.048	0.157
141	58.71	52.80	1.0568	0.6792	25.0	0.014	0.020
142	31.06	0.30	0.1156	0.0058	412.0	0.104	1.079
143	30.94	0.05	0.1143	0.0057	413.5	0.104	1.096
144	29.55	liq. N_2	0.1012	zero	433.5	0.109	1.229
145	30.78	"	0.1127	"	416.0	0.104	1.061
150	32.15	"	0.1271	"	396.8	0.100	0.901
151	30.26	"	0.1076	"	423.5	0.106	1.130

Table 18. Fractionated Benzyl Alcohol - Bulk Liquid at 30.6°C

Results Corrected for Surface Cooling.

Run N°	Temperature (°C)		Pressure (mm. Hg.)		Mass Flux, W x 10^5 (g./cm.^{2}sec.)	α	
	t_1	t_2	P_1	P_2		Before Correction	After Correction
153	28.21	20.70	0.0900	0.0453	33.4	0.146	0.214
154	28.10	20.70	0.0889	0.0453	35.0	0.155	0.230
155	29.71	25.35	0.1026	0.0550	12.4	0.067	0.072
156	30.06	26.35	0.1059	0.0760	7.6	0.062	0.073
157	30.32	28.75	0.1081	0.0942	4.0	0.068	0.085
158	30.29	28.80	0.1079	0.0946	4.3	0.077	0.095
159	21.20	0.05	0.0474	0.0057	131.7	0.360	0.893
160	21.42	0.05	0.0484	0.0057	128.4	0.351	0.851
161	22.17	5.00	0.0519	0.0096	118.0	0.335	0.792
162	25.46	9.25	0.0585	0.0149	100.0.	0.299	0.651
163	25.38	13.35	0.0697	0.0224	73.1	0.237	0.441
164	25.69	17.05	0.0716	0.0321	68.8	0.251	0.496
165	28.20	20.75	0.0897	0.0455	33.5	0.147	0.217
166	20.27	liq. N_2	0.0435	zero	144.7	0.375	0.941
167	20.00	"	0.0424	"	148.4	0.385	0.992
168	29.30	25.65	0.0989	0.0715	18.2	0.152	0.191
169	29.69	27.35	0.1023	0.0832	12.8	0.133	0.192
170	27.14	17.85	0.0817	0.0346	48.5	0.183	0.295
171	25.34	17.05	0.0695	0.0321	73.6	0.269	0.561
172	23.09	11.65	0.0565	0.0189	105.2	0.329	0.795
173	21.75	6.95	0.0499	0.0118	124.0	0.360	0.923
174	20.87	2.95	0.0460	0.0077	136.2	0.379	1.007

Table 18 cont^{d}

Run N^{o}	Temperature (^{o}C)		Pressure (mm. Hg.)		Mass Flux, W x 10^{5} ($g./cm.^{2}sec.$)	α	
	t_1	t_2	P_1	P_2		Before Correction	After Correction
175	28.47	25.15	0.0921	0.0682	29.8	0.200	0.357
176	28.54	25.40	0.0925	0.0698	28.8	0.202	0.354
177	29.34	27.10	0.0993	0.0813	17.6	0.171	0.281
178	26.51	20.80	0.0771	0.0457	57.3	0.252	0.521
179	19.70	liq. N_2	0.0412	zero	152.7	0.396	1.046
180	19.60	"	0.0408	"	154.0	0.399	1.067

Table 19. n-Butyric Acid - t_1 = 20.0^{o}C. Results Recalculated Using Vapour Pressure Data of Skylarenko et al. (P_1 = 1.2823 mm. Hg.)

Run N^{o}	t_2 (^{o}C)	P_2 (mm. Hg.)	Mass Flux, W x 10^{5} ($g./cm.^{2}sec.$)	α x 10^{3}
103	16.67	0.9099	4.8	4.0
104	18.75	1.1272	1.9	3.8
105	0.20	0.1476	92.1	25.4
106	4.85	0.2523	42.2	12.8
107	9.05	0.4027	19.6	7.0
108	13.05	0.6209	9.1	4.3
109	0.07	0.1455	83.9	23.1
110	2.50	0.1928	54.6	15.7
111	liquid N_2	zero	270.0	65.9
115	"	"	249.8	60.9

Table 20. n-Butyric Acid - $t_1 = 20.0^{\circ}C$ ($P_1 = 0.6760$ mm. Hg.). Results Recalculated Using Schrage's "Velocity of Approach" Factor.

Run N°	t_2 (°C)	P_2 (mm. Hg.)	Γ	"Effective" Pressure (ΓP_2)	Mass Flux, W x 10^5 (g./cm.^{2}sec.)	Corrected α x 10^3
103	16.67	0.5269	1.000	0.5269	4.8	10.0
104	18.75	0.6160	1.000	0.6160	1.9	9.9
105	0.20	0.1438	0.900	0.1293	92.1	52.7
106	4.85	0.2074	0.967	0.2008	42.2	27.8
107	9.05	0.2914	0.989	0.2880	19.6	15.9
108	13.05	0.3993	0.996	0.3978	9.1	10.2
109	0.07	0.1390	0.905	0.1258	83.9	47.8
110	2.50	0.1707	0.950	0.1620	54.6	33.8
111	liquid N_2	zero	0.000	zero	270.0	125.2
115	"	"	0.000	"	249.8	115.7

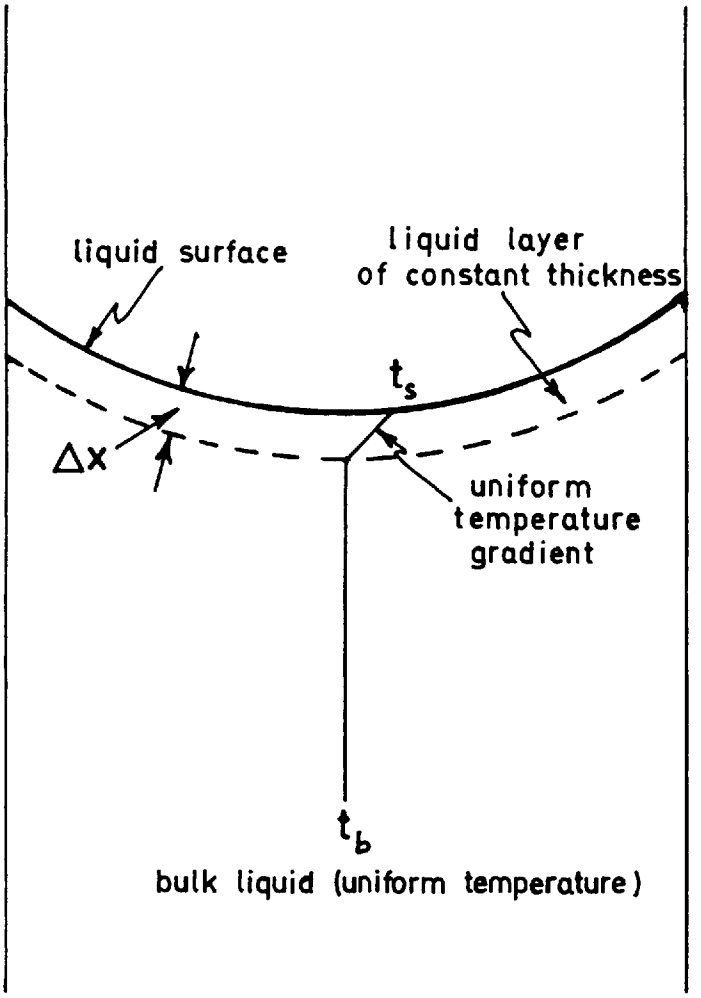

FIG 28 A MODEL FOR HEAT TRANSFER AT THE LIQUID SURFACE

APPENDIX 7

A MODEL FOR HEAT TRANSFER AT THE LIQUID SURFACE.

Consider all of the heat transfer resistance at the surface to be confined to a layer of liquid of constant thickness Δx (see Fig. 28). Also consider that heat is transferred through the layer by conduction only. Then for the case of evaporation $(t_s < t_b)$ the following equation results:-

$$W\lambda = k.\frac{(t_b - t_s)}{\Delta x} \qquad \text{(A9-1)}$$

where W = mass flux

λ = latent heat of vaporisation

k = thermal conductivity of liquid

Rearranging equation (A9-1) we obtain:-

$$W = \frac{k}{\lambda \Delta x}.(t_b - t_s)$$

$$= \frac{k}{\lambda \Delta x}.(\text{Surface Cooling}) \qquad \text{(A9-2)}$$

Since Δx is assumed to be constant and k and λ can be taken as constants over a small range of temperature, it is clear from equation (A9-2) that the relationship between W and Surface Cooling should be linear on the basis of this model. Hence, the surface cooling data presented in Fig. 19 fits the model quite well.

From Fig. 19, the slope of the line drawn through the surface cooling data (corrected for surface area)is 1.4×10^{-4} g./cm.^{2}sec.$^\circ$C. i.e.:- from equation (A9-2),

$$\frac{k}{\lambda \Delta x} = 1.4 \times 10^{-4} \qquad \text{(A9-3)}$$

A value of thermal conductivity for benzyl alcohol was not

readily available so the value for benzene was taken to be a reasonable estimate.

k for benzene at $60^{\circ}C$ = 0.0036 cal/cm.^{2}sec.($^{\circ}C$/cm.) (Kaye and Laby[53], p.53)

The latent heat of vaporisation for benzyl alcohol at its boiling point ($208^{\circ}C$) is given by Perry[49](p.216) as 112.28 cal./g.. A value of 112 cal./g. was considered to be an adequate estimate for use here.

Substituting the above values of k and λ in equation (A9-3) the following was obtained:-

$$\frac{5.6 \times 10^{-4}}{1.12 \times 10^{2}\ \Delta x} = 1.4 \times 10^{-4}$$

from which $\Delta x = 2.3 \times 10^{-2}$ cm. approx.

Hence, if the above model for heat transfer is assumed to be applicable to the data in Fig. 19, the whole of the temperature drop from bulk liquid to liquid surface must occur across a surface layer about 0.2 mm. thick.

APPENDIX 8

PRIMARY DATA

Table 21. Primary Data for Untreated Benzyl Alcohol.

Run No.	Temperature (°C)		Meniscus (cm.)		Capillary Reading (cm.)		Evap^{n} Time		Stirrer Speed
	t_1	t_2	Width	Depth	Initial	Final	min.	sec.	(r.p.m.)
13	60.90	42.10	0.845	0.204	2.0	8.0	32	-	zero
35	60.80	56.60	0.855	0.186	6.9	10.6	130	-	"
36	60.90	51.40	0.866	0.201	3.0	8.6	79	-	"
39	"	16.25	0.856	0.195	2.0	10.0	3	40	710
40	60.80	25.50	0.842	0.193	2.0	10.0	15	07	710
41	"	37.80	0.860	0.167	2.0	9.0	32	-	720
42	"	22.10	0.852	0.196	1.6	9.5	7	59	720
45	56.70	16.30	0.865	0.204	2.0	10.0	9	24	720
46	56.80	24.00	0.868	0.205	5.6	10.6	10	40	750
47	"	20.20	0.867	0.196	2.5	10.0	11	17	750
48	"	31.40	0.866	0.180	2.0	8.6	32	13	760
49	"	45.75	0.861	0.195	1.6	5.5	63	-	720
50	"	55.30	0.844	0.205	4.8	7.7	172	-	700
51	40.50	15.70	0.858	0.199	2.2	8.7	41	-	730
52	"	29.70	0.871	0.217	1.7	5.5	45	-	750
53	"	27.05	0.845	0.209	8.7	11.0	37	-	720
54	"	35.05	0.877	0.200	2.9	7.0	172	-	730
55	"	0.60	0.875	0.212	5.0	11.0	7	28	750

Table 22. Primary Data for n-Butyric Acid.

Run No.	Temperature (°C)		Meniscus (cm.)		Capillary Reading (cm.)		Evap^{n} Time		Stirrer Speed
	t_1	t_2	Width	Depth	Initial	Final	min.	sec.	(r.p.m.)
61	30.05	14.85	0.857	0.203	2.0	10.0	7	53	700
62	30.10	18.20	0.857	0.210	2.4	10.0	17	18	700
63	"	22.35	0.843	0.194	2.0	9.8	38	-	700
64	"	0.30	0.862	0.319	2.0	10.5	-	35	700
65	"	26.65	0.847	0.197	1.5	9.7	84	-	720
66	"	liq. N_2	0.847	0.397	2.3	10.6	-	25	500
67	"	8.80	0.852	0.225	2.0	8.0	-	58	low
68	"	4.10	0.831	0.206	1.7	10.0	2	19	700
69	"	8.60	0.874	0.209	2.0	11.0	3	30	700
70	"	15.10	0.844	0.188	1.7	10.0	8	33	700
71	"	0.45	0.867	0.193	1.9	10.0	2	07	800
72	"	3.00	0.865	0.222	1.6	10.0	2	28	700
73	"	0.15	0.870	0.232	1.9	8.9	1	40	750
74	"	liq. N_2	0.816	0.199	2.0	9.9	1	09	800
75	"	0.20	0.867	0.229	1.8	10.0	1	55	700
76	"	9.52	0.879	0.194	1.9	10.6	3	17	700
77	30.15	14.80	0.890	0.204	2.0	10.3	4	34	700
78	30.12	14.85	0.879	0.212	2.0	10.5	7	44	700
79	30.10	23.30	0.876	0.192	2.0	9.6	23	50	700
80	"	0.20	0.870	0.210	2.0	10.0	2	00	750
81	30.15	15.85	0.871	0.197	2.0	10.0	5	59	750
82	"	0.10	0.862	0.212	2.0	10.0	2	01	750
83	"	23.40	0.856	0.181	2.1	9.5	26	18	750

Table 22 cont^{d}

Run N^{o}	Temperature (°C)		Meniscus (cm.)		Capillary Reading (cm.)		Evap^{n} Time		Stirrer Speed (r.p.m.)
	t_1	t_2	Width	Depth	Initial	Final	min.	sec.	
84	30.15	28.25	0.840	0.189	1.5	6.3	90	-	750
85	"	19.40	0.852	0.190	2.0	10.0	14	20	750
86	30.20	18.65	0.835	0.179	1.5	10.3	19	44	zero
87	30.15	18.70	0.860	0.182	1.5	10.0	16	44	450
88	"	18.75	0.870	0.168	2.6	10.0	14	41	600
89	"	18.75	0.866	0.191	2.0	10.0	15	37	830
90	30.20	15.30	0.841	0.192	1.5	10.0	13	17	zero
91	"	15.30	0.869	0.196	1.5	10.1	9	43	450
92	"	15.30	0.864	0.180	2.5	10.0	12	05	600
93	"	15.30	0.871	0.209	1.5	10.0	9	56	850
94	30.20	0.00	0.893	0.221	3.1	10.4	3	47	zero
95	30.15	0.00	0.873	0.187	1.5	10.6	3	02	550
96	30.15	0.05	0.858	0.229	1.8	10.1	2	04	770
97	30.20	0.00	0.853	0.185	1.6	10.6	2	26	650
98	"	liq. N_2	0.861	0.214	1.8	10.3	1	26	zero
99	"	"	0.854	0.219	1.7	10.4	1	29	370
100	"	"	0.870	0.212	1.6	10.5	1	23	450
101	"	"	0.866	0.203	1.8	10.5	1	17	630
102	"	"	0.863	0.200	1.7	10.5	1	18	770
103	20.00	16.67	0.876	0.198	1.7	7.3	68	-	820
104	"	18.75	0.849	0.181	1.6	5.0	114	-	840
105	"	0.20	0.856	0.189	1.7	10.5	5	53	800
106	"	4.85	0.849	0.188	1.7	10.5	13	03	850

Table 22 cont[d]

Run N[o]	Temperature (°C)		Meniscus (cm.)		Capillary Reading (cm.)		Evap[n] Time		Stirrer Speed (r.p.m.)
	t_1	t_2	Width	Depth	Initial	Final	min.	sec.	
107	20.00	9.05	0.861	0.180	1.5	10.5	28	20	830
108	"	13.05	0.871	0.190	1.6	9.5	52	-	840
109	"	0.07	0.861	0.173	1.6	10.6	6	43	840
110	"	2.50	0.856	0.178	1.7	10.5	9	43	850
111	"	liq. N_2	0.875	0.207	1.6	10.6	1	55	800
112	"	"	0.878	0.218	1.7	10.5	2	22	zero
113	"	"	0.884	0.213	1.7	10.5	2	11	400
114	"	"	0.882	0.195	1.8	10.5	2	04	600
115	"	"	0.884	0.216	2.0	10.6	1	55	770

Table 23. Primary Data for Fractionated Benzyl Alcohol.

Run N[o]	Temperature (°C)		Meniscus (cm.)		Capillary Reading (cm.)		Evap[n] Time		Stirrer Speed (r.p.m.)
	t_1	t_2	Width	Depth	Initial	Final	min.	sec.	
120	60.50	22.05	0.885	0.199	3.0	10.5	2	03	750
124	"	22.00	0.895	0.170	3.0	10.5	1	52	790
126	"	31.50	0.908	0.192	3.5	11.5	2	29	770
127	"	31.50	0.898	0.176	3.5	10.5	2	12	770
128	"	31.50	0.890	0.198	3.5	10.5	2	20	800
129	"	41.15	0.924	0.170	2.0	10.5	4	17	780
130	"	49.65	0.917	0.188	2.7	10.7	19	00	790
132	"	49.70	0.895	0.145	2.0	10.0	20	-	760
133	"	49.70	0.893	0.163	2.0	10.0	18	-	750

Table 23 cont^{d}

Run N^{o}	Temperature (°C)		Meniscus (cm.)		Capillary Reading (cm.)		Evap^{n} Time		Stirrer Speed (r.p.m.)
	t_1	t_2	Width	Depth	Initial	Final	min.	sec.	
134	60.50	56.70	0.910	0.175	1.4	5.6	36	-	750
135	"	45.70	0.897	0.158	2.0	10.0	8	10	800
136	"	35.50	0.890	0.161	2.0	10.0	3	55	820
137	"	26.20	0.865	0.148	2.5	10.0	2	01	830
138	"	35.40	0.901	0.188	2.0	10.0	3	49	730
139	"	56.40	0.895	0.159	5.7	10.7	36	-	780
140	"	41.10	0.894	0.179	2.1	10.1	4	58	800
141	"	52.80	0.896	0.211	1.6	10.0	29	-	800
142	"	0.30	0.903	0.201	3.6	10.6	1	28	780
143	"	0.05	0.915	0.203	1.6	10.6	1	50	780
144	"	liq. N_2	0.914	0.191	1.9	10.6	1	44	780
145	"	"	0.905	0.202	1.7	10.7	1	52	760
146	"	"	0.915	0.180	1.6	10.5	2	46	zero
147	"	"	0.915	0.207	1.8	10.6	2	09	580
148	"	"	0.884	0.196	1.8	10.7	1	56	650
149	"	"	0.909	0.205	1.8	10.6	1	54	710
150	"	"	0.925	0.200	1.8	10.6	1	51	750
151	"	"	0.925	0.197	1.7	10.7	1	47	790
153	30.60	20.70	0.891	0.167	3.2	10.7	21	-	790
154	"	20.70	0.918	0.178	1.9	10.5	21	27	800
155	"	23.35	0.907	0.165	3.0	10.1	52	-	830
156	"	26.35	0.894	0.171	1.8	8.2	78	-	830
157	"	28.75	0.917	0.153	2.2	6.3	94	-	840

Table 23 cont^{d}

Run N^{o}	Temperature (°C)		Meniscus (cm.)		Capillary Reading (cm.)		Evap^{n} Time		Stirrer Speed (r.p.m.)
	t_1	t_2	Width	Depth	Initial	Final	min.	sec.	
158	30.60	28.80	0.894	0.176	2.0	6.0	83	-	840
159	"	0.05	0.929	0.163	2.0	10.6	5	42	870
160	"	0.05	0.914	0.162	1.5	10.6	6	23	860
161	"	5.00	0.907	0.163	1.5	10.7	7	06	850
162	"	9.25	0.907	0.153	1.5	10.7	8	31	820
163	"	13.35	0.900	0.153	2.9	10.7	10	01	830
164	"	17.05	0.908	0.179	2.5	10.7	10	37	830
165	"	20.75	0.900	0.138	1.5	10.2	26	18	850
166	"	liq. N_2	0.905	0.189	1.8	10.7	5	25	870
167	"	"	0.901	0.171	1.5	10.7	5	39	870
168	"	25.65	0.900	0.168	1.5	10.2	44	-	870
169	"	27.35	0.902	0.162	1.5	8.3	49	-	880
170	"	17.85	0.910	0.168	1.6	10.7	16	55	870
171	"	17.05	0.900	0.157	1.5	10.7	11	40	860
172	"	11.65	0.904	0.166	1.5	10.7	7	58	860
173	"	6.95	0.915	0.185	1.5	10.7	6	28	860
174	"	2.95	0.902	0.179	1.6	10.7	6	01	850
175	"	25.15	0.889	0.152	2.0	10.7	28	-	860
176	"	25.40	0.904	0.137	1.6	10.7	30	-	850
177	"	27.10	0.903	0.183	2.0	10.7	44	-	840
178	"	20.80	0.897	0.174	1.6	10.7	14	30	850
179	"	liq. N_2	0.896	0.174	1.8	10.7	5	21	860
180	"	"	0.909	0.148	1.7	10.7	5	24	860

Table 23 cont[d]

Run N[o]	Temperature (°C)		Meniscus (cm.)		Capillary Reading (cm.)		Evap[n] Time		Stirrer Speed (r.p.m.)
	t_1	t_2	Width	Depth	Initial	Final	min.	sec.	
181	60.70	liq. N_2	0.903	0.181	1.7	10.8	1	45	790
182	20.30	"	0.899	0.165	1.5	10.7	9	40	900
183	20.30	"	0.908	0.183	1.5	10.7	9	44	850
184	0.20	"	0.882	0.151	1.5	8.9	39	-	850
185	- 0.10	"	0.875	0.173	1.7	10.5	49	-	870
186	25.00	"	0.898	0.168	1.5	10.7	7	33	870
187	35.65	"	0.902	0.173	1.8	10.7	4	24	830
188	40.35	"	0.896	0.193	1.5	10.7	3	39	830
189	45.10	"	0.905	0.169	1.7	10.7	2	57	840
190	50.10	"	0.913	0.168	1.7	10.7	2	25	840
191	25.35	"	0.901	0.173	1.9	10.7	7	00	880
192	34.35	"	0.904	0.181	1.9	10.7	4	28	850
193	39.55	"	0.899	0.160	1.5	10.7	3	51	830
194	44.85	"	0.905	0.207	1.5	10.7	3	06	800
195	50.30	"	0.910	0.191	1.5	10.7	2	33	840
196	55.10	"	0.905	0.190	1.6	10.7	2	13	780
197	55.10	"	0.924	0.194	1.6	10.7	2	10	790

APPENDIX 9

SAMPLE CALCULATIONS

Calculation of Evaporation Coefficient.

When W is expressed in terms of g./cm.^{2}sec. and $(P_1 - P_2)$ is expressed in terms of mm. Hg., equation (1.1-6) becomes:-

$$W = \alpha\, 5.83 \times 10^{-2} . (M/T_1)^{\frac{1}{2}} . (P_1 - P_2) \qquad \text{(A9-1)}$$

Consider Run 120 (Table 23, Appendix 8).

Width of meniscus = 0.885 cm.

Depth of meniscus= 0.199 cm.

Surface area is determined as outlined in Appendix 5:-

$$\text{Area} = \pi \left[\left(\frac{0.885}{2} \right)^2 + (0.199)^2 \right]$$

$$= 0.741 \text{ cm.}^2$$

The volume of benzyl alcohol displaced is equivalent to a 7.5 cm. length of capillary.

Capillary calibration is 2.64×10^{-2} cc./cm.

Density of benzyl alcohol at room temperature is 1.043 g./cc. (Perry,[49] p.132).

Hence, mass of benzyl alcohol evaporated

$$= 7.5 \times 2.64 \times 10^{-2} \times 1.043$$

$$= 0.2066 \text{ g.}$$

Evaporation time = 123 sec.

Hence, mass flux $$W = \frac{0.2066}{0.741 \times 123}$$

$$= 2.268 \times 10^{-3} \text{ g./cm.}^2\text{sec.}$$

Evaporating temperature, t_1 = 60.5°C

i.e.:- $T_1 = (60.5 + 273.16)^{\circ}K$

$= 333.66^{\circ}K$

so that $1/T_1 = 0.002997062$

Vapour pressure is calculated from the following equation (Section 3.4):-

$$\log P(\text{mm. Hg.}) = 10.597 - 3509. \frac{1}{T}$$

Hence $\log P_1 = 10.597 - 3509 \times 0.002997062$

$= + 0.080$

i.e.:- $P_1 = 1.2023$ mm. Hg.

similarly $P_2 = 0.0514$ mm. Hg.

and hence $(P_1 - P_2) = 1.1509$ mm. Hg.

Molecular weight of benzyl alcohol, M = 108.13.

Hence $(M/T_1)^{\frac{1}{2}} = \left(\frac{108.13}{333.66}\right)^{\frac{1}{2}}$

$= 0.569$

Substituting for W, $(M/T_1)^{\frac{1}{2}}$ and $(P_1 - P_2)$ in equation (A9-1) we obtain:-

$$2.268 \times 10^{-3} = \alpha \times 5.83 \times 10^{-2} \times 0.569 \times 1.1509$$

from which $\alpha = 5.94 \times 10^{-2}$

Calculation of Surface Cooling for Free Evaporation Runs Assuming $\alpha = 1$.

Rearranging equation (A9-1) we obtain:-

$$\alpha = \frac{W}{5.83 \times 10^{-2} . (M/T_1)^{\frac{1}{2}} . (P_1 - P_2)}$$

For free evaporation runs, $P_2 = 0$ and the equation reduces to:-

$$\alpha = \frac{W}{5.83 \times 10^{-2} . (M/T_1)^{\frac{1}{2}} . P_1}$$

or

$$\alpha = \frac{W}{5.83 \times 10^{-2} . M^{\frac{1}{2}} . (P_1/T_1^{\frac{1}{2}})} \qquad \text{(A9-2)}$$

The only factor in equation (A9-2) affected by surface cooling is $(P_1/T_1^{\frac{1}{2}})$. Rearranging equation (A9-2) we obtain:-

$$(P_1/T_1^{\frac{1}{2}})_{exp.} = \frac{W}{5.83 \times 10^{-2} . M^{\frac{1}{2}} . \alpha_{exp.}} \qquad \text{(A9-3)}$$

where the subscript "exp." refers to experimental values.

It is clear from equation (A9-2) that if the true value of α is assumed to be unity, then the true value of $(P_1/T_1^{\frac{1}{2}})$ must be given by:-

$$(P_1/T_1^{\frac{1}{2}})_{actual} = \frac{W}{5.83 \times 10^{-2} . M^{\frac{1}{2}}}$$

Also, from equation (A9-3):-

$$\alpha_{exp.} . (P_1/T_1^{\frac{1}{2}})_{exp.} = \frac{W}{5.83 \times 10^{-2} . M^{\frac{1}{2}}}$$

Hence $$(P_1/T_1^{\frac{1}{2}})_{actual} = \alpha_{exp.} . (P_1/T_1^{\frac{1}{2}})_{exp.}$$

i.e.:- $$\log (P_1/T_1^{\frac{1}{2}})_{actual} = \log \left[\alpha_{exp.} . (P_1/T_1^{\frac{1}{2}})_{exp.} \right]$$

or $$\log P_{1_{actual}} - \tfrac{1}{2} \log T_{1_{actual}} = \log \left[\alpha_{exp.} . (P_1/T_1^{\frac{1}{2}})_{exp.} \right] \qquad \text{(A9-4)}$$

The vapour pressure of benzyl alcohol is represented by:-

$$\log P = 10.597 - 3509 . \frac{1}{T} \qquad \text{(A9-5)}$$

Substituting for $\log P_{1_{actual}}$ in equation (A9-4) we obtain:

$$10.597 - \frac{3509}{T_{1_{actual}}} - \tfrac{1}{2} \log T_{1_{actual}} = \log \left[\alpha_{exp.} \cdot (P_1/T_1^{\frac{1}{2}})_{exp.} \right] \qquad (A9\text{-}6)$$

Solution of equation (A9-6) by trial-and-error gives $T_{1_{actual}}$ and the surface cooling is then obtained from:-

$$\text{Surface Cooling} = T_{1_{exp.}} - T_{1_{actual}}$$

Consider Run 184 (Table 23, Appendix 8).

Evaporating temp., $t_1 = 0.20^{\circ}C$

i.e.:- $T_1 = 273.36^{\circ}K$

and from equation (A9-5) $P_1 = 0.005754$ mm. Hg.

Hence $$(P_1/T_1^{\frac{1}{2}})_{exp.} = \frac{0.005754}{(273.36)^{\frac{1}{2}}}$$

$$= 0.0003484$$

also $\alpha_{exp.} = 0.621$ (Table 14, Appendix 6)

so that $$\alpha_{exp.} (P_1/T_1^{\frac{1}{2}})_{exp.} = 0.621 \times 0.0003484$$

$$= 0.0002162$$

and $$\log \left[\alpha_{exp.} (P_1/T_1^{\frac{1}{2}})_{exp.} \right] = \overline{4}.33486$$

$$= -3.665 \text{ approx.}$$

Substituting in equation (A9-6):-

$$10.597 - \frac{3509}{T_{1_{actual}}} - \tfrac{1}{2} \log T_{1_{actual}} = -3.665$$

A trial-and-error solution gives:-

$$T_{1_{actual}} = 268.9^{\circ}K \text{ approx.}$$

Hence $$\text{Surface Cooling} = T_{1_{exp.}} - T_{1_{actual}}$$

$= 273.36 - 268.9$

$= 4.5^{\circ}C$

Correction of Evaporation Coefficients for Surface Cooling.

Consider Run 134 (Table 12, Appendix 6).

Originally calculated mass flux $= 7.2 \times 10^{-5}$ g./cm.^{2}sec.

Applying area correction, $W = 7.2 \times 10^{-5} \times 1.45$

$= 10.4 \times 10^{-5}$ g./cm.^{2}sec.

(the corresponding value of α corrected by the surface area factor is given by $0.007 \times 1.45 = 0.011$)

The slope of the line through the surface cooling data shown in Fig. 19 is 1.4×10^{-4} g./cm.^{2}sec.$^{\circ}$C.

Hence, surface cooling is estimated as follows:-

$$\text{Surface Cooling} = \frac{10.4 \times 10^{-5}}{1.4 \times 10^{-4}}$$

$= 0.75^{\circ}C$

Temperature of bulk liquid $= 60.5^{\circ}C$

Hence $t_{1_{actual}} = 60.5 - 0.75$

$= 59.75^{\circ}C$

i.e.:- $T_{1_{actual}} = 332.91^{\circ}K$

and from equation (A9-5), $P_{1_{actual}} = 1.1403$ mm. Hg.

From Table 12, Appendix 6, $P_2 = 0.9099$ mm. Hg.

Hence $(P_1 - P_2)_{actual} = 0.2304$ mm. Hg.

$M = 108.13$

Hence $$(M/T_1)^{\frac{1}{2}}_{actual} = \left(\frac{108.13}{532.91}\right)^{\frac{1}{2}}$$

$$= 0.569$$

Substituting the estimated actual values of W, $(P_1 - P_2)$ and $(M/T_1)^{\frac{1}{2}}$ in equation (A9-1) we obtain:-

$$10.4 \times 10^{-5} = \alpha_{actual} \times 5.83 \times 10^{-2} \times 0.569 \times 0.2304$$

from which $$\alpha_{actual} = 0.014$$

(compared with value of 0.011 when not corrected for surface cooling)

Ignoring the small change of $(M/T)^{\frac{1}{2}}$ caused by small temperature changes, it can be seen that if α_{actual} were in fact unity in this case, then the required value of $(P_1 - P_2)_{actual}$ would be given by:-

$$(P_1 - P_2)_{actual} = \frac{10.4 \times 10^{-5}}{5.83 \times 10^{-2} \times 0.569}$$

$$= 0.00314 \text{ mm. Hg.}$$

Hence $$P_{1_{actual}} = 0.00314 + 0.9099$$

$$= 0.9130 \text{ mm. Hg.}$$

From equation (A9-5), the value of $T_{1_{actual}}$ corresponding to $P_{1_{actual}} = 0.9130$ mm. Hg. is $329.9^{\circ}K$.

i.e.:- $$t_{1_{actual}} = 329.9 - 273.16$$

$$= 56.7^{\circ}C$$

i.e.:- Surface Cooling required $= (60.5 - 56.7)^{\circ}C$

$$= 3.8^{\circ}C$$

Estimated Surface Cooling $= 0.75^{\circ}C$

Hence, the estimated surface cooling would have to be in error by an amount of the order of 3°C if α_{actual} were in fact unity in this case.

Inclusion of Schrage's "Velocity of Approach" Factor.

Consider Run 105 (Table 11, Appendix 6).

Schrage[44](p.35) gives a chart expressing the correction factor, Γ, as a function of a quantity ϕ defined as follows:-

$$\phi = \frac{1}{2\pi^{\frac{1}{2}}} \cdot \frac{W}{W_{s+}} \cdot (T_o/T_s)^{-\frac{1}{2}} \cdot \left(\frac{\gamma_o}{\gamma_s}\right)^{-1} \qquad (A9\text{-}7)$$

where W = net mass flux at surface

W_{s+} = kinetic evaporation flux of the material

T_o, T_s = temperature of vapour at interface and liquid surface respectively

γ_o = mass density of vapour at interface

γ_s = mass density of vapour in equilibrium with liquid surface

As pointed out in Section (5.3), it is reasonable to assume $T_o = T_s$, so that mass density of vapour can be taken to be proportional to vapour pressure as follows:-

$$\left(\frac{\gamma_o}{\gamma_s}\right)^{-1} = (P_2/P_1)^{-1} = (P_1/P_2)$$

For Run 105 (n-butyric acid evaporating at 20.0°C), P_1 = 0.6760 mm. Hg. and $(M/T)^{\frac{1}{2}}$ = 0.548. The kinetic evaporation flux is obtained from equation (A9-1) by putting $P_2 = 0$ and $\alpha = 1$ to give the following:-

$$W_{s+} = 5.83 \times 10^{-2} \times 0.548 \times 0.6760$$
$$= 2.158 \times 10^{-2} \text{ g./cm.}^2\text{sec.}$$

Hence, for n-butyric acid evaporating at 20.0°C, equation (A9-7) can be written as follows:-

$$\phi = \frac{1}{2\pi^{\frac{1}{2}}} \cdot \left(\frac{W}{2.158 \times 10^{-2}}\right) \cdot \left(\frac{0.6760}{P_2}\right)$$
$$= 8.85 \, (W/P_2)$$

For Run 105,
$$\phi = 8.85 \times \frac{92.1 \times 10^{-5}}{0.1458}$$
$$= 5.67 \times 10^{-2}$$

From Schrage's chart, $1 - \Gamma = 0.1$ approx.

i.e.:- $\Gamma = 0.9$

The corrected equation given by Schrage (equation (1.4-1)) is equivalent to equation (A9-1) corrected in the following form:-

$$W = \alpha \times 5.83 \times 10^{-2} \cdot (M/T)^{\frac{1}{2}} \cdot (P_1 - \Gamma P_2) \qquad \text{(A9-8}$$

For Run 105, $(P_1 - \Gamma P_2) = (0.6760 - 0.9 \times 0.1458)$
$$= 0.5467 \text{ mm. Hg.}$$

Substituting in equation (A9-8):-

$$92.1 \times 10^{-5} = \alpha \times 5.83 \times 10^{-2} \times 0.548 \times 0.5467$$

from which $\alpha = 52.7 \times 10^{-3}$

(uncorrected value of $\alpha = 54.3 \times 10^{-3}$)

APPENDIX 10

REFERENCES

1. H.Herz, Ann. Phys., 17, 177 (1882).

2. I. Langmuir, Phys. Rev., 8, 2 (1916).

3. M. Knudsen, Ann. Phys., 47, 697 (1915).

4. O. Knacke and I. N. Stranski, Progr. Metal Phys., 6, 181-235 (1956).

5. T. Alty, Proc. Roy. Soc., A161, 68 (1937).

6. R. S. Bradley, Proc. Roy. Soc., A205, 553 (1951).

7. G. S. Trick and Sir Eric Rideal, Trans. Far. Soc., A210, 261 (1952).

8. R. F. Strickland-Constable and E. W. Bruce, Trans. Inst. Chem. Eng., 32, 192 (1954).

9. T. K. Sherwood and K. Johannes, A.I.Ch.E. Journal, 8, 590-3 (1962).

10. R. Jaeckel an d W. Peperle, Z. phys. Chem., 217, 321-36 (1961).

11. B. Paul and L. G. Lyon, Am. Inst. Aeron. Astron. J., 3, 6, 1067-71 (1965).

12. H. Cordes and H. Cammenga, Z. phys. Chem., 45, 3/4, 186-95 (1965).

13. R. N. Haward, Trans. Far. Soc., 35, 1401 (1939).

14. Sir Eric Rideal and P. M. Wiggins, Proc. Roy. Soc., A210, 291 (1952).

15. S. A. Kitchener and R. F. Strickland-Constable, Proc. Roy. Soc., A245, 93-110 (1958).

16. R. Littlewood and Sir Eric Rideal, Trans. Far. Soc., 52, 1598-1608 (1956).

17. G. Burrows, J. App. Chem., 7, 375-84 (1957).

18. T. Alty, Proc. Roy. Soc., A131, 554 (1931).

19. T. Alty and C. A. Mackay, Proc. Roy. Soc., A149, 104 (1935).

20. M. Baranaev, Zh. Fiz. Chim., 13, 1635 (1939).

21. W. Prüger, Z. Phys., 115, 202 (1940).

22. K. Hammeke and E. Kappler, Z. Geophysik, Sonderband 181 (1953).

23. H. Bucka, Z. phys. Chem., 195, 260 (1950).

24. L. Bogdandy, H. G. Kleist and O. Knacke, Z. Elektrochem., 59, 460 (1955).

25. L. J. Delaney, R. W. Houston and L. C. Eagleton, Chem. Eng. Sci., 19, 2, 105 (1964).

26. H. D. Chu, L. J. Delaney and L. C. Eagleton, Chem. Eng. Sci., 20, 6, 601-5 (1965).

27. L. J. Delaney, N. J. Psaltis and L. C. Eagleton, Chem. Eng. Sci., 20, 6, 607-10 (1965).

28. G. Wyllie, Proc. Roy. Soc., A197, 383 (1949).

29. J. Birks and R. S. Bradley, Proc. Roy. Soc., A198, 226 (1949).

30. R. S. Bradley and A. D. Shellard, Proc. Roy. Soc., A198, 240 (1949).

31. R. S. Bradley and G. C. S. Waghorn, Proc. Roy. Soc., A206, 65 (1951).

32. K. C. D. Hickman and D. J. Trevoy, I.E.C., 44, 1882 (1952).

33. D. J. Trevoy, I.E.C., 45, 2366 (1953).

34. K. C. D. Hickman, I.E.C., 46, 1442 (1954).

35. W. J. Heideger and M. Boudart, Chem. Eng. Sci., 17, 1-10 (1962).

36. K. Nabavian and L. A. Bromley, Chem. Eng. Sci., 18, 10, 651 (1963).

37. R. S. Silver and H. C. Simpson, "The Condensation of Superheated Steam",p.39, H.M.S.O. (1962).

38. J. Miller and J. Daen, J. Phys. Chem., 69, 9, 3006-13 (1965).

39. D. J. Jamieson, Nature, 202, 4932, 583 (1964).

40. J. P. Hirth and G. M. Pound, "Condensation and Evaporation", Pergamon (1963).

41. K. Herzfeld, J. Chem. Phys., 3, 319 (1935).

42. E. M. Mortensen and H. Eyring, J. Phys. Chem., 64, 846 (1960).

43. J. F. Kincaid and H. Eyring, J. Chem. Phys., 6, 620 (1938).

44. R. W. Schrage, "A Theoretical Study of Interphase Mass Transfer", Columbia University Press, N.Y. (1953).

45. S. A. Zwick, J. Appl. Phys., 31, 10, 1735-41 (1960).

46. D. J. Wilhelm, "Condensation of Metal Vapours: Mercury and the Kinetic Theory of Condensation", U.S. At. Energy Comm. Report ANL - 6948 (1964).

47. R. K. M. Johnstone, "The Construction of a Large Mach-Zehnder Interferometer and its Application to the Study of Gas/Liquid Transfer Processes", Ph.D. Thesis, University of London (1964).

48. H. S. Carslaw and J. C. Jaeger, "Conduction of Heat in Solids", 2nd Edition, Clarendon Press (1959).

49. J. H. Perry (Editor), "Chemical Engineers' Handbook", 3rd Edition, M^{c}Graw-Hill (1950).

50. F. H. Newman and V. H. L. Searle, "The General Properties of Matter", 4th Edition, Edward Arnold (1948).

51. Landolt-Börnstein, "Zahlenwerte und Funktionen", 6th Edition, Volume II/2a, Springer Verlag (1960).

52. H. S. Mickley, T. K. Sherwood and C. E. Reed, "Applied Mathematics in Chemical Engineering", 2nd Edition, M^{c}Graw-Hill (1957).

53. G. W. C. Kaye and T. H. Laby, "Physical and Chemical Constants", 11th Edition, Longmans Green (1956).

54. S. I. Skylarenko, B. I. Markin and Y. V. Samson, Zhur. Fiz. Chim.,

32, 692 (1958). Reported in Chem. Abstr., 52, 14266h, (1958).